Rheological Properties of Polymer Liquids(Dissertation_全文)

AUTHOR(S):

Masuda, Toshiro

RHEOLOGICAL PROPERTIES

OF

POLYMER LIQUIDS

TOSHIRO MASUDA

RHEOLOGICAL PROPERTIES OF POLYMER LIQUIDS

TOSHIRO MASUDA

Department of Polymer Chemistry

Faculty of Engineering

Kyoto University

JAPAN

Preface

The state of polymer molecules which appear in the course of research on the rheological properties of polymeric materials can be typically classified into three categories: isolated molecules in dilute solutions, correlated molecules in concentrated systems, and restricted molecules in crystalline structures. What we are concerned about here are rheological properties in the second state, especially those for concentrated systems of uncrosslinked amorphous polymers, such as concentrated solutions and melts. These will be defined here as "polymer liquids". As is well-known, the rheological behavior of such polymer liquids is strongly affected by entanglement couplings, which are typically described as relatively strong interactions between polymer molecules in the amorphous state. At present, however, the nature of entanglement couplings is not very clear.

Beginning in 1960, when the author first became interested in polymer rheology, he has engaged in research on the rheological properties of polymer liquids. His investigations have extended over the subjects of the rheological properties of polymer melts, polymer solutions, polymer blends, branched polymers, and disperse systems. The main objective has centered on the systematic collection of experimental data for the effects of temperature, concentration, molecular weight, molecular weight distribution, branching of polymer chain, and dispersed particles in polymer liquid; and on seeking out the relations between the measured properties and molecular structure.

The present thesis is based on studies carried out by the author in the Department of Polymer Chemistry, Kyoto University, from 1965 to 1972, except for the works on the rheological properties of branched polymers and disperse systems. Therefore, the subject of this thesis is mainly concerned with the effects of temperature, molecular weight and its distribution and concentration. An additional aim is to contribute something to the elucidation of the nature of entanglement couplings.

The constitution of the present thesis is as follows: Chapter 1 gives introductory remarks and a brief review of the rheological behavior of polymer liquids, and provides a basis for the subsequent discussions. The preparation and characterization of sample materials employed in this study, and the measuring techniques are summarized in Chapter 2. The sample codes and fundamental molecular parameters such as molecular weight and its distribution are also tabulated. In Chapter 3, the experimental results of rheological properties of polymer melts are described. The molecular weight and temperature dependence of some rheological parameters are discussed on the basis of the current molecular theories. Chapter 4 gives some description of the effects of concentration on the viscous and elastic behavior of polymer solutions. Chapter 5 deals with the rheological properties of polymer blends. Discussion and suggestion for the feature of entanglement couplings in polymer blend are given on the basis of the experimental data for narrow-distribution polymers. In Chapter 6, some current blending theories are reviewed. The predictions of the theories are tested with the experimental data obtained in Chapter 5. Moreover, a comparison of theories is made.

TOSHIRO MASUDA

March,1973

Acknowledgments

The author is deeply indebted to

Professor Shigeharu Onogi

for his continual guidance and encouragement during the course of this research. This research has been carried out in collaboration with a number of students and coworkers, for whose help the author wishes to express his sincere thanks.

The special thanks of the author also go to

Professors Michio Kurata and Tadao Kotaka,

who introduced him into polymer rheology, and to

Professor Hisashi Odani and Doctor Kunihiro Osaki,

all of whom have given helpful comments and advice on many occasions.

The author wishes to tender the sincere thanks also to

Professors John D. Ferry and Donald C. Bogue

for their useful discussions during their visits in our department at Kyoto University.

This study was supported in part by a grant for scientific research from the Ministry of Education of Japan, which support is gratefully acknowledged.

TOSHIRO MASUDA

Contents

CHAPTER 1

Introduction

1.1 GENERAL PERSPECTIVE

Rheology, "the science of deformation and flow", may be approached in two quite different ways: one is phenomenological and the other is molecular-theoretical. The phenomenological rheology aims to look for a common relation between strain and stress(in terms of time)for many materials. This approach to rheology is often referred to as "continuum mechanics", which includes the classical theory of elasticity, fluid mechanics, plasticity theory and the mechanical theory for viscoelastic body. This part of rheology has a physical aspect, because it deals with the common properties of materials. The other approach to rheology is more chemical, in the sense that it is closely related to the internal structure of the materials or molecules. In other words, it is an application of rheology to each of the branches of materials science. This study, as it is with the rheological properties of polymer liquid, falls in this second category. From the historical point of view, however, the progress of both parts of rheology has been motivated, first, by colloid science, and then by the rapid growth of polymer science, since polymeric materials show typical viscoelastic behavior.

As is well-known, the physical properties of polymeric materials generally depend on the molecular weight. By this fact, polymeric substances distinguish themselves from low molecular weight substances. However, with increasing molecular weight, some properties become less

dependent on it, and other become more and more strongly dependent on it. Melting point, tensile strength and viscoelastic properties in the transition and glassy zones are examples of the former, while the viscoelastic properties in the rubbery and terminal (or flow) zones typically belong to the latter. Accordingly, the rheological properties of the rubbery and terminal zones are significantly affected by the molecular weight distribution also.

Polymer rheology, as a branch of the material science, deals with the relation between the rheological properties and the structure of polymers, such as molecular weight, molecular weight distribution, chain branching and others. From an industrial point of view, the rheology of polymeric materials, especially of polymer liquids, is of special importance in connection with polymer processing, such as spinning, film formation, molding of plastics etc.

The viscoelastic behavior of concentrated systems of high polymers, such as concentrated solutions and melts, has been studied for a long time by many authors, because of the broad academic and industrial interest. Theoretical and experimental investigations hitherto published have been revealed that entanglement couplings between molecules constitute one of the most significant factors which determine the rheological properties of these concentrated systems. However, there still remain some unsolved problems on the true nature of the entanglement couplings and their effect on the rheological behavior of polymer liquids. A difficulty met the theoretical treatments of the entanglement couplings in concentrated systems in that we cannot describe satisfactorily very strong interactions between molecular chains or segments.

Many investigations concerning the effect of molecular weight, its

distribution and branching, have been shown qualitatively that rheological properties of polymer liquids are strongly affected by such a structure, especially in the terminal and rubbery zones. However, polymer samples having a broad distribution of molecular weight cannot afford exact information on these problems. Unusual behavior has often been desultorily attributed to molecular weight distribution or branching. One of the weak points of some studies published previously seems to be in the samples employed. Although the influence of molecular weight distribution are contained in the experimental results, we cannot extract it from the data quantitatively, because the samples are not well-characterized. Bold conclusions deduced on the basis of such experiments has led to more of the same kind of experimental data and, in some cases at least, amplified confusion.

In order to escape from this pattern, well-characterized samples and accurate measurements on them over wide ranges of temperatures and time scales are necessary. The same arguments may be appropriate for reseach on the effect of branching on the rheological properties.

Unfortunately, we do not have suitable parameters to represent the width and shape of molecular weight distributions. Therefore, even if the distribution is known in detail, quantitative relations between the distribution and the properties of polymers cannot be formulated. This is the reason that an investigation using order-made samples, prepared by blending narrow-distribution polymers with different molecular weights, is essential. In the blend samples, some parameters such as molecular weights of the components, their ratios and the blending ratios are known.

In conclusion, then, we feel that the most effective means of understanding the rheological properties of complex materials, such as

those having broad molecular-weight distributions, is first to accumulate reliable experimental data for narrow-distribution polymers. The experimental investigations described in this thesis have been conducted with this objective in mind.

In this chapter is given a review of the theoretical background, including the phenomenological and molecular theories for polymer liquids, which will serve as a basis for discussion in succeeding chapters.

1.2 RHEOLOGICAL BEHAVIOR OF POLYMER LIQUIDS

1.2.1 Simple Shearing Flow and Stress

In most of the experimental studies for rheological properties of polymer liquids, "simple shearing flow" has been applied on the tested materials as a "viscometric flow".[1] A simple shearing flow is illustrated in Fig.1-1. There is a non-zero component of velocity v_1 in only a single direction; in this case x_1. The coordinate system adopted here is a cartesian coordinate system (x_1,x_2,x_3), and subscripts, 1, 2, and 3 denote, respectively, the flow direction, the direction of the velocity gradient and the neutral direction. The simple shearing flow is defined by

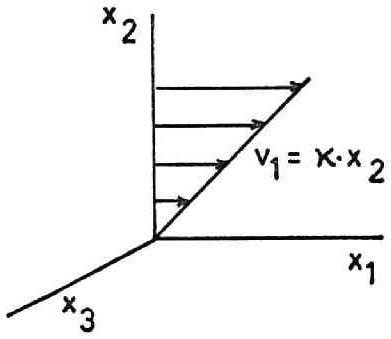

FIG.1-1. Simple shearing flow.

$$\mathbf{v} = (v_1 , 0 , 0) \qquad (1\text{-}1)$$

$$\dot{\gamma} = \kappa \begin{pmatrix} 0 & 1 & 0 \\ 1 & 0 & 0 \\ 0 & 0 & 0 \end{pmatrix} \qquad (1\text{-}2)$$

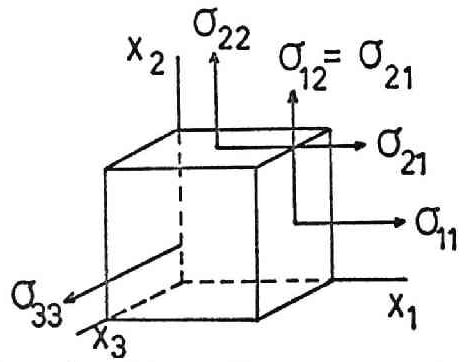

FIG.1-2. Identification of the components of stress tensor.

$\mathbf{v}$ is the velocity of fluid and $\dot{\boldsymbol{\gamma}}$ is the rate of deformation tensor, a basic measure of deformation of fluid, whose cartesian components $\dot{\gamma}_{ij}$ are, in general,

$$\dot{\gamma}_{ij} = \left(\frac{\partial v_i}{\partial x_j} + \frac{\partial v_j}{\partial x_i} \right) = \dot{\gamma}_{ji} \tag{1-3}$$

κ is a shear component of the rate of deformation tensor and a scalar function of x_2-coordinate:

$$\kappa = \frac{\partial v_1}{\partial x_2} = \frac{v_1(x_2)}{x_2} \tag{1-4}$$

The stress tensor $\boldsymbol{\sigma}$ has, in general, nine components, written as follows in matrix form:

$$\boldsymbol{\sigma} = \begin{pmatrix} \sigma_{11} & \sigma_{12} & \sigma_{13} \\ \sigma_{21} & \sigma_{22} & \sigma_{23} \\ \sigma_{31} & \sigma_{32} & \sigma_{33} \end{pmatrix}. \tag{1-5}$$

where the component of the stress tensor σ_{ij} is defined as the stress acting on the plane perpendicular to the x_i-axis and in the direction of x_j-axis, as illustrated in Fig.1-2. An significant feature of the stress tensor for most real fluids, is the symmetry relation,[2,3]

$$\sigma_{ij} = \sigma_{ji} \tag{1-6}$$

and then only six components of eq(1-5) are independent.

1.2.2 Constitutive Equations

For an incompressible material*, the equation of continuity, which express the principle of conservation of mass, is written in cartesian coordinates as

$$\frac{\partial v_i}{\partial x_i} = 0 \tag{1-7}$$**

---

* Incompressibility of material is always assumed hereafter.

** Repeated subscripts imply summation over that subscript in tensor analysis.[2~4]

The equation of motion, expressing the principle of conservation of momentum, is

$$\rho \left(\frac{\partial v_i}{\partial t} + v_j \frac{\partial v_i}{\partial x_j} \right) = \rho F_i + \frac{\partial \sigma_{ij}}{\partial x_j} \tag{1-8}$$

where ρ is the density of an incompressible material subjected to an external force $\mathbf{F}$.

Besides these two conservation equations, one other fundamental equation connecting the stress tensor with the strain or rate of strain tensor is required in order to determine the mechanical behavior of the materials completely. This material equation is the so-called "constitutive equation", which is sometimes called the rheological equation.* [2~5] An example of the most simple constitutive equation is Newton's law for the Newtonian fluid in simple shearing flow:

$$\sigma_{12} = \eta_0 \kappa \tag{1-9}$$

where η_0 is a constant, called the coefficient of viscosity.

In the course of extensive theoretical investigations on continuum mechanics, many constitutive equations for viscoelastic fluids, with polymer liquids in mind, have been proposed.[6] Current constitutive equations can be classified into two categories:[4,7] the differential and integral types of the equations. What is necessary here is a constitutive equation described by single integral of the history of deformation, although more general forms may be written as an expansion of a series of integrals of the history, as for example in the case of the second-order simple fluid.[8]

---

* There are two important requirements for constitutive equations:[3,4]

(1) A constitutive equation should be of a form independent of the coordinate system selected for reference(the principle of material objectivity), and

(2) it should be able to be written in a coordinate system embedded in the material.

The major merit of integral representations is that they are explicit in stress, being of the form:[4]

$$\text{stress} = \int_{-\infty}^{t} (\text{memory function})(\text{strain history})dt' \qquad (1\text{-}10)$$

This equation shows that the present response (stress) can be expressed explicitly by the history of deformation at all times t' in the past up to the present time, t. The general form of the single integral type of the constitutive equation is as well-known:[4,6]

$$\boldsymbol{\sigma}(t) = -p\mathbf{1} + \int_{-\infty}^{t}\{\mu_1[\mathbf{C}^{-1} - \mathbf{1}] + \mu_2[\mathbf{C} - \mathbf{1}]\, dt' \qquad (1\text{-}11)$$

where $\mathbf{1}$ is the unit tensor, p isotropic pressure, $\mathbf{C}$ is the Cauchy-Green relative strain tensor at t' relative to the present time t, $\mathbf{C}^{-1}$ is the inverse* of $\mathbf{C}$ which is called the Finger tensor. μ_1 and μ_2 are memory functions, being some functions of the invariants of the strain tensor and/or rate of strain tensor in the non-linear case. The constitutive equation whose memory function is a function of the second invariant of rate of strain tensor, II_d, has been discussed in connection with polymer liquids. The representation is in the form:

$$\boldsymbol{\sigma}(t) = -p\mathbf{1} + \int_{-\infty}^{t} \mu[t-t';II_d(t')][(1+\varepsilon)(\mathbf{C}^{-1} - \mathbf{1}) + \varepsilon(\mathbf{C} - \mathbf{1})]dt' \qquad (1\text{-}12)$$

where ε is a constant, giving the ratio of the second normal stress difference, $(\sigma_{22} - \sigma_{33})$ to the first one, $(\sigma_{11} - \sigma_{22})$, which is believed to be small compared with unity. If $\varepsilon=0$, eq(1-12) is simplified to[9]

$$\boldsymbol{\sigma}(t) = -p\mathbf{1} + \int_{-\infty}^{t} \mu[t-t';II_d(t')](\mathbf{C}^{-1} - 1)dt' \qquad (1\text{-}13)$$

For a simple shearing flow, $\mathbf{C}$, $\mathbf{C}^{-1}$ and II_d are respectively given as

---

* $\mathbf{C}\mathbf{C}^{-1} = \mathbf{1}$

$$\mathbf{C} = \begin{pmatrix} 1 & -\kappa t & 0 \\ -\kappa t & 1+\kappa^2 t^2 & 0 \\ 0 & 0 & 1 \end{pmatrix} \tag{1-14}$$

$$\mathbf{C}^{-1} = \begin{pmatrix} 1+\kappa^2 t^2 & \kappa t & 0 \\ \kappa t & 1 & 0 \\ 0 & 0 & 1 \end{pmatrix} \tag{1-15}$$

and

$$II_d = 2\kappa^2 \tag{1-16}$$

1.2.3 Viscoelastic Behavior of Polymer liquids

When the memory function μ is independent of II_d, eq(1-13) gives the constitutive equation for linear viscoelasticity, that is,[5]

$$\boldsymbol{\sigma}(t) = -p\mathbf{1} + \int_{-\infty}^{t} \mu(t-t')(\mathbf{C}^{-1} - \mathbf{1})dt' \tag{1-17}$$

The Boltzmann superposition principle for liquids,[10,11] which is valid only for infinitesimal strain, is given as follows:

$$\sigma(t) = \int_{-\infty}^{t} G(t-t')\dot{\gamma}(t')dt' \tag{1-18}$$

or

$$\sigma(t) = \int_{-\infty}^{t} \mu(t-t')\gamma(t')dt' \tag{1-19}$$

This is the one dimensional case of eq(1-17). Here G(t-t') is the relaxation function (or modulus), which is related to the memory function by

$$\mu(t-t') = -\frac{dG(t-t')}{dt'} \tag{1-20}$$

Now we introduce the relaxation spectrum $H(\tau)$ in terms of relaxation time by

$$G(t-t') = \int_{-\infty}^{\infty} H(\tau)\exp[-(t-t')/\tau]d\ln\tau \tag{1-21}$$

or

$$\mu(t-t') = -\int_{-\infty}^{\infty} \frac{H(\tau)}{\tau} \exp[-(t-t')/\tau]d\ln\tau \qquad (1\text{-}22)$$

From eqs(1-18)∿(1-22), the relaxation modulus G(t), complex modulus G*(iω), and its real and imaginary parts G'(ω) and G"(ω) in shear can be obtained as follows.

Let the infinitesimal strain history be

$$\gamma(t') = 0, \quad t' < 0 \quad \text{and} \quad \gamma(t') = \gamma_0, \quad t' \geq 0 \qquad (1\text{-}23)$$

Then the relaxation modulus G(t) is given by

$$G(t) = \sigma(t)/\gamma_0 = \int_{-\infty}^{\infty} H(\tau) \exp(-t/\tau)d\ln\tau \qquad (1\text{-}24)$$

When the material is subjected to a sinusoidal small strain,

$$\gamma^* = \gamma_0 \exp(i\omega t') \qquad (1\text{-}25)$$

the complex modulus G*(iω) is given by

$$G^*(i\omega) = \sigma^*/\gamma^* = G'(\omega) + iG''(\omega)$$

$$= i\omega \int_0^{\infty} G(s) \exp(-i\omega s)ds = \int_0^{\infty} \mu(s) \exp(-i\omega s)ds \qquad (1\text{-}26)$$

The storage modulus G' and loss modulus G" are written, respectively, as

$$G'(\omega) = \omega\int_0^{\infty} G(s)\sin(\omega s)ds = \int_0^{\infty} \mu(s)\cos(\omega s)ds \qquad (1\text{-}27)$$

and

$$G''(\omega) = \int_0^{\infty} G(s)\cos(\omega s)ds = \int_0^{\infty} \mu(s)\sin(\omega s)ds \qquad (1\text{-}28)$$

The complex viscosity η*(iω) is also defined by

$$\eta^*(i\omega) = G^*(i\omega)/i\omega = \eta'(\omega) - i\eta''(\omega) = \int_0^{\infty} G(s)\exp(-i\omega s)ds \qquad (1\text{-}29)$$

and then

$$\eta'(\omega) = \int_0^{\infty} G(s)\cos(\omega s)ds \qquad (1\text{-}30)$$

$$\eta''(\omega) = \int_0^{\infty} G(s)\sin(\omega s)ds \qquad (1\text{-}31)$$

The relations between these material functions and the relaxation spectrum can be deduced as

$$G'(\omega) = \int_{-\infty}^{\infty} H(\tau) \frac{\omega^2\tau^2}{1+\omega^2\tau^2} d\ln\tau \tag{1-32}$$

$$G''(\omega) = \int_{-\infty}^{\infty} H(\tau) \frac{\omega\tau}{1+\omega^2\tau^2} d\ln\tau \tag{1-33}$$

and

$$\eta'(\omega) = \int_{-\infty}^{\infty} H(\tau) \frac{\tau}{1+\omega^2\tau^2} d\ln\tau \tag{1-34}$$

Using the linear constitutive equation, eq(1-17), and eq(1-15), we can obtain the stress comoponents in steady state for a simple shearing flow. The result is

$$\boldsymbol{\sigma} = -p\mathbf{I} + \begin{pmatrix} \theta_0\kappa^2 & \eta_0\kappa & 0 \\ \eta_0\kappa & 0 & 0 \\ 0 & 0 & 0 \end{pmatrix} \tag{1-35}$$

That is, the shear stress $\sigma_{12} = \sigma_{21}$, the first normal stress difference, $\sigma_{11} - \sigma_{22}$, and the second normal stress difference, $\sigma_{22} - \sigma_{33}$, are, respectively,

$$\sigma_{12} = \eta_0\kappa \tag{1-36}$$

$$\sigma_{11} - \sigma_{22} = \theta_0\kappa^2 \tag{1-37}$$

$$\sigma_{22} - \sigma_{33} = 0 \tag{1-38}$$

where η_0 and θ_0 are called the zero-shear or Newtonian viscosity and the first normal stress coefficient, which are also written as

$$\eta_0 = \int_0^{\infty} G(s)ds = \int_{-\infty}^{\infty} \tau H(\tau) d\ln\tau \tag{1-39}$$

$$\theta_0 = 2\int_0^{\infty} G(s)sds = 2\int_{-\infty}^{\infty} \tau^2 H(\tau) d\ln\tau \tag{1-40}$$

If we use the non-linear constitutive equation, eq(1-13) instead of eq(1-17) and define the rate-dependent relaxation spectrum $H(\tau;II_d)$ with[9]

$$\mu(t-t';II_d) = \int_{-\infty}^{\infty} \frac{H(\tau;II_d)}{\tau} \exp[-(t-t')/\tau] d\ln\tau \qquad (1-41)$$

then the stress tensor is of the following form:

$$\sigma = -p\mathbf{I} + \begin{pmatrix} \theta(\kappa)\kappa^2 & \eta(\kappa)\kappa & 0 \\ \eta(\kappa)\kappa & 0 & 0 \\ 0 & 0 & 0 \end{pmatrix} \qquad (1-42)$$

Then the rate of shear dependent viscosity and normal stress coefficient can be expressed as

$$\eta(\kappa) = \sigma_{12}/\kappa = \int_{-\infty}^{\infty} \tau H(\tau;\kappa) d\ln\tau \qquad (1-43)$$

$$\theta(\kappa) = (\sigma_{11} - \sigma_{22})/\kappa^2 = 2\int_{-\infty}^{\infty} \tau^2 H(\tau;\kappa) d\ln\tau \qquad (1-44)$$

where the function of the second invariant II_d are rewritten as function of κ, because $II_d=2\kappa^2$[eq(1-16)]. Eqs(1-43) and (1-44) show that the rate of shear dependences of $\eta(\kappa)$ and $\theta(\kappa)$ are caused by the rate-dependent relaxation spectrum. The explicit expressions for $H(\tau;\kappa)$ have been proposed by many authors but it is not required here to discuss these in detail. In general, however, $H(\tau;\kappa)$ should be a decreasing function of κ.

The extinction angle χ of the stress tensor eq(1-42) is obtained as

$$2\cot 2\chi = (\sigma_{11} - \sigma_{22})/\sigma_{12} \qquad (1-45)$$

This angle can be measured by the flow birefringence experiments.

1.2.4 Some Characteristic Constants for Rheological Behavior of Polymer Liquids

The phenomenological behavior of polymer liquids mentioned above, gives some important rheological parameters characteristic of the materials,

especially in the terminal zone. Since the rate-dependent relaxation spectrum $H(\tau;\kappa)$ tends to the linear relaxation spectrum $H(\tau)$ with $\kappa\to 0$, the zero-shear viscosity η_0 is given by

$$\eta_0 = \lim_{\kappa\to 0}\eta(\kappa) = \lim_{\omega\to 0}[G''(\omega)/\omega] = \lim_{\omega\to 0}\eta'(\omega)$$

$$= \int_0^\infty G(s)ds = \int_{-\infty}^\infty \tau H(\tau)d\ln\tau \qquad (1\text{-}46)$$

making use of eqs(1-28), (1-30), (1-32), (1-34), (1-36) and (1-43). Similarly, eqs(1-27), (1-33), (1-37) and (1-44) give the relation between the storage modulus $G'(\omega)$ and the first normal stress difference, $\sigma_{11}-\sigma_{22}$, at long time scale.

$$A_G = \lim_{\omega\to 0}[G'(\omega)/\omega^2] = \lim_{\kappa\to 0}[(\sigma_{11}-\sigma_{22})/2\kappa^2]$$

$$= \theta_0/2 = \int_0^\infty sG(s)ds = \int_{-\infty}^\infty \tau^2 H(\tau)d\ln\tau \qquad (1\text{-}47)$$

where A_G is called the elasticity coefficient.[11] Another important parameter is the steady-state compliance J_e^0, defined as

$$J_e^0 = \lim_{\kappa\to 0}[(\sigma_{11}-\sigma_{22})/2\sigma_{12}^2] = \lim_{\omega\to 0}[G'(\omega)/G''(\omega)^2]$$

$$= A_G/\eta_0^2 = \int_0^\infty sG(s)ds/[\int_0^\infty G(s)ds]^2$$

$$= \int_{-\infty}^\infty \tau^2 H(\tau)d\ln\tau/[\int_{-\infty}^\infty \tau H(\tau)d\ln\tau]^2 \qquad (1\text{-}48)$$

which may be a measure of the deformability in slow flow of an entanglment structure in polymer liquids. It also corresponds to the inverse of spring constant in the Maxwell element, which is the most simple mechanical model of viscoelastic liquid. At a finite κ, we can define a rate-dependent compliance function, $J_e(\kappa)$ and recoverable elastic strain, $s(\kappa)$ as

$$J_e(\kappa) = (\sigma_{11} - \sigma_{22})/2\sigma_{12}^2 \qquad (1\text{-}49)$$

$$s(\kappa) = J_e(\kappa)\sigma_{12}(\kappa) \qquad (1\text{-}50)$$

which are naturally the functions of σ_{12} as well.

The important parameters in the rubbery zone for the conceptual scheme of entanglement couplings are the quasi-equilibrium modulus G_{eN}^0 which is the modulus at the rubbery plateau, the entanglement compliance[11] J_{eN}^0 and the average molecular weight between the coupling loci, M_e. An analogy to the kinetic theory of crosslinked rubber gives the relation:

$$G_{eN}^0 = 1/J_{eN}^0 = g_N \rho RT/M_e \qquad (1\text{-}51)$$

where ρ is the density of polymer and g_N a front factor near unity.

1.3 MOLECULAR THEORIES FOR POLYMER LIQUIDS

1.3.1 General View of Molecular Theories

The molecules of different polymer species have their own structures, characterized by the bond angles in the backbone chain, the side groups or chains and the configurations. In order to formulate the mechanical properties of such diverse and complicated molecules, they must necessarily be represented by as simple a molecular model as possible without overlooking the essential characteristics. Therefore, a molecular theory should be appraised not only by the agreement of the predictions with experimental results but also by the physical validity of the proposed model. The molecular theory whose physical model does not reasonably represent the real polymer, is of no value, even though it can explain the behavior of polymers very well.

From this point of view, so-called "bead-spring" theories for isolated molecules can almost completely describe the linear viscoelastic behavior of very dilute polymer solutions. The theory based on the bead-spring model or the Rouse model was first proposed by Rouse[12] and then developed by Zimm[13], Tschoegl[14] and others[15], taking account of hydrodynamic interaction[16] between segments and excluded volume effects. Unfortunately, however, the current molecular theories for polymer liquids have met with less success. No theory is able to predict the famous, empirical law that the viscosity of the polymer liquids is proportional to the 3.5 power of the molecular weight:[11,17,18]

$$\eta_0 = \text{const. } M^{3.5} \tag{1-52}$$

The difficulty seems to lie in the following question: "how can the nature of entanglement couplings be embodied in the molecular model?" This author believes firmly that the first goal for a successful molecular theory must be the interpretation of the 3.5 power law for viscosity. The empirical law is preassumed a priori in all of the theories proposed up to the present. The most typical two molecular theories, among others, are selected and reviewed here.

1.3.2 An Extension of the Rouse Theory; the FLW Theory

The Rouse theory[12] is based upon the bead-spring model, made up of N+1 Stokesian beads of friction factor ζ_0 and N Hookian springs of the equilibrium length l and the spring constant,

$$\kappa_0 = 3kT/l^2 \tag{1-53}$$

This is illustrated in Fig.1-3. The theory is one of the bead-spring theories[15] and is just the case of free draining and no excluded volume

effect, that is, there is no hydrodynamic interaction between the beads in the solvent, and the conformation of the model is taken as Gaussian. For this model suspended in the flowing solvent with the velocity v_α in the α-direction, the equation of motion can be written as eq(1-54). Where $\boldsymbol{\alpha}$, $\mathbf{v}_\alpha$ and $\partial/\partial\boldsymbol{\alpha}$ are the vectors in the normal coordinates, with N+1 components for α-coordinate of bead, velocity of solvent, and differential operator, respectively. $\mathbf{A}$ is the Rouse matrix of dimensions, (N+1)x(N+1), and ψ is a probability function for the chain conformation.

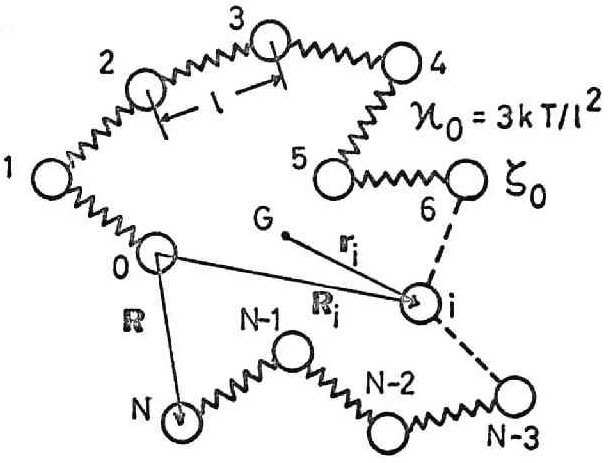

FIG.1-3. The Rouse or bead-spring model.

$$\zeta_0(\dot{\boldsymbol{\alpha}} - \mathbf{v}_\alpha) + \kappa_0 \mathbf{A}\boldsymbol{\alpha} + kT(\partial/\partial\boldsymbol{\alpha})\ln\psi = 0 \qquad (1\text{-}54)$$

The normal coordinate analysis on the dynamics of the model under the sinusoidal simple shearing vibration [eq(1-25)], yield the following results:

$$G'(\omega) = nkT \,\Sigma\, \frac{\omega^2\tau_p^2}{1+\omega^2\tau_p^2} \qquad (1\text{-}55)^*$$

$$G''(\omega) = nkT \,\Sigma\, \frac{\omega\tau_p}{1+\omega^2\tau_p^2} + \omega\eta_s \qquad (1\text{-}56)$$

$$\tau_p = \zeta_0/2\kappa_0\lambda_p \qquad (1\text{-}57)$$

---

* Σ means $\sum_{p=1}^{N}$ in this section.

where n is the number of chains per unit volume, η_s is the viscosity of solvent and λ_p is the p-th (in order of the magnitude) eigen value of **A**. The explicit expressions for τ_1, the so-called maximum relaxation time, and τ_p are respectively,

$$\tau_1 = \frac{N^2 l^2}{6\pi^2 kT} \zeta_0 \qquad (1\text{-}58)$$

$$\tau_p = \tau_1 / p^2, \qquad p = 1, 2, \ldots N \qquad (1\text{-}59)$$

The first attempt to describe the rubbery plateau in connection with the entanglement couplings was an extension of the Rouse theory proposed by Ferry-Landel-Williams (FLW) in 1955.[11,19] The effects of entanglement are introduced by giving a high value of τ_p for long times, such that the viscosity is proportional to $M^{3.5}$. The τ_p's are divided into the two groups,

$$\tau_p = N^2 l^2 \zeta_0 Q_e / 6\pi^2 p^2 kT, \qquad p \leq p_e \qquad (1\text{-}60)$$

and

$$\tau_p = N^2 l^2 \zeta_0 / 6\pi^2 p^2 kT, \qquad p > p_e \qquad (1\text{-}61)$$

where

$$Q_e = (M/M_C)^{2.5}, \qquad M > M_C \qquad (1\text{-}62)$$

The p_e value can be determined as the p_e-th relaxation time of a polymer having molecular weight M is equal to the maximum relaxation time of polymer with $M = M_C$, the critical molecular weight for entanglement. Eq(1-61) is identically equal to eq(1-59), and eq(1-60) meams that the friction factor in the Rouse theory, ζ_0, is multiplied by a factor Q_e in longer time region. This theory predicts the following relations:

$$\eta_0 = (cRT/M)\Sigma\ \tau_p = 1.645\ (cRT/M)\tau_1 \qquad (1\text{-}63)$$

$$J_e^0 = (M/cRT) \cdot \Sigma \tau_p^2/(\Sigma \tau_p)^2 = 0.40 \ (M/cRT) \qquad (1\text{-}64)$$

$$G_{eN}^0 = cRT/M \qquad (1\text{-}65)$$

with the concentration or density of polymer c (g-polymer/ml-liquid).

Similar molecular theories are the Marvin-Oser theory[20] and the Chompff-Duiser theory[21]. The former substituted the FLW's idea with a mechanical model and gave a closed expressions for $G^*(\omega)$ and other viscoelastic functions. The latter theory calculated the relaxation spectra by localizing the highly frictional portions,"slow point", on a polymer chain. The predictions of these theories are not so different from the FLW theory.

1.3.3 The Graessley Theory

A new molecular theory was proposed by Graessley[22] for linear viscoelastic behavior in the entanglement region. The molecular model employed is shown in Fig.1-4. As illustrated in this figure, let the i-th entanglement locus of a polymer chain having E loci interact with the j-th of another chain at P. The most significant assumption in this theory is that the entanglement slippage should be caused by slipping off the shorter fragment of chain [23], i.e., if i> j ($i \leq E/2$, $j \leq E/2$), j fragment slips off. Another assumptions for the spring constant at i, κ_i, and the friction factor at P, ζ_{ij}, are

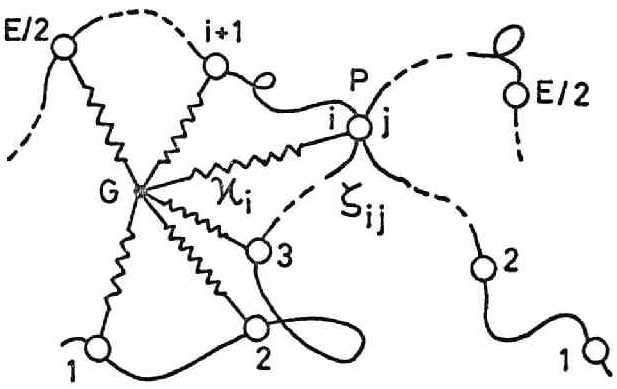

FIG.1-4. The molecular model empolyed in the Graessley theory.
P: entanglement coupling locus
G: center of gravity of molecule

$$\kappa_i = 3kT/2\langle S^2\rangle\,[1 - 3(i/E) + 3(i/E)^2] \tag{1-66}$$

$$\zeta_{ij} = 2N_e E^{5/2}(i/E)^2[1 - (i/E)]^{1/2}\zeta_0, \quad i<j$$
$$= 2N_e E^{5/2}(j/E)^2[1 - (j/E)]^{1/2}\zeta_0, \quad i>j \tag{1-67}$$

where $\langle S^2\rangle$, N_e and ζ_0 are, respectively, the mean-square radius of gyration, the number of segments between entanglement loci and the segmental friction factor. Then the relaxation time characteristc of the entanglement τ_{ij} is given as

$$\tau_{ij} = \zeta_{ij}/\kappa_i = (4\langle S^2\rangle N_e E^{5/2}/3kT)\,\zeta_0\phi_{ij} \tag{1-68}$$

where

$$\phi_{ij} = [1-3(i/E)+3(i/E)^2](i/E)^2[1-(i/E)]^{1/2}, \quad i<j$$
$$= [1-3(i/E)+3(i/E)^2](j/E)^2[1-(j/E)]^{1/2}, \quad i>j \tag{1-69}$$

Using the values of*

$$(2/E)^2{}_{\Sigma\Sigma}\ \phi_{ij} = 1.236\times10^{-2} \quad \text{and} \quad (2/E)^2{}_{\Sigma\Sigma}\ \phi_{ij}^2 = 2.735\times10^{-4},$$

the final results are

$$\eta_0 = (4n\langle S^2\rangle N_e E^{7/2}/3)\,\zeta_0[(2/E)^2{}_{\Sigma\Sigma}\ \phi_{ij}]$$
$$= 0.01648n\langle S^2\rangle N_e E^{7/2}\zeta_0 \tag{1-70}$$

$$J_e^0 = (nEkT)^{-1}\{(2/E)^2{}_{\Sigma\Sigma}\ \phi_{ij}^2/[(2/E)^2{}_{\Sigma\Sigma}\ \phi_{ij}]^2\}$$
$$= 1.789/nEkT \tag{1-71}$$

and the maximum relaxation time

$$\tau_m = 3.575\ \eta_0/nEkT \tag{1-72}$$

---

* $\Sigma\Sigma$ means $\sum_{i=1}^{2/E}\sum_{j=1}^{2/E}$ in this section.

Moreover, the storage and loss moduli are expressed in the form,

$$G'(\omega) = nEkT\ (2/E)^2 \Sigma\Sigma \frac{(\omega\tau_m\lambda_{ij})^2}{1+(\omega\tau_m\lambda_{ij})^2} \tag{1-73}$$

$$G''(\omega) = nEkT\ (2/E)^2 \Sigma\Sigma \frac{\omega\tau_m\lambda_{ij}}{1+(\omega\tau_m\lambda_{ij})^2} \tag{1-74}$$

with $\lambda_{ij} = 32\phi_{ij}/2^{1/2}$

Taking account of $nEkT=cRT/M_e$ and $M_e \propto 1/c$,* the predictions of the theory are tabulated in TABLE 1-I as well as those of the FLW theory. As shown in this table, some marked differences between the predictions of both theories, especially for the steady-state compliance and the quasi-equilibrium modulus, are there.

TABLE 1-I

THE PREDICTIONS OF THE MOLECULAR THEORIES FOR VISCOELASTIC BEHAVIOR OF POLYMER LIQUIDS

Parameter	The FLW theory	The Graessley theory
η_0	$\propto c^{3.5} M^{3.5} \zeta_o$+	$\propto c^{3.5} M^{3.5} \zeta_o$
A_G	$\propto c^{6}\ M^{8}\ \zeta_o^2$	$\propto c^{5}\ M^{7}\ \zeta_o^2$
J_e^o	$\propto c^{-1}\ M^{1}$	$\propto c^{-2}\ M^{0}$
τ_m	$\propto c^{2.5} M^{4.5} \zeta_o$	$\propto c^{1.5} M^{3.5} \zeta_o$
G_{eN}^0	$\propto c^{1}\ M^{-1}$	$\propto c^{2}\ M^{0}$

+ ζ_o is a function of c and T in general, but it can be regarded as constant at the iso-free volume state.

* " $A \propto B$ " means that A is proportional to B

1.4 EFFECT OF TEMPERATURE AND FREE VOLUME

As is well-known, the temperature dependence of viscoelastic properties of amorphous polymer has been well represented by the WLF equation[11], which was proposed by Williams-Landel-Ferry[24]:

$$\log a_T = \frac{- c_1^r(T - T_r)}{c_2^r + (T - T_r)} \tag{1-75}$$

where a_T is the shift factor, which is obtained from the shifts of the viscoelastic functions according to the time-temperature superposition principle. T_r is the reference temperature and c_1^r and c_2^r are numerical constants corresponding to T_r. Another definition of the shift factor is

$$a_T = \eta_0(T)/\eta_0(T_r) \tag{1-76}$$

with the zero-shear viscosity at T and T_r.

The famous empirical equation, eq(1-75) can be described from the free volume theory for liquids.[11] According to Doolittle[25], as well as Cohen and Turnbull[26], the viscosity of liquids can be given by

$$\ln\eta = \ln A + Bv/(v-v_0) \tag{1-77}$$

where A and B are constants for liquid, v is the specific volume, and v_0 the occupied volume at temperature T. The fractional free volume f is defined by $f = (v - v_0)/v$, which is also a function of temperature. Above the glass transition temperature T_g, f can be written approximately as[18,24]

$$f = (v - v_0)/v = f_g + \alpha_f(T - T_g) = \alpha_f(T - T_0) \tag{1-78}$$

where α_f is the temperature coefficient of the fractional free volume, f_g is the fractional free volume at T_g, and T_0 is an imaginary temperature well known as the Vogel temperature, at which the free volume would vanish.

Using eq(1-78), eq(1-77) may be rewritten as

$$\ln\eta = \ln A + \frac{B/\alpha_f}{(T - T_0)} \tag{1-79}$$

This equation is usually referred to as the Vogel equation[18] or the modified Arrhenius equation.[27] The WLF equation can be derived from eq(1-79) in the following form:

$$\log a_T = \frac{-c_1^{\,g}(T - T_g)}{c_2^{\,g} + (T - T_g)}, \quad c_1^{\,g}=B/2.303f_g \text{ and } c_2^{\,g}=f_g/\alpha_f \tag{1-80}$$

or

$$\log a_T = \frac{-c_1^{\,r}(T - T_r)}{c_2^{\,r} + (T - T_r)}, \quad c_1^{\,r}=B/2.303f_r \text{ and } c_2^{\,r}=f_r/\alpha_f \tag{1-81}$$

with the reference temperature T_r, and f_r, the fractional free volume at T_r. Eq(1-81) shows that the plot of $-(T - T_r)/\log a_T$ against $(T - T_r)$ shoud give a straight line, and that from its slope and intercept, $c_1^{\,r}$, $c_2^{\,r}$, f_r, α_f, and T_0 can be evaluated, assuming B = 1.[18,24]

REFERENCES

1. B. D. Coleman, H. Markovitz, and W. Noll, "Viscometric Flows of Non-Newtonian Fluids", Springer, New York, 1966.
2. R. Aris, "Vectors, Tensors, and the Basic Equations of Fluid Mechanics", Prentice-Hall, Englewood Cliffs, 1964.
3. A. G. Fredrickson, "Principles and Applications of Rheology", Prentice-Hall, Englewood Cliffs, 1964.
4. S. Middleman, " The Flow of High Polymers", Interscience, New York, 1968.
5. A. S. Lodge, "Elastic Liquids", Academic Press, New York, 1964.
6. D. C. Bogue and J. L. White, "Engineering Analysis of Non-Newtonian Fluids", Agardograph Series of NASA, 1970.

7. T. W. Spriggs, J. D. Huppler, and R. B. Bird, Trans. Soc. Rheology, 10, 191 (1966)

8. B. D. Coleman and W. Noll, Rev. Mod. Phys., 33, 239 (1961)

9. M. Yamamoto, Trans. Soc. Rheology, 15, 331 (1971)

10. L. Boltzmann, Pogg. Ann. Phys., 7, 624 (1876)

11. J. D. Ferry, "Viscoelastic Properties of Polymers", 2nd. Ed., John Wiley, New York, 1970.

12. P. E. Rouse, Jr., J. Chem. Phys., 21, 1272 (1953)

13. B. H. Zimm, J. Chem. Phys., 24, 269 (1956)

14. (a) N. W. Tschoegl, J. Chem. Phys., 39, 149 (1963)
(b) N. W. Tschoegl, J. Phys. Chem., 40, 473 (1964)

15. K. Osaki, Adv. Polym. Sci.; in press

16. J. G. Kirkwood and J. Riseman, J. Chem. Phys., 16, 565 (1956)

17. T. G. Fox, S. Gratch, and S. Loshaek, "Rheology", F. R. Eirich Ed., Vol. I., Academic Press, New York, 1956, Chap.12.

18. G. C. Berry and T. G. Fox, Adv. Polym. Sci., 5, 261 (1968)

19. J. D. Ferry, R. F. Landel, and M. L. Williams, J. Appl. Phys., 26, 359 (1955)

20. (a) R. S. Marvin and H. Oser, J. Res. NBS, 66B, 171 (1962)
(b) H. Oser and R. S. Marvin, J. Res. NBS, 67B, 87 (1963)

21. (a) A. J. Chompff and J. A. Duiser, J. Chem. Phys., 45, 1505 (1966)
(b) A. J. Chompff and W. Prins, J. Chem. Phys., 48, 235 (1968)

22. W. W. Graessley, J. Chem. Phys, 54, 5143 (1971)

23. (a) W. W. Graessley, J. Chem. Phys., 43, 2696 (1965)
(b) W. W. Graessley, J. Chem. Phys., 47, 1942 (1967)

24. M. L. Williams, R. F. Landel, and J. D. Ferry, J. Am. Chem. Soc., 77, 3701 (1955)

25. (a) A. K. Doolittle, J. Appl. Phys., 22, 1471 (1951)

(b) A. K. Doolittle and B. D. Doolittle, J. Appl. Phys., 28, 901 (1957)

26. (a) M. H. Cohen and D. Turnbull, J. Chem. Phys., 31, 1164 (1959)

(b) D. Turnbull and M. H. Cohen, J. Chem. Phys., 34, 120 (1961)

27. A. A. Miller, J. Polym. Sci., Part A, 1, 1857; 1865 (1963); 2, 1095 (1964)

CHAPTER 2

Experimental

2.1 INTRODUCTION

As mentioned in the previous chapter, the quantitative discussion of the rheological properties of polymer liquids, necessarily requires well-characterized polymeric materials. When the experimental results are compared with the predictions of the current molecular theories with respect to the molecular weight dependence, the molecular weight distribution should be as narrow as possible; it is to be desired that they are "mono-disperse". In the case of blended samples of different molecular weights, the situation is the same essentially as that for the component polymers.

To obtain samples having a narrow distribution of molecular weight, several fractionation techniques have been developed[1] over a period of many years. The fractional precipitation method, above all, has often been utilized in the preparation of samples for rheological experiments, because the method can produce a large amount of the fraction. Another large contribution to the preparation of good samples has been brought about by the development of the anionic polymerization technique[2]. We can get the polymer samples whose molecular weight distribution is so narrow that it can be regarded as "mono-disperse". The polymer samples empolyed in this study are those obtained by both the fractionation of raw polymers with broad distributions and also prepared by anionic polymerization. A polymer prepared by aninic polymerization will hereafter

be called an "anionic polymer". On the other hand, the polymer prepared by thermal or radical polymerization will be referred to as a "radical polymer".

Another condition for a thorough understanding of experimental results is that the measurements of the rheological properties are carried out accurately and over wide ranges of temperature and time. In this chapter are brought together the methods of preparation of the sample materials and also a tabulation of the molecular parameters, such as molecular weights, molecular weight distribution, tacticity and so on. Moreover, the experimental methods for measuring rheological properties of polymer liquids are described briefly.

2.2 PREPARATION AND CHARACTERIZATION OF SAMPLES

2.2.1 Polystyrenes (PS)

Radical Polystyrenes. In preparation of polystyrene, the purified styrene was polymerized by heating without initiator for 100,37,16, and 8 hr at 80,100,115 and 130°C,respectively, giving polymers having different molecular weights. The polymers were fractionated by precipitation with methyl ethyl ketone-methanol mixture. The fractions were purified by extraction with methanol and dried in a vacuum oven. The molecular weight M_w determined from intrinsic viscosity $[\eta]$ in toluene at 30°C using the following equation,[3] are shown in Table 2-I.

$$[\eta] = 1.2 \times 10^{-4} M_w^{0.71} \qquad (2\text{-}1)$$

These samples are used in Section 4.2.

TABLE 2-I

THE MOLECULAR WEIGHT OF RADICAL POLYSTYRENE SAMPLES

Sample	$M_w \times 10^{-4}$
80-1	191
80-2	148
80-3	92.5
80-4	70.4
80-5	29.0
100-1	105
100-3	65.6
100-4	26.9
111-1	137
140-2	20.6
130	35.7
115	55.7
100	90.6
80	167

Anionic Polystyrenes. The narrow-distribution polystyrenes employed throughout this study were prepared by anionic polymerization[2] at a low temperature (-78°C) in high vacuum below 10^{-6} mmHg, using tetrahydrofran as the solvent and n-butyl lithium as the initiator. The polymerization procedure was similar to that reported by Morton et al.[4], with certain improvements introduced by the author. The concentration of the initiator was 0.232 N in n-hexane. The weight of polymer obtained in each batch was 60-100 g. The polymer was precipitated and purified with methanol. Some of the polymers were fractionated by precipitation in benzene-methanol systems to remove higher and lower molecular weight fractions present in small amounts. The samples thus prepared were dried in a vacuum oven at 60°C.

The weight-average molecular weights M_w of the anionic polystyrenes were obtained from the intrinsic viscosity in cyclohexane at 34.5°C, using the following equation proposed by Altares et al.[5] for narrow-distribution polystyrene:

$$[\eta] = 8.5 \times 10^{-4} M_w^{0.5} \qquad (2\text{-}2)$$

The number-average molecular weight M_n, on the other hand, was determined by osmotic pressure technique using High Speed Membrane Osmometer, Model 502, of Mecrolab Inc.

The molecular weight distribution of the samples was measured by means of the Gel Permeation Chromatograph, Model 200, manufactured by Waters Associates Inc. The measurements were carried out with tetrahydrofran as the solvent at room temperature. The flow rate was 1 ml/min. The weight- and number-average molecular weights were also evaluated from the gel permeation chromatogram.

The weight- and number-average molecular weights and their ratios thus determined are tabulated in Table 2-II. M_w and M_n values determined by GPC

TABLE 2-II

THE WEIGHT- AND NUMBER-AVERAGE MOLECULAR WEIGHTS AND THEIR RATIO FOR THE ANIONIC POLYSTYRENE SAMPLES

Sample	Mol. wt. x 10^{-4}			Mol. wt.(GPC) x 10^{-4}		
	M_w	M_n	M_w/M_n	M_w	M_n	M_w/M_n
L2*	189	177	1.07	-	-	-
L3	2.45	2.26	1.08	2.74	1.97	1.39
L4*	402	383	1.05	-	-	-
L5	35.1	33.0	1.06	40.9	36.3	1.13
L9	0.89	0.88	1.01	1.19	0.91	1.31
L10	1.93	1.82	1.06	2.27	1.61	1.41
L12	1.48	1.29	1.15	2.08	1.51	1.38
L14	2.89	2.83	1.02	2.91	2.43	1.20
L15	21.5	21.5	1.00	22.9	20.3	1.13
L16	5.87	6.22	-	5.90	5.23	1.13
L18	58.1	55.0	1.06	61.6	56.3	1.09
L19	51.3	47.1	1.09	54.7	49.8	1.10
L20*	153	147	1.04	-	-	-
L22	27.5	25.7	1.07	31.8	28.8	1.10
L23*	440	386	1.14	-	-	-
L26	58.5	53.3	1.10	60.4	54.2	1.11
L27	16.7	19.9	-	18.5	16.4	1.13
L33	3.65	4.17	-	3.36	2.90	1.16
L34	4.69	4.95	-	4.31	3.84	1.12
L37	11.3	11.3	1.00	13.1	10.8	1.21
L40	20.5	23.4	-	26.6	22.9	1.16
L43*	183	171	1.07	-	-	-
L44	76.2	73.6	1.04	70.5	61.3	1.15
L45	73.8	68.7	1.08	70.0	62.4	1.14
L46	10.4	9.05	1.15	12.0	10.5	1.14
L47	13.7	16.0	-	13.5	12.1	1.11
L48*	102	96.5	1.06	82.9	72.5	1.14
L49	55.6	51.5	1.08	-	-	-
L50	29.8	27.6	1.08	31.5	27.5	1.15
L53	1.05	-	-	1.01	0.77	1.31
L56	-	-	-	56.5	45.0	1.25
L60	-	-	-	9.42	8.50	1.11
PS7**	30.3	19.3	1.57	31.3	17.0	1.84

* The molecular weights are too high to be determined acculately.

** Polystyrene prepared by radical polymerization, listed here for the sake of a comparison.

method coincide fairly well with those obtained by viscosity and osmotic pressure methods, but the ratios of M_w/M_n from the GPC have somewhat larger values than those from the other methods. For a comparison, similar measurements were carried out for the "standard" polystyrene polymers prepared by Pressure Chemical Co., and the result is shown in Table 2-III. The values of M_w and M_n in the second and third columns of the table are taken from the data sheets issued by Pressure Chemical Co., and were obtained by light scattering and osmotic pressure methods, respectively.

Comparing Table 2-II with Table 2-III, it is clear that the samples prepared here have molecular weight distributions as narrow as the standard polystyrenes.

TABLE 2-III

THE WEIGHT- AND NUMBER-AVERAGE MOLECULAR WEIGHTS AND THEIR RATIO FOR THE STANDARD POLYSTYRENES OBTAINED FROM PRESSURE CHEMICAL CO.

Sample	Mol. wt. x 10^{-4}			Mol. wt.(GPC) x 10^{-4}		
	M_w	M_n	M_w/M_n	M_w	M_n	M_w/M_n
S1	86.7	77.3	1.12	83.9	73.66	1.14
S2	41.1	39.2	1.05	48.3	42.84	1.13
S3	17.3	16.4	1.05	17.8	15.9	1.12
S4	9.82	9.62	1.02	10.04	9.12	1.10
S5	5.10	4.90	1.04	5.15	4.70	1.10
S6	1.985	1.965	1.01	1.97	1.80	1.09
S7	1.03	0.97	1.06	1.08	0.98	1.10
S8	0.500	0.460	1.09	0.570	0.520	1.10

2.2.2 Polymethyl Methacrylates (PMMA)

Radical Polymethyl Methacrylates.

In preparation of radical PMMA, purified monomer was polymerized by heating with around 2% of azobisisobutyronitrile as the initiator for around 40 min at 50°C, giving polymers of different molecular weights. The conversion was about 30%. The polymers were precipitated and purified with methanol. Each polymer thus obtained was fractionated by precipitation in acetone-n-hexane mixtures, and the fractions were purified and dried. The weight-average molecular weight of the fractions was determined from the intrinsic viscosity in acetone at 25°C by the following equation[6]:

$$[\eta] = 7.5 \times 10^{-5} M_w^{0.70} \qquad (2\text{-}3)$$

TABLE 2-IV

THE WEIGHT- AND NUMBER-AVERAGE MOLECULAR WEIGHTS AND THEIR RATIO FOR THE RADICAL PMMA SAMPLES

Sample	Mol. wt. x 10^{-4}		
	M_w	M_n	M_w/M_n
712	40.8	25.1	1.62
713	27.8	20.3	1.37
714	22.9	17.5	1.31
715	19.1	15.1	1.26
702	17.4	13.9	1.25
717	14.3	11.6	1.23
703	11.4	9.90	1.15
903	10.1	5.00	2.01
905	9.45	4.65	2.03
907	8.01	5.03	1.59
909	6.58	4.31	1.53
910	5.21	3.75	1.39
911	4.08	3.28	1.24
913	2.91	2.10	1.39
914	1.89	0.93	2.04
MS	4.10	-	-

The number-average molecular weight was measured by means of the Membrane Osmometer. The result is listed in Table 2-IV.

Anionic Polymethyl Methacrylates. This type of polymer samples of different molecular weights was prepared by anionic polymerization at low temperature (-78°C) under pressures below 10^{-6} mmHg, using tetrahydrofuran as the solvent and sodium naphthalene as the initiator. Each polymer thus prepared had a rather broad distribution of molecular weight and therefore was

fractionated in acetone-n-hexane systems. The fraction was purified and dried.

The weight-average molecular weight of each fraction was determined using eq(2-3). The number-average molecular weight M_n was determined by osmotic pressure measurements. The values for the weight- and number-average molecular weights and the ratio M_w/M_n are tabulated in Table 2-V.

TABLE 2-V

THE WEIGHT- AND NUMBER-AVERAGE MOLECULAR WEIGHTS AND THEIR RATIO FOR ANIONIC PMMA SAMPLES

Sample	Mol. wt. x 10^{-4}		
	M_w	M_n	M_w/M_n
MF2	34.2	22.4	1.53
MF3	27.0	18.8	1.44
MF5	19.7	14.6	1.35
MF6	15.8	13.9	1.14
MF7	11.6	9.80	1.18
MF8	9.63	7.18	1.34
MF9	6.39	5.28	1.21
MF10	4.52	3.71	1.22
MF11	3.51	2.53	1.39
MF12	2.84	1.80	1.58
MF13	1.14	0.91	1.25

The tacticity of the samples prepared by anionic polymerization was examined by nuclear magnetic resonance (NMR) spectroscopy and compared with that of PMMA obtained by the radical polymerization. An example of the NMR spectrum for anionic PMMA is shown in Fig. 2-1 together with that for radical PMMA. The tacticity parameters proposed by several authors[7~9], triad (I, H and S), diad(i and

TABLE 2-VI

THE TACTICITY PARAMETERS FOR ANIONIC AND RADICAL PMMA

Sample	$M_w x10^{-4}$	I	H	S	i	s	B
MF2	34.2	0.141	0.519	0.340	0.401	0.599	1.080
MF7	11.6	0.141	0.512	0.347	0.397	0.603	1.063
702	17.4	0.065	0.370	0.565	0.250	0.750	0.987
910	5.20	0.063	0.406	0.531	0.266	0.734	1.040

s) and heterogeneity parameter B were evaluated from these spectra, and the results are shown in Table 2-VI. In this table, the sample MF2 and MF7 are the anionic PMMA, while 702 and 910 are the radical PMMA.

The NMR spectra shown in Fig.2-1 and the tacticity parameters in Table 2-VI show that the samples of anionic PMMA are slightly isotactic as compared with the radical PMMA which is ideally atactic. Furthermore, the amorphous character of the samples, as determined by the X-ray diffraction method, was found to be about the same in the anionic material as in the radical material.

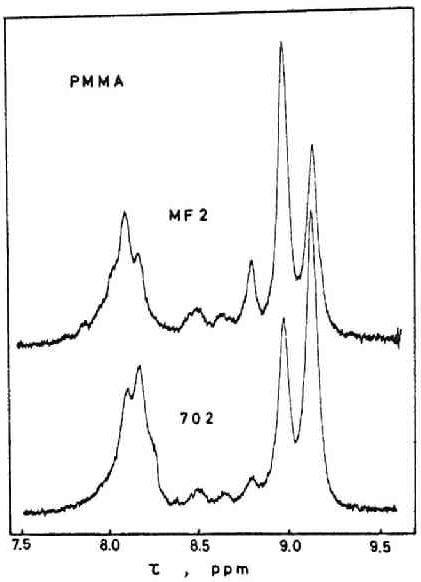

FIG.2-1. An example of the NMR spectra for anionic PMMA (MF2), compared with that for radical PMMA (702)

2.2.3 Polyvinyl Acetates (PVAc)

Linear Polyvinyl Acetates. The linear polyvinyl acetates was prepared by two methods: the photopolymerization of vinyl acetate at low temperature and the reacetylation of polyvinyl alcohol (PVA). The photopolymerization was carried out using α,α'-azodiisobutyronitrile as the initiator under a reduced pressure at -20°C. The conversion was controlled not to exceed 10%. The acetylation of PVA was

TABLE 2-VII

THE MOLECULAR WEIGHTS OF LINEAR POLYVINYL ACETATE SAMPLES

Sample	$M_w \times 10^{-4}$
A1	107
A2	68.8
H121	58.7
H122	40.4
H123	25.2
H13	21.8
H22	11.6
L11	75.6
L12	37.9
L21	32.0
L22	16.8
L13	13.6
L23	6.63

performed by the conventional method. One part of PVA was heated with 10 parts of pyridine-acetic anhydride mixture (2:1 in volume) for 4~6 hrs at 100°C. The degree of acetylation attained was substantially 100%.

Each polymer thus obtained was fractionated by precipitation in acetone-water mixtures, and the fractions were purified in boiling water and then dried in a vacuum oven. The weight-average molecular weight M_w shown in Table 2-VII, was determined from the intrinsic viscosity in acetone at 30°C by the following equation given by Matsumoto et al.[10]:

$$[\eta] = 1.02 \times 10^{-4} M_w^{0.72} \qquad (2\text{-}4)$$

The signs H and L in the first column of this table, mean that the fractions were obtained by the fractionation of PVAc prepared from PVA having the degree of polymerization of 2700 and 1600, respectively. A denotes the photopolymerized samples. These samples are employed in Sections 3.2 and 4.2.

Branched Polyvinyl Acetates. The preparation of branched PVAc was carried out according to the method described by Matsumoto et al.[11] by heating the purified monomer with 0.05% of azodiisobtyronitrile as the initiator in the stream of nitrogen for 8~10hrs at 60°C. The conversion was 80~90%. The polymers were fractionated, purified and dried as in the case of the linear polymers. The weight-average molecular weight for several fractions was determined by light scattering method, and a linear relationship was obtained between M_w and the intrinsic viscosity. From this relationship, M_w for other fractions was evaluated. The light-scattering measurements were carried out with solutions in methyl ethyl ketone at 30°C. The degree of branching, d, was evaluated by the following equation[12]:

$$d = (P_{no}/P_n - 1)/P_{no} \qquad (2\text{-}5)$$

where P_{no} and P_n are the number-average degree of polymerization of PVAc

before and after the saponification, respectively. The values of M_w, P_{no}, P_n and d, are tabulated in Table 2-VIII. As shown in this table, the value of d for most fractions was approximately 1.5×10^{-4}.

TABLE 2-VIII

THE MOLECULAR WEIGHT AND DEGREE OF BRANCHING FOR BRANCHED POLYVINYL ACETATE SAMPLES

Sample	$M_w \times 10^{-4}$	$P_{no} \times 10^{-4}$	$P_n \times 10^{-3}$	$d \times 10^4$
S11	443	-	-	-
F11	389	3.07	5.37	1.54
S121	335	-	-	-
S131	253	-	-	-
F12	252*	1.90	4.71	1.60
F13	228	1.69	4.61	1.52
F15	182	1.30	4.29	1.40
F16	181*	1.29	4.29	1.55
S21	180	-	-	-
F171	145	1.00	4.17	1.40
F21	128*	-	-	-
S122	80.5	-	-	-
S22	58.6*	-	-	-
S132	50.2	-	-	-
F110	49.1	0.285	1.97	1.57
F22	29.2*	-	-	-
F192	26.3	0.138	1.05	2.27
F23	9.68	-	-	-

* Measured by the light scattering.

2.2.4 Solution Samples

The polymer solutions employed in this study are not the dilute but the moderately concentrated and concentrated solutions. The terminology "concentrated" means that the entanglement couplings in the solution are fully developed, and "moderately concentrated" does the intermediate region between "dilute" and "concetrated", as defined in Section 4.1.

Polyvinyl acetates, polystyrenes and polymethyl methacrylates are used as the solute polymers. Many solvents are employed, such as methyl ethyl ketone (MEK) and ethyl n-butyl ketone (EBK) for PVAc, toluene (T), decalin (D), diethyl phthalate (DEP) and partially chlorinated diphenyls (KC4 and KC5)* for polystyrene, and DEP for PMMA. Among these combinations of polymer-solvent, PVAc-EBK at 29°C and PS-D at 15°C are, respectively, exactly and very closely in θ-conditions. This decalin contained cis and trans isomers in the ratio of 38.5 : 61.5, as determined from gas chromatography.

To prepare polymer solutions in highly viscous solvents, such as DEP, KC4 and KC5, the suitable mixture of the polymer and the solvent was first dissolved in light solvent, such as benzene and dichloroethane, and the light solvent was removed by evaporation from thin film of the solution. For the preparation of the other solutions, polymer was directly dissolved in the solvent by stirring. The solution series, their solute polymers and solvents are given in Table 2-IX. Here, SC and MC denote the solutions of anionic polystyrenes and radical polymethyl methacrylates, respectively.

TABLE 2-IX

THE SOLUTE POLYMERS, THEIR MOLECULAR WEIGHTS AND THE SOLVENTS FOR SOLUTION SAMPLES

Series	Polymer	$M_w \times 10^{-4}$	Solvent
SC1	L26(PS)	58.5	DEP
SC2	L50(PS)	29.8	KC5
MC1	715(PMMA)	19.1	DEP
MC2	714(PMMA)	22.9	DEP

2.2.5 Blend Samples

The blend samples of anionic polystyrenes, as well as those of

* KC4 and KC5 are different in the degree of chlorination.

radical polymethyl methacrylates were employed for measurements of the rheological properties of polymer blends. The blending of the component polymers was carried out by dissolving suitable mixtures of two or three components in benzene at about 30% concentration accompanied by shaking. The solvent was removed by freeze-drying and in a vacuum oven at 60°C. In Table 2-X, are shown the weight-average molecular weights of the components, M_1 and M_2, and the ratio for binary blend series. The subscripts 1 and 2 denote the lower and higher molecular weight components, respectively. The only one ternary blend sample, BT1 contains equal amounts of L18, L16 and L9. In this table, BB and MB denote the blends of anionic polystyrenes and polymethyl methacrylates, respectively.

TABLE 2-X

THE MOLECULAR WEIGHTS OF THE COMPONENT POLYMERS AND THE RATIO FOR BINARY BLEND SERIES

Series	$M_1 \times 10^{-4}$	$M_2 \times 10^{-4}$	M_2/M_1
BB1	5.87(L16)	58.1(L18)	9.90
BB2	21.5 (L15)	35.1(L5)	1.63
BB3	4.69(L34)	16.7(L27)	3.56
BB4	10.4 (L46)	73.8(L45)	7.10
BB5	3.65(L33)	76.2(L44)	20.9
BB6	1.05(L53)	102 (L48)	97.1
BB7	13.7 (L47)	29.8(L50)	2.18
BB8	9.42(L60)*	56.5(L56)	6.00
MB1	5.21(910)	17.4(702)	3.34
MB2	4.10(MS)	17.4(702)	4.24

* Evaluated from GPC.

The weight-average molecular weight of the blend sample $\bar{M}$ was calculated by

$$\bar{M} = w_1 M_1 + w_2 M_2 \qquad (2\text{-}6)$$

where M_1 and M_2 are the weight-average molecular weights, and w_1 and w_2 are the weight fractions of the low and high molecular weight components, respectively.

The gel permeation chromatograms of blends are shown in Figs. 2-2 and 2-3. The blend sample BB25 is composed of equal amounts of two components and the weight fraction of the high molecular weight component in the BB3 series varies from 0.8 to 0.2. The molecular weight distributions of the components are completely separated from each other for BB3 series, but not for BB25.

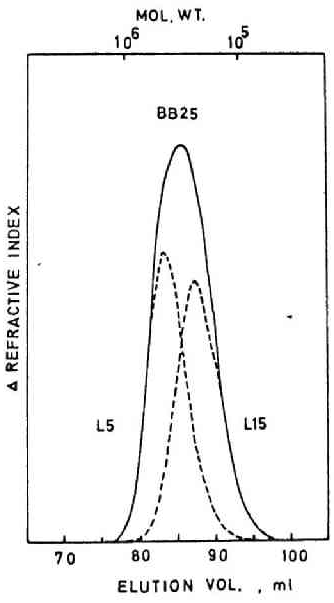

FIG.2-2. Gel permeation chromatograms for the BB25 and the components. The scale of the refractive index is arbitrary.

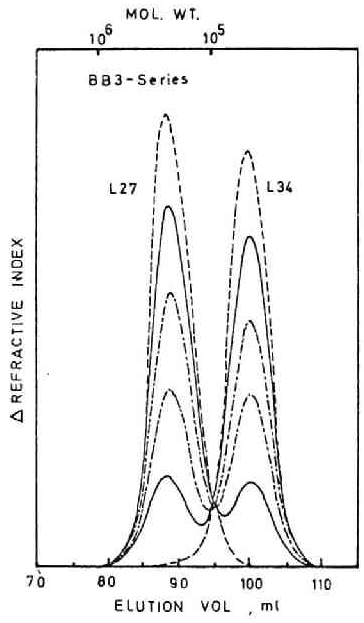

FIG.2-3. Gel permeation chromatograms for the BB3 series and the components. The scale of the refractive index is arbitrary.

2.3 EXPERIMENTAL METHODS

2.3.1 Concentric Cylinder Rheometer

The concentric cylinder-type rheometer[13] was used to measure the storage and loss modulus , G' and G", the dynamic viscosity η' and apparent viscosity (= non-Newtonian viscosity $\eta(\kappa)$). A merit of this rheometer is that it can be used as a torsionally oscillating rheometer or a Couette-type viscometer by a minor change in the driving system. Another merit is that the oscillation and rotation of the outer and/or inner cylinders during the measurements are changed into electric potential by means of a differential transformer device, and after being amplified are recorded on a X-Y recorder.

The thermostat has been designed to keep temperature constant from room tremperature to 300°C, and inert gas flows under a slight positive pressure through a spiral pipe in the thermostat over the surface of the sample in order to minimize chemical degradation at higher temperatures. By using many torsion wires and bobs having different diameters, a very wide range of rheological properties can be measured. The frequency and number of revolutions of the cup range from 5×10^{-4} to 1 Hz and from 0.122 to 240 rpm, respectively.

When the rheometer is used as a torsionally oscillating rheometer, the complex viscosity η^* can be evaluated from the following equation, which is a reduced form of a general equation given by Markovitz[14]:

$$\eta^* = \frac{[(A_1 + B_1\rho)\omega - C_1/\omega][\sin\phi/m - i(1 - \cos\phi/m)]}{(\sin\phi/m)^2 + (1 - \cos\phi/m)^2} \qquad (2\text{-}7)$$

where A_1, B_1 and C_1 are apparatus constants, ω is the angular frequency, m is the amplitude ratio, ϕ is the phase angle between the cup and bob, ρ

is the density of the sample, and $i = \sqrt{(-1)}$.

When the rheometer is used as a Couette-type viscometer, the flow curves of non-Newtonian liquids can be determined accurately by the single-bob method proposed by Krieger and Maron[15]. The reciprocal of the apparent viscosity η_a is given by the following equation:

$$1/\eta_a = f(\sigma)/\sigma = \Phi_\alpha[1 + k_1(\frac{d\log\Phi_\alpha}{d\log\sigma}) + k_2(\frac{d\log\Phi_\alpha}{d\log\sigma})^2] \qquad (2\text{-}8)$$

where

$$k_1 = \frac{\alpha^2 - 1}{2\alpha^2}(1 + \frac{2}{3}\ln\alpha) \qquad (2\text{-}9)$$

$$k_2 = \frac{\alpha^2 - 1}{6\alpha^2}\ln\alpha \qquad (2\text{-}10)$$

and

$$\sigma = T/2\pi R_1^2 L \qquad (2\text{-}11)$$

$$\Phi_\alpha = \frac{2\Omega}{\sigma[1 - (1/\alpha^2)]} \qquad (2\text{-}12)$$

where $f(\sigma)$ is the rate of shear ($= \kappa$), σ and T are the shear stress and torque at the wall of the bob, respectively. Ω is the angular velocity of rotating cup and α the ratio of the radii of the bob to the cup. Φ_α is often called the apparent fluidity.

2.3.2 Capillary Viscometers

Two types of capillary viscometers are utilized in this study. One is the Maron-Krieger-Sisko viscometer[16], which was used for measurements of zero-shear viscosity for polymer solutions of low viscosity. The other is a variable-pressure capillary rheometer, very similar to the Merz-Colwell Extrusion (Instron type) Rheometer[17], which was used for meassuring the non-Newtonian viscosity of polymer melts and highly viscous solutions.

The non-Newtionan viscosity η_a can be calculated by the following equations[15]:

$$1/\eta_a = f(\sigma)/\sigma = \Phi_\alpha[1 + \frac{1}{4}(\frac{d\log \Phi_\alpha}{d\log \sigma})] \tag{2-13}$$

$$\sigma = \Delta PR/2L \tag{2-14}$$

$$\Phi_\alpha = 8LQ/\pi R^4 \Delta P \tag{2-15}$$

where ΔP is the pressure drop throughout the capillary tube, Q the volumetric flow rate, and R and L are the radius and the length of the capillary. The other notations are the same as for the concentric cylinder rheometer.

2.3.3 Flow Birefringence

Flow birefringence technique has been employed here, to evaluate the first normal stress difference, $\sigma_{11} - \sigma_{22}$, of the moderately concentrated solutions.[18,19] The value of $(\sigma_{11} - \sigma_{22})$ is connected with the extinction angle χ by eq(1-45). In this study was used the Edsall-Rao type flow birefringence apparatus[20], which was manufactured by Rao Instrument Co., and whose optical alignment is illustrated in Fig.2-4. This apparatus enables one to obtain the extinction angle χ and the birefringence Δn as the functions of the rate of shear. The extinction angle can be measured directly and the birefringence is calculated by the following well-known equation:

$$\Delta n = (\delta/2\pi)(\lambda/L) \tag{2-16}$$

where δ is the phase difference, λ the wave length (550mμ, here) and L is the height of the cylinders (10cm, here). The measuring technique and the details of the apparatus have appeared elsewhere.[19-21]

The correspondence of stress and the flow birefringence parameters, for example eq(1-45), is based on the following assumptions:

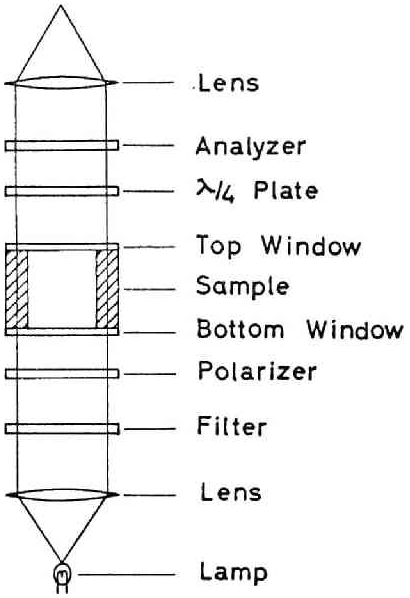

FIG.2-4. The optical alignment of the flow birefringence apparatus.

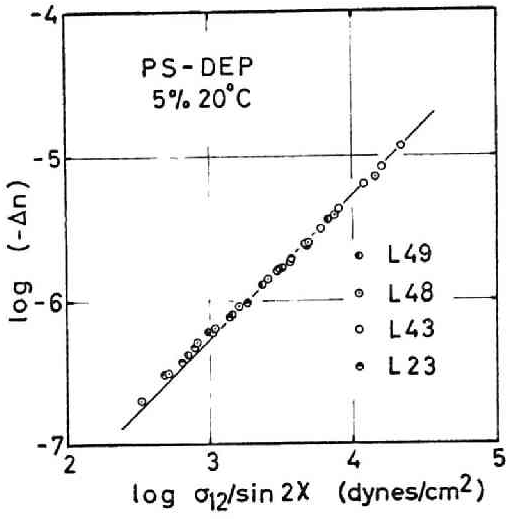

FIG.2-5. Logarithm of birefringence plotted against $\log(\sigma_{12}/\sin 2\chi)$, to test the stress-optical law.

(1) The stress-optical coefficient, C, is independent of stress, and (2) the principal axis of the stress-ellipsoid coincides with that of the refractive index-ellipsoid. These principles are called " stress-optical law" and can be expressed using the constant stress-optical coefficient,[18, 22]

$$C = |\Delta n|/\Delta\sigma \tag{2-17}$$

as

$$|\Delta n|\sin 2\chi = 2C\sigma_{12} \tag{2-18}$$

$$|\Delta n|\cos 2\chi = C(\sigma_{11} - \sigma_{22}) \tag{2-19}$$

The stress-optical law can be easily tested by plotting $\log(|\Delta n|)$ against $\log(\sigma_{12}/\sin 2\chi)$. An example is shown in Fig.2-5 measured for 5% DEP solutions of polystyrenes. The slope of the straight line is just unity, indicating the validity of the stress-optical law. The intercept of the line furnishes

the value of the stress-optical coefficient. The experiments for various solution samples show that the stress-optical law is valid and the stress-optical coefficient is independent of molecular weight and its distribution, but it slightly increases with concentration. The values of C at 5% are 2715 and 5800 Br (Brewster = 10^{-13} cm^2/dyne) for PS-DEP and PS-KC4 systems, respectively. The latter value agrees very well with the literature value[23].

REFERENCES

1. M. J. R. Cantow,Ed., "Polymer Fractionation", Academic Press, New York, 1967.
2. L. Reich and A. Schindler, "Polymerization by Organo-metallic Compounds", Interscience, New York, 1966, Chapter VII.
3. T. Oyama, K. Kawahara, and M. Ueda, J. Chem. Soc. Japan (Pure Chem. Sect.) 79, 727 (1958)
4. (a) M. Moton, P. Milkovich, D. B. McIntyre, and L. J. Bradley, J. Polym. Sci., Part A, 1, 443 (1963)
   (b) M. Moton. A. A. Rembaum, and J. L. Hall, J. Polym. Sci, Part A, 1, 461, (1963)
5. T. Altares, Jr., D. P. Wyman, and V. R. Allen, J. Polym. Sci., Part A, 2, 4533 (1964)
6. G. V. Schulz, H. J. Cantow, and G. Meyerhoff, J. Polym. Sci., 10, 79 (1953)
7. F. A. Bovey and G. V. D. Tiers, J. Polym. Sci., 44, 173 (1960)
8. G. Natta, J. Polym. Sci., 16, 143 (1955)
9. R. L. Miller and L. E. Nielsen, J. Polym. Sci.,46, 303 (1960)
10. M. Matsumoto and Y. Oyanagi, J. Polym. Sci., 46, 441 (1960)
11. M. Matsumoto and M. Maeda, Kobunshi Kagaku, 12, 428 (1955)

12. (a) S. Tsuchiya, Y. Sakaguchi, and I. Sakurada, Kobunshi Kagaku, 18, 346 (1961)

(b) D. J. Stein and G. V. Schulz, Macromol. Chem., 52, 249 (1962)

13. M. Horio, S. Onogi, and S. Ogihara, J. Japan Soc. Testing Mater., 10, 350 (1961)

14. (a) H. Markovitz, J. Appl. Phys., 23, 1070 (1952)

(b) H. Markovitz, P. M. Yavorsky, R. C. Harper, Jr., L. J. Zapas, and T. W. DeWitt, Rev. Sci. Instr., 23, 430 (1952)

15. (a) I. M. Krieger and S. H. Maron, J. Appl. Phys., 23, 147 (1952)

(b) I. M. Krieger and S. H. Maron, J. Appl. Phys., 25, 72 (1954)

16. S. H. Maron, I. M. Krieger, and A. W. Sisko, J. Appl. Phys., 25, 971 (1954)

17. J. R. VanWazer, J. W. Lyons, K. Y. Kim, and R. E. Colwell, "Viscosity and Flow Measurement", Interscience; New York, 1963, p.231.

18. (a) A. S. Lodge, Trans. Faraday Soc., 52, 127 (1956)

(b) A. S. Lodge, Nature, 176, 838 (1955)

19. H. Janeschitz-Kriegl, Adv. Polym. Sci., 6, 170 (1960)

20. R. Cerf and H. A. Scheraga, Chem. Rev., 51, 185 (1952)

21. V. N. Tsvetkov, "Newer Methods of Polymer Characterization", B. Ke, Ed., Interscience, New York, 1964, Chapter XIV.

22. W. Philippoff, Nature, 178, 811 (1956)

23. W. Philippoff, Proc. 4th Intern. Congr. Rheology, Part 2, Interscience, New York, 1965, p.343.

CHAPTER 3

Rheological Properties of Polymer Melts

3.1 INTRODUCTION

The rheological properties of polymer melts are important in connection with understanding their internal structure and also with improving their processing such as in the melt spinning process in the textile industry and in the molding process in the plastics industry, and therefore have been studied by many authors.[1] These studies have provided much information about the molecular motion of polymer chains under shear and the relationships to processability. Especially, there are many indications that the elasticity manifested by polymer melts is a more significant factor in the processability than the viscosity. Many of the characteristic phenomena of polymer melts, such as spinnability, the Weissenberg effect, the swelling (or Barus) effect and melt fracture, which are encountered in polymer processes, are all connected with elasticity.

Another purpose of such studies was to generalize the effect of entanglement couplings. However, it was impossible to clarify fully the true nature of the entanglements, mainly because the samples employed in these studies had rather broad molecular weight distributions, even when some of them were fractionated.

In the present chapter, viscoelastic properties have been measured for various polymeric materials, such as polyvinyl acetates (PVAc), polymethyl methacrylates (PMMA) and polystyrenes (PS), in molten state over wide ranges of temperature and frequency. First, preliminary experimental

results for fractions of PVAc and PMMA melts are given and the general features of the effects of temperature, molecular weight, molecular weight distribution and branching, are presented. In the succeeding sections, the molecular weight dependence of zero-shear viscosity, steady-state compliance, and the shear modulus characteristic of entanglement networks are evaluated quantitatively and discussed for narrow-distribution polymers. The current molecular theories for entanglement couplings are discussed on the basis of these experimental results. The temperature and molecular weight dependences of the shift factor are also discussed; in addition, the parameters having to do with the free volume, such as the Vogel temperature and the temperature coefficient of the fractional free volume, are presented for the narrow-distribution polymers.

3.2 THE PRELIMINARY EXPERIMENTAL RESULTS OF RHEOLOGICAL PROPERTIES OF POLYMER MELTS

3.2.1 Effect of Temperature

The dynamic viscosity and rigidity curves illustrated in Fig.3-1 for PMMA fraction 703 (see Table 2-IV) at five temperatures can be superposed by the shift along a straight line having the slope of -1 and along the abscissa, respectively, giving master curves shown in Fig.3-2. The reference temperature of the superposition is arbitrarily chosen as 220°C. The values of the shift factor log a_T, determined from the data of η' and G' are substantially the same, and moreover, they are independent of the molecular weight, excepting PMMA fractions 913 and 914 having extremely low molecular weights.

The temperature dependence of log a_T can well be represented by the following WLF-type equations over the entire range of temperature:

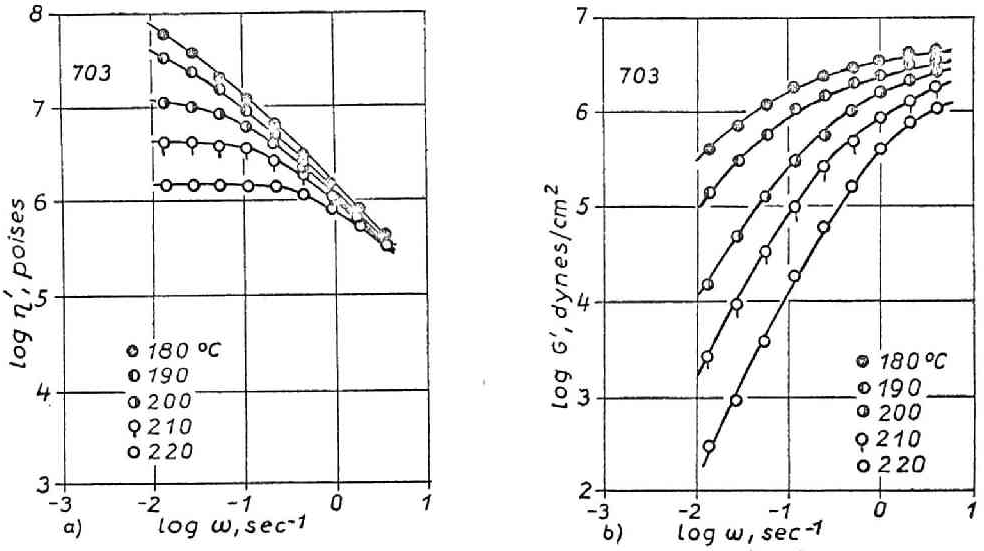

FIG.3-1. Dynamic viscosity η' and rigidity G' plotted against angular frequency ω for PMMA fraction 703 at different temperatures.

$$\log a_T = \frac{-18.25(T - T_g)}{121.9 + (T - T_g)} \qquad (\text{PMMA}, T_g = 105^\circ\text{C}) \qquad (3\text{-}1)$$

$$\log a_T = \frac{-17.09(T - T_g)}{49.1 + (T - T_g)} \qquad (\text{PVAc}, T_g = 32^\circ\text{C}) \qquad (3\text{-}2)$$

In Figs.3-3 and 3-4, $\log a_T$ for PMMA and PVAc is plotted against the difference of temperature from T_g. The solid lines in these figures show the calculated values from above equations and the circles experimental ones.

The numerical constants, c_1^g and c_2^g can be related with the fractional free volume at T_g, according to eq(1-80):

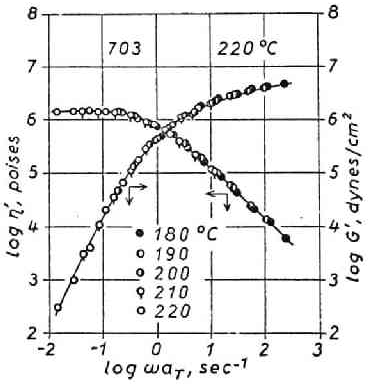

FIG.3-2. Master curves of η' and G' for PMMA 703. The reference temperature is 220°C.

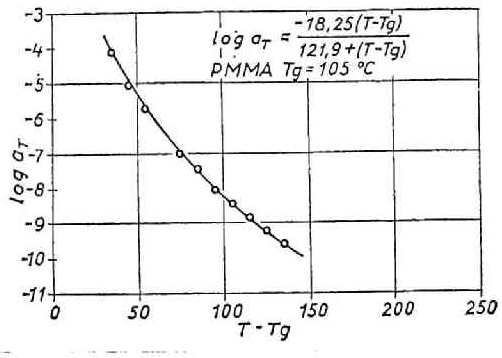

FIG.3-3. Log a_T plotted against $(T - T_g)$ for the radical PMMA. T_g is assumed to be 105°C.

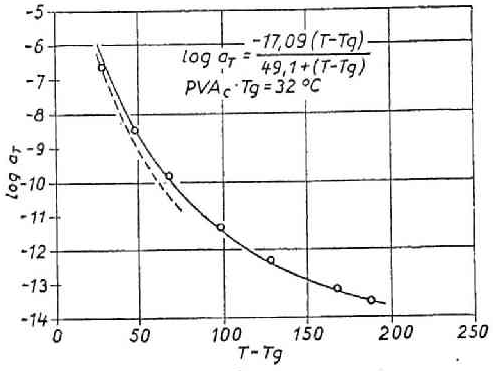

FIG.3-4. Log a_T plotted against $(T - T_g)$ for PVAc. T_g is assumed to be 32°C.

$$f_g = 1/2.303\ c_1^g \tag{3-3}$$

$$\alpha_f = 1/2.303\ c_1^g\ c_2^g \tag{3-4}$$

The values of f_g evaluated from eq(3-3) for PMMA and PVAc are respectively 0.024 and 0.025, showing good agreement with the well-known value of 0.025 [1,2]. The values of α_f evaluated from eq(3-4) for PMMA and PVAc are respectively, 1.95×10^{-4} and 5.16×10^{-4} deg^{-1}.

3.2.2 A Comparison of Dynamic Viscosity with Steady-State One

Previously, the dynamic viscosity η' was compared with the apparent viscosity η_a for the melts of polystyrenes, polyethylenes and polypropylenes by Onogi et al.[3,4] The conclusion was that the experimental results did not coincide with those predicted by several current theories but accorded with the empirical law of Cox and Merz.[5] A similar comparison has been attempted for PMMA and PVAc. Figs. 3-5 and 3-6 show the result of the comparison for PMMA fraction 905 and PVAc fraction H122. As seen from these figures, η_a plotted against the rate of shear κ coincides with the

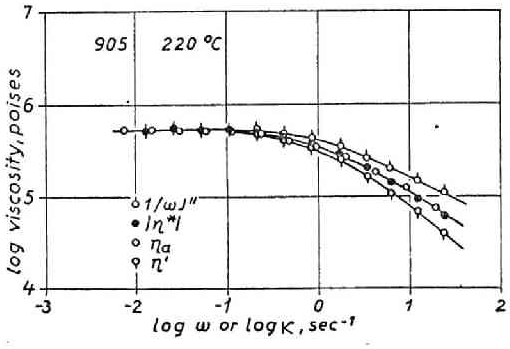

FIG.3-5. A comparison of η_a with η', $1/\omega J''$ and $|\eta^*|$ for the PMMA 905 at 220°C.

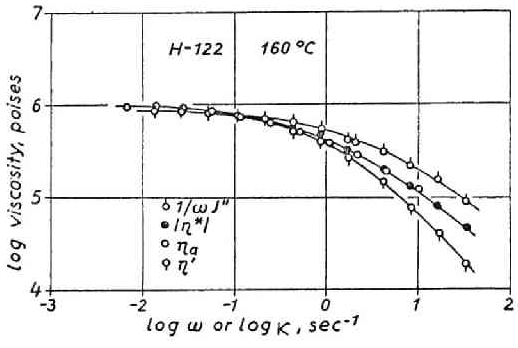

FIG.3-6. A comparison of η_a with η', $1/\omega J''$ and $|\eta^*|$ for the PVAc H122 at 160°C.

absolute value of complex viscosity $|\eta^*|$ plotted against the angular frequency ω. These figures indicate that here again the empirical law proposed by Cox and Merz is best of all the theories just as in the case of polyethylene and polystyrene. The curve of η' decreases more rapidly and that of $1/\omega J''$ does so less rapidly than the η_a curve, indicating that the theories of DeWitt[6] and Pao[7] are not suitable at least for the melts of PMMA and PVAc.

3.2.3 Effect of Molecular Weight

In Fig.3-7, the master curves of η' at the reference temperature of 220°C are given for fourteen fractions of the radical PMMA differing in their molecular weights from each other. As seen from this figure, η' at lower frequencies depends very strongly upon the molecular weight, while it becomes less sensitive to the molecular weight at higher frequencies. Moreover, the viscosity curves for the samples having molecular weights higher than a certain critical value M_d, unite into one curve at angular frequency of about 10^3 sec^{-1}. The slope of this united curve is equal to

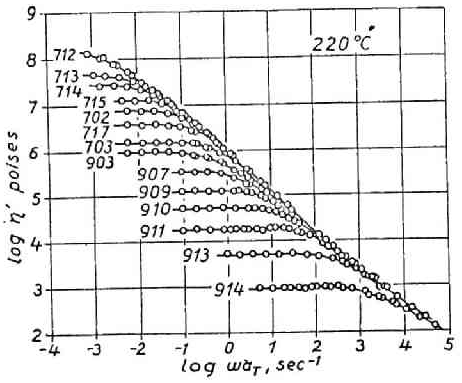

FIG.3-7. Master curves of η' for the radical PMMA samples having different molecular weights at 220°C.

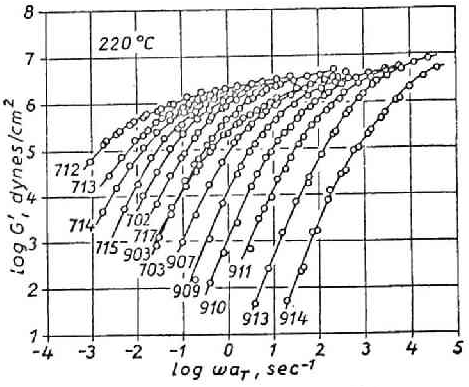

FIG.3-8. Master curves of G' for the radical PMMA samples having different molecular weights at 220°C.

-1/2, and this slope is the same as predicted from the Rouse theory. On the other hand, the viscosity curve for the sample having molecular weight lower than M_d, the sample 914, joins the united curve at a much higher frequency.

The corresponding rigidity curves for the same samples are shown in Fig.3-8. Here again, the effect of molecular weight is very pronounced only at lower frequencies. It is noteworthy in this figure that the rigidity curves do not unite into one even at higher frequencies than where the viscosity curves come together.

These results are very suggestive to us, because they indicate that at higher frequencies various polymers having different molecular weights and the distributions cannot be distinguished from each other by their viscosities alone; the polymers show difference only in their rigidities. When various polymers of the same kind manifest different processabilities at higher rate of shear or frequencies as in the case of melt spinning and molding of plastics, the difference in the processability can be ascribed to the difference in the elastic properties than the viscous ones.

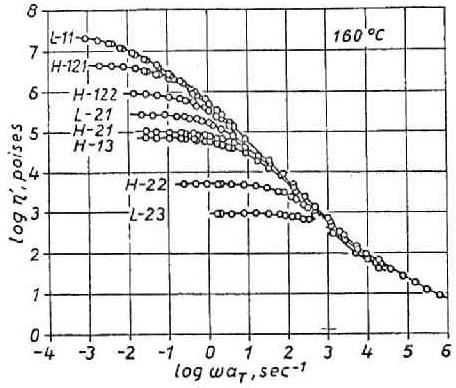

FIG.3-9. Master curves of η' for the PVAc samples having different molecular weights at 160°C.

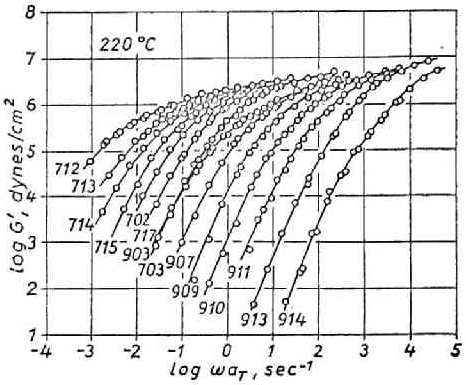

FIG.3-10. Master curves of G' for the PVAc samples having different molecular weights at 160°C.

In Fig.3-9 and Fig.3-10 are shown master curves of η' and G' for the eight fractions of PVAc at reference temperature of 160°C. The viscosity and rigidity curves in these figures have similar features to those for PMMA discussed above. The viscosity curves unite into one curve at angular frequency of about $10^3 sec^{-1}$, but the rigidity still differs greatly from sample to sample at the same frequency. The fraction H13 shows quite different frequency dependences of η' and G' from fraction H21, suggesting that the former is likely to have a broader distribution of molecular weight than the latter. Such a phenomenon was first observed by Onogi et al. in the study of viscoelasticity of solutions of polyvinyl alcohol[8], and thereafter similar results on the effect of molecular weight distribution upon the rate of shear dependence of steady flow viscosity have been reported by several authors[9,10] This problem will discussed in detail in Chapter 5 again.

The M_d value seems to be very close to the critical molecular weight M_c, which is generally accepted as a molecular weight at that a continuous

structure due to entanglements between molecular chains is formed in a polymer system.[11] Anyway the above mentioned M_d is considered to be the molecular weight that makes entanglement essential to the rheological properties.

3.2.4 Frequency Dependence of the Viscosity - Molecular Weight Relation

In Figs.3-11 and 3-12, log η' and log $|\eta^*|$ are respectively plotted against log M_w for PMMA samples using the angular frequency as the parameter. Figs.3-13 and 3-14 give similar plots for PVAc. As seen from Figs.3-11 and 3-12, the curves for log η' and log $|\eta^*|$ at $\omega = 0$ for PMMA are straight and have the slope of 4.0, which is somewhat higher than the expected value of 3.5. On the other hand, the viscosity curves for PVAc in Figs.3-13 and 3-14 are straight only for molecular weights below 3.3×10^5. Above this limit of molecular weight, the curves are concave upwards, and the

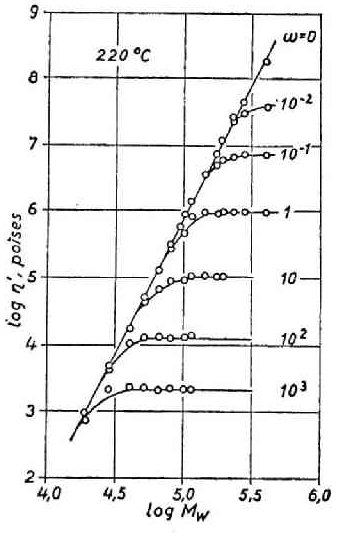

FIG.3-11. Log η' versus log M_w at different angular frequencies for PMMA at 220°C.

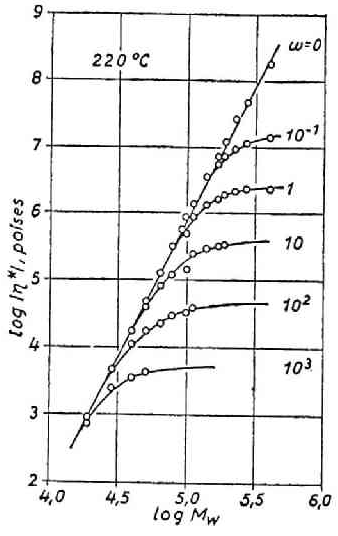

FIG.3-12. Log $|\eta^*|$ versus log M_w at different angular frequencies for PMMA at 220°C.

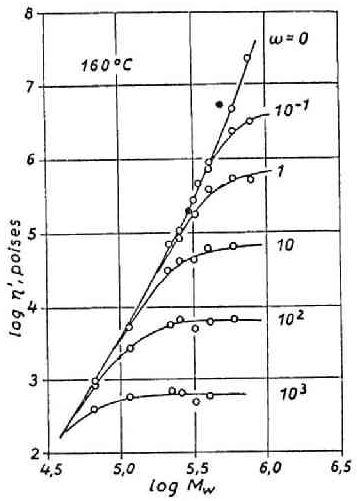

FIG.3-13. Log η' versus log M_w at different angular frequencies for PVAc at 160°C. The closed circles represent the branched PVAc.

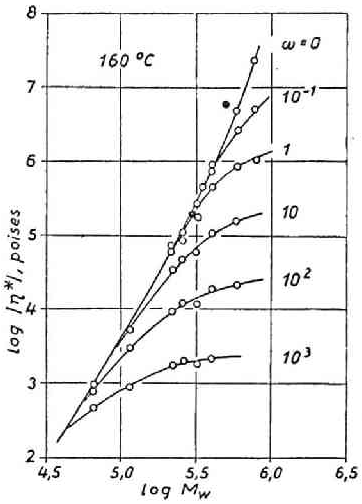

FIG.3-14. Log $|\eta^*|$ versus log M_w at different angular frequencies for PVAc at 160°C. The closed circles represent the branched PVAc.

slope increase from 3.5 to considerably high values. Quite a similar result for PVAc has been reported by Ninomiya et al.[12], though it was obtained at lower temperatures. Long et al.[13] have also reported the value of 3.65 for PVAc.

The viscosity vs. molecular weight curves at higher frequencies are not straight, and their slopes decrease gradually with increasing frequency. At very high frequencies, the curves for high molecular weight fractions are practically horizontal, as was previously found for polystyrenes[4]. Some results similar to those described above have been presented by a few authors.[9,14]

3.2.5 Effect of Blending of Two Fractions

The effect of blending of two components differing only in molecular

weight upon the rheological properties has been reported for polyethylene [15], polypropylene[16] and polystyrene[4]. So far as the range of frequency is not very high, log (η'/η_0) plotted against log ω for blends of two components could be superposed into a master curve by the shift in the horizontal direction by log a_M. On the other hand, log G' vs. log ω curves could be superposed by shifting them first horizontally by log a_M and then vertically by log c_M. The shift factors a_M and c_M depended not only upon the average molecular weight but also the molecular weight difference between the components. When the molecular weight difference was small, log a_M and log c_M bore straight-line relationship between log (η_2/η_b), where η_2 and η_b are respectively the zero-shear viscosity for the component and the blend.

The viscosity and rigidity curves for three blend samples of PMMA fractions 717 and 907 are shown in Figs.3-15 and 3-16. These curves have been superposed by the method described above, giving master curves in Fig.3-17.

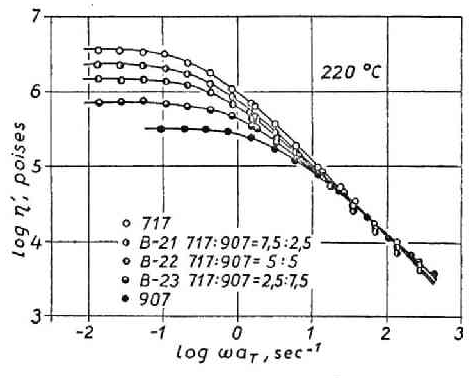

FIG.3-15. Master curves of η' for the blends of PMMA, and the components 717 and 907, at 220°C.

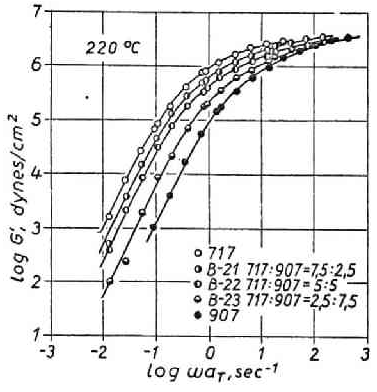

FIG.3-16. Master curves of G' for the blends of PMMA, and the components 717 and 907, at 220°C.

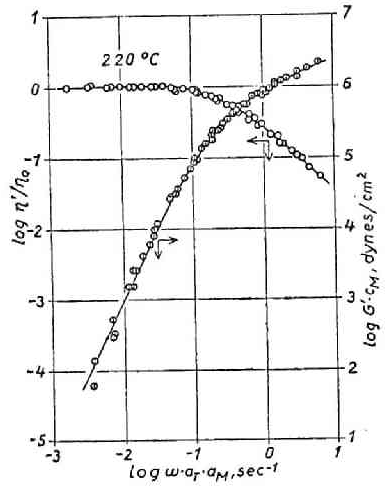

FIG.3-17. Master curves of η' and G' for the blends of PMMA samples, 717 and 907, having different compositions. The reference component is the sample 717.

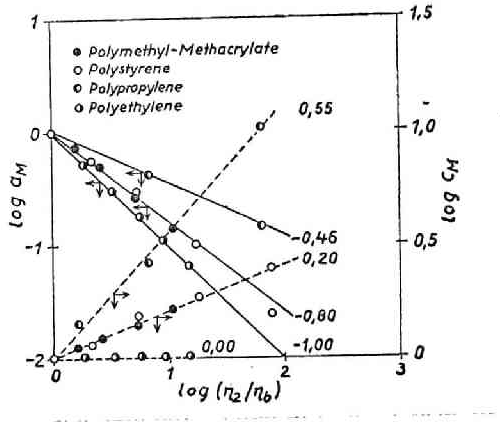

FIG.3-18. Log a_M and log c_M plotted against log (η_2/η_b) for polyetyrene, polypropylene, polystyrene and PMMA.

The compositions in the blend samples are as indicated in the figures. The reference component is the higher molecular weight fraction 717. The variation of the shift factors, a_M and c_M, with the viscosity ratio η_2/η_b for the same systems is compared with those for other materials in Fig.3-18. It is clear that the a_M corresponds to the shift in the viscoelastic time constants by blending, and has the same meaning as the parameter λ_2 in the Ninomiya theory for binary blend[12]. Furthermore, c_M is equal to the ratio of the steady-state compliance for the blend, J^0_{eb}, to that for the component, J^0_{e2}.

In Figs.3-19 and 3-20, are shown the frequency dependences of viscoelastic functions for the blend samples, B11, B12 and B13, and their components, as well as a radical PMMA sample 703. B11, B12 and B13 contain

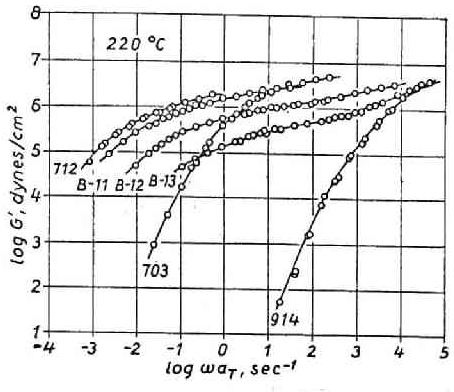

FIG.3-19. Master curves of G' for the blends of PMMA, the components 712 and 914, and a radical PMMA 703 at 220°C.

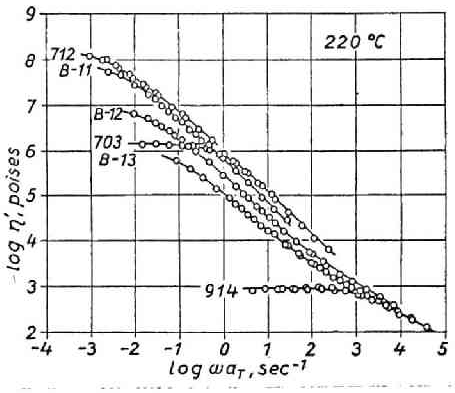

FIG.3-20. Master curves of η' for the blends of PMMA, the components 712 and 914, and a radical PMMA 703 at 220°C.

the higher molecular weight component 712, by 75, 50 and 25%, respectively. These blends containing the highest molecular weight fraction give somewhat abnormal viscosity and rigidity curves. When one compares the curves for blend B13 with those for fraction 703 having almost the same M_w, the effect of bimodal distribution will be definite.

These results show that the frequency dependence of viscoelastic properties depends intensively upon the molecular weight distribution. Therefore, the generalization of the frequency (as well as rate of shear) dependence of the viscosity[17~20], will be non-sense unless the molecular weight distribution of all the samples is the same.

The relaxation spectra calculated by the so-called zero-order approxima-

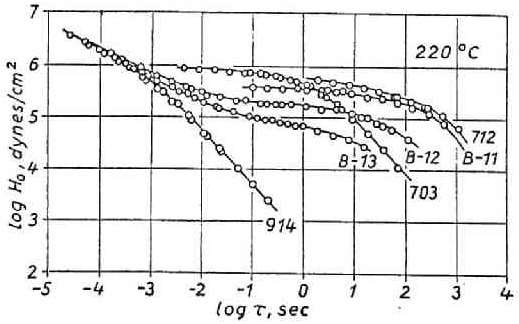

FIG.3-21. Relaxation spectra for the blends of PMMA, the components 712 and 914, and a radical PMMA 703, at 220°C.

tion for the blend of bimodal distribution are compared with those for the components and other fraction in Fig.3-21. As the content of the lower molecular weight component increases, the longest relaxation time of the blends becomes shorter than that for the higher molecular weight component. At the same time, the intensity of the spectra in rubbery region decreases because of the dilution effect by the lower molecular weight component.

These interesting behavior of the binary blends of polymers will be discussed further in detail and a complete interpretation will be given in Chapter 5, on the basis of the experimental data for very narrow-distribution polymers and their blends.

3.2.6 Effect of Branching

One of the well-known effects of branching on the flow properties of polymer liquids is that branched polymers manifest lower viscosities than linear ones having the same molecular weights[21-24]. Some other investigations[13,25], however, showed that branched polymers gave rather higher viscosities than linear ones. Another effect of branching is greater dependences of the viscosity upon molecular weight and conentration [22,26]. Such a behavior of branched polymers may be due to their liability to forming a somewhat different entanglment structure from that for linear polymers.

In Figs.3-22 and 3-23 are compared the frequency dependences of the viscoelastic functions for two samples of branched PVAc, F110 and F22, with those for linear PVAc, H121, H122 and H21. The molecular weights and other molecular parameters of the samples are listed in Table 2-VII and Table2-VIII. As seen from these figures, the branched samples show larger dependence of viscosity and smaller dependence of the rigidity upon frequency. The difference between the linear and branched polymers is also clear in their

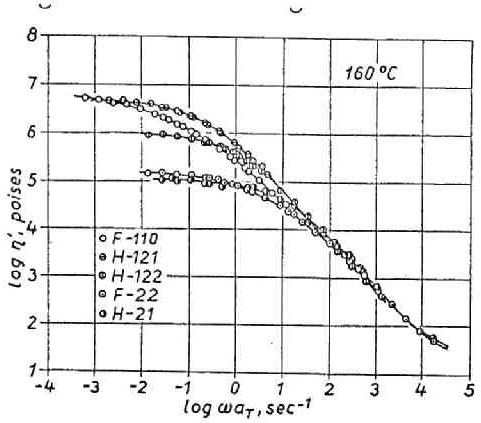

FIG.3-22. A comparioson of the frequency dependence of η' for the branched PVAc, F110 and F22, with that for the linear PVAc, H121, H122 and H21, at 160°C.

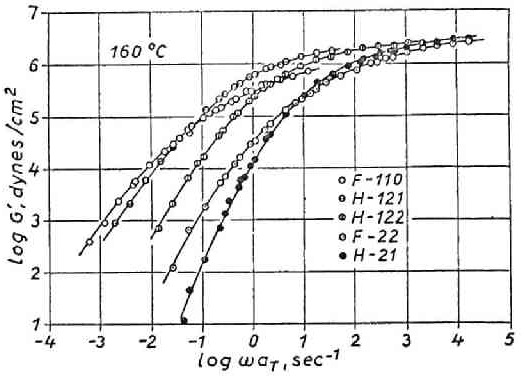

FIG.3-23. A comparison of the frequency dependence of G' for the branched PVAc, F110 and F22, with that for the linear PVAc, H121, H122 and H21, at 160°C.

relaxation spectra shown in Fig.3-24. The spectra for the branched samples are broader than the linear ones. The values of M_w/M_n of the linear PVAc H121 and H122 are respectively 1.71 and 2.68, but the viscosity and rigidity curves for these two samples are quite similar in their shape. In other words, H122 has not too broad a distribution to show abnormal frequency dependences of η' and G'. The branched fraction F22, on the other hand, has almost the same value of M_w/M_n as the above linear sample H122, but it shows apparently different curves from the linear samples. Therefore, it must be concluded that the abnormal behavior manifested by

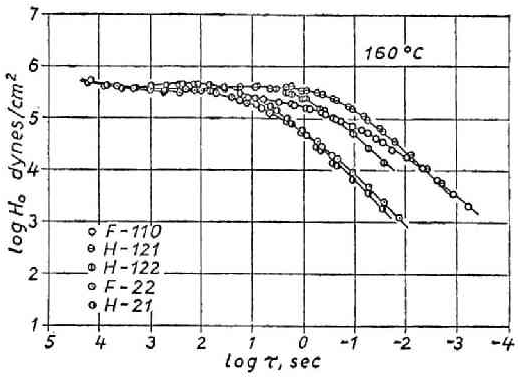

FIG.3-24. A comparison of relaxation spectra for the branched PVAc with those for the linear PVAc.

the branched polymers is no other than the effect of branching.

In Figs.3-13 and 3-14 are compared the zero-shear viscosity for the branched samples with those for linear ones with the closed circles. It is clear from these figures that the log-log polt of the viscosity against molecular weight for the branched polymers should have higher slope than the linear polymers[13,24,25].

More recently, very interesting investigations on the rheological properties of branched polymers have been extensively carried out by us and others[27~32]; the samples employed there are well chracterized with respect to the type of branching, and the number and length of the branches. Such a subject, however, is outside of this thesis and no more is described.

3.3 FREQUENCY DEPENDENCE OF VISCOELASTIC FUNCTIONS

Anionic Polystyrenes

In Fig. 3-25, the storage modulus G' at various temperatures is logarithmically plotted against the angular frequency for one of the anionic polystyrenes, L27, having molecular weight of 167,000, as an example. Such log G' vs. log ω curves as well as the similar curves for the loss modulus G" and dynamic viscosity η' at various temperatures can always be superposed into respective master curves by use of the time-temperature superposition principle.

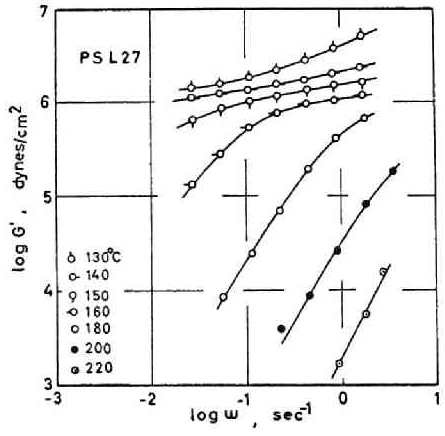

FIG.3-25. Frequency dependence of G' for anionic polystyrene L27 at various temperatures.

In Fig.3-26 are shown the master curves of G' for the narrow-distribution polystyrenes having different molecular weights. The abscissa of the figure is the reduced angular frequency ωa_T, and the reference temperature is 160°C. The molecular weights of the samples range from 581,000 (L18) to 8,900(L9)(see Table 2-II). As may be seen from this figure, the master curve includes not only the flow or terminal zone but also rubbery and glass transition zones. The terminal zone shifs progressively to the low frequency side and the rubbery plateau becomes longer and longer as the molecular weight increases. The samples having very low molecular weights, such as L14, L12 and L9, do not manifest the rubbery plateau. The height of the rubbery plateau for the samples of higher molecular weights seems to be independent of molecular weight, and has a value of about 2.0×10^6 dynes/cm^2. The G' curves for high molecular weight samples unite in the transition zone, while those for low molecular weight samples do not unite but shift to the high frequency side because of the excess free volume, as will be discussed later. Each G' curve shows a very sharp transition from the rubbery to the terminal zone, where the curve has the slope of 2.0. The extremely flat rubbery plateau and the very sharp rubbery-flow transition are chracteristic features most remarkable in the narrow-distribution polymers.

Fig.3-27 shows master curves of G" for the same samples as in Fig.3-26. The reference temperature is 160°C here again. The shift factors a_T determined in the course of the time-temperature superposition of the G" curves are the same as those for G'. As is evident from Fig.3-27, the effect of molecular weight on G" also very marked. For the samples having molecular weights higher than the 167,000 of L27, the G" curve

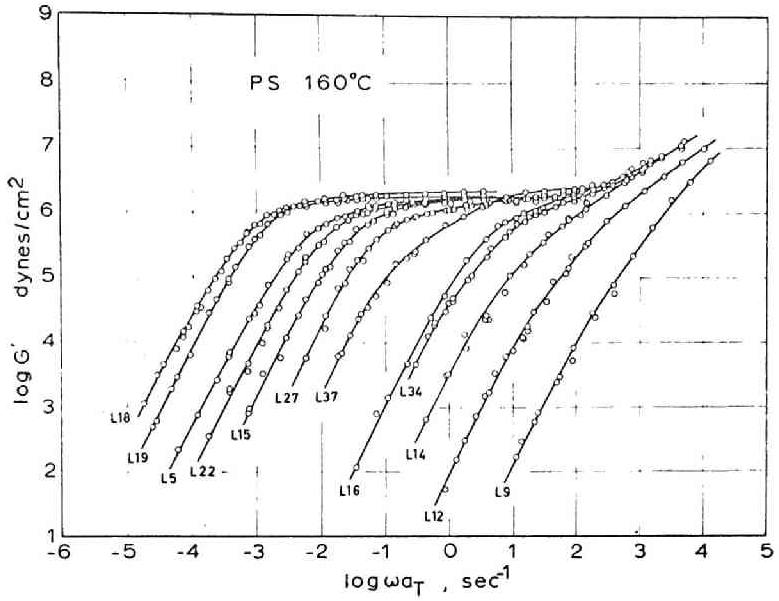

FIG.3-26. Master curves of G' for narrow-distribution (anionic) polystyrenes having different molecular weights. The reference temperature is 160°C.

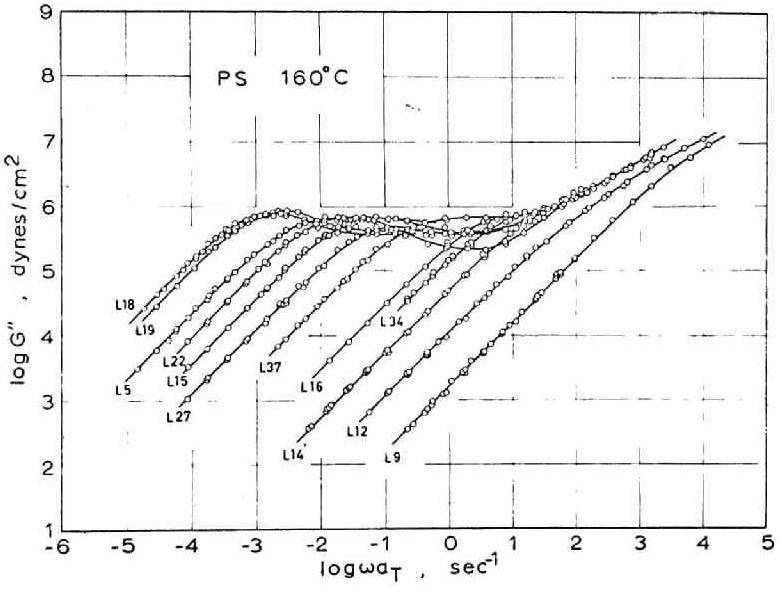

FIG.3-27. Master curves of G'' for narrow-distribution (anionic) polystyrenes having different molecular weights. The reference temperature is 160°C.

shows a peak at the low frequency end of the rubbery zone. This indicates that narrow-distribution polystyrenes having very high molecular weight have two sets of relaxation times corresponding to two relaxation mechanisms separated in the time scale. The two sets of relaxation times, of course, correspond to the glass transition in the high frequency region, which is not fully observed in this study, and the entanglement slippage in the low frequency region, which appears as a peak of the G" curve in Fig.3-27. For polymers such as L37, L16 and L34 having molecular weights low but higher than the critical molecular weight M_c, the above two sets of relaxation times approach and overlap each other, and hence the peak in G" disappears and only a plateau can be observed.

Anionic Polymethyl Methacrylates

In Figs.3-28 and 3-29 are shown, respectively, the master curves of the storage shear modulus G' and loss modulus G" for the anionic PMMA samples having different molecular weights. The reference temperature is 220°C. The molecular weight of the samples ranges from 342,000 to 11,400 (see Table 2-V). As seen from these figures, the master curves also include not only the terminal and rubbery zones but the long time end of glass transition zone. In the terminal zone, the G' and G" curves have, respectively, the slopes of 2.0 and 1.0, and shift to the low frequency side and the rubbery plateau becomes longer and longer as the molecular weight increases.

All G' and G" curves unite in the glass transition zone, excepting those for the sample MF13 having low molecular weight. The G' curves for the samles having higher molecular weights manifest the rubbery plateau, whose intensity is about 3~6 x 10^6 dynes/cm^2. The rubbery

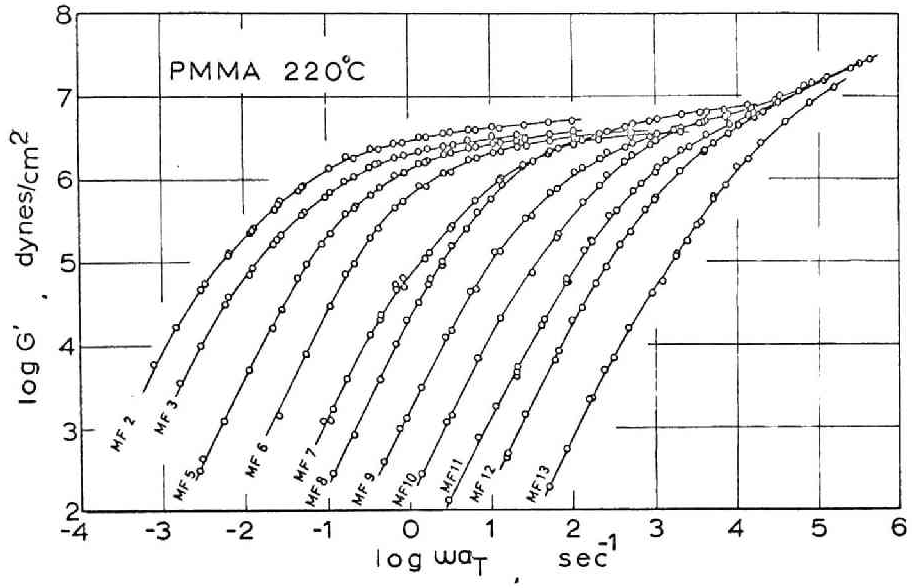

FIG.3-28. Master curves of G' for the anionic PMMA having different molecular weights. The reference temperature is 220°C.

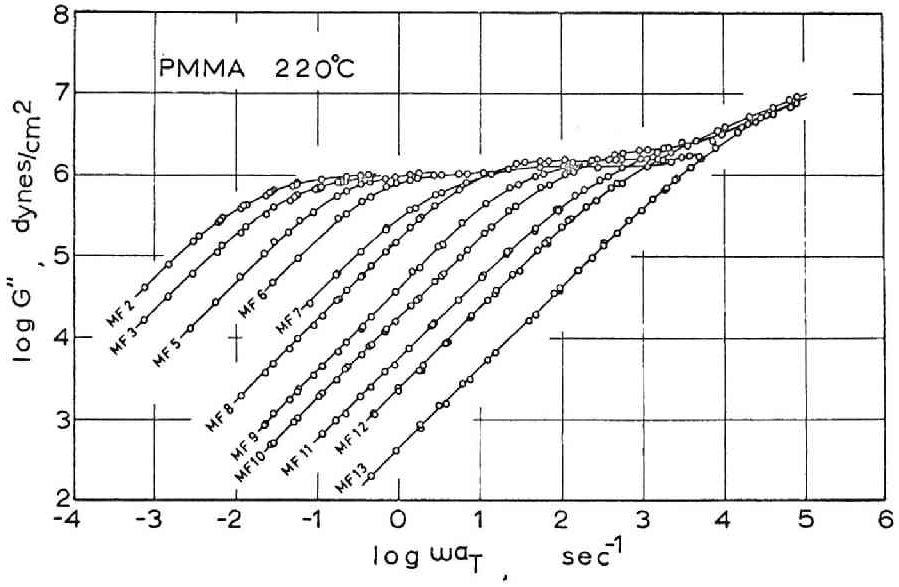

FIG.3-29. Master curves of G'' for the anionic PMMA having different molecular weights. The reference temperature is 220°C.

plateau is not very flat and the rubbery-flow transition in G' curves is less sharp, as compared with those for anionic polystyrenes.

3.4 RHEOLOGICAL BEHAVIOR IN THE TERMINAL ZONE

Anionic Polystyrenes

The rheological properties of polymer liquid in the long time region or terminal zone can be characterized by such parameters as the zero-shear viscosity η_0, the elasticity coefficient A_G, the normal stress coefficient θ_0, and the steady-state compliance J_e^0, which are defined respectively by eqs(1-46), (1-47) and (1-48). According to eq(1-47) as well as the second-order fluid theory[33,34], A_G is equal to $\frac{1}{2}\theta_0$. This has also been confirmed by experimental results obtained by several authors[35~37].

The molecular weight dependence of zero-shear viscosity η_0 for the narrow-distribution polystyrenes is shown in Fig.3-30. It is clear from this figure that, above M = 40,000, the dependence can be represented by a straight line having the slope of 3.7; η_0 is proportional to $M^{3.7}$. The value of this exponent of M for anionic polystyrene reported recently by different authors[38~42] ranges from 3.14 to 4.0. The small deviations of these values from the well-known value of 3.5[43,44] seem not to be essential, when one allows for the difference in the measureing methods employed by different authors.

The critical molecular weight of entanglement couplings M_C for the narrow-distribution polystyrenes cannot be accurately determined from Fig.3-30 itself,but it must have a value between 30,000 and 40,000, which is consistent with the reliable values of 31,200 and 38,000 published in recent papers[1,39,44].

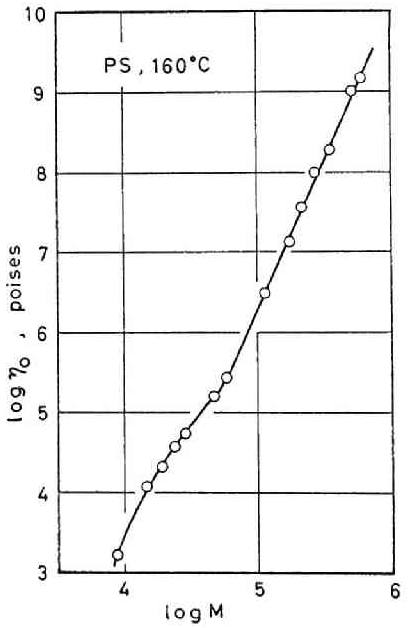

FIG.3-30. Molecular weight dependence of zero-shear viscosity η_0 for narrow-distribution (anionic) polystyrenes at 160°C.

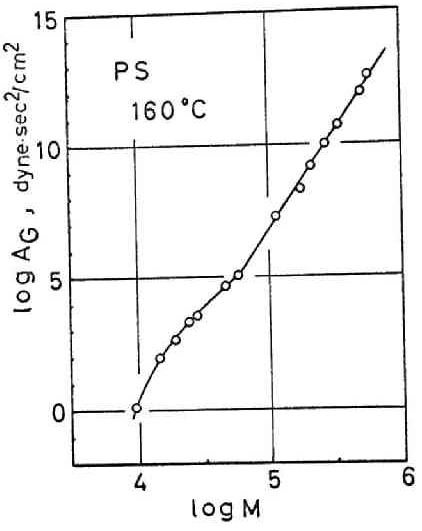

FIG.3-31. Molecular weight dependence of elasticity coefficient A_G for narrow-distribution (anionic) polystyrenes at 160°C.

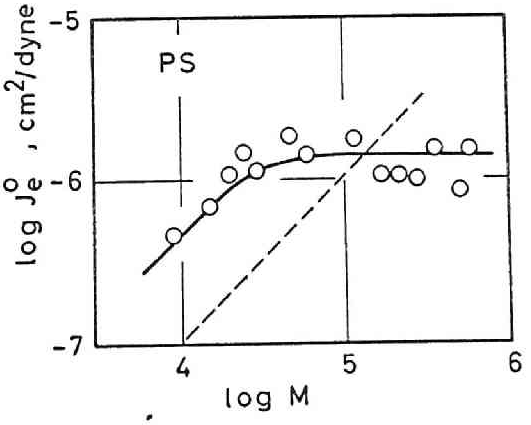

FIG.3-32. Molecular weight dependence of steady-state compliance J_e^0 for narrow-distribution (anionic) polystyrenes at 160°C.

The relationship between log η_0 and log M below M_c cannot be approximated by a straight line, but in the iso-free-volume state (see Section 3.6 in this chapter) it can be represented by a straight line having the slope of unity[44,45].

The values of A_G calculated by eq(1-47) are plotted logarithmically against molecular weight in Fig.3-31. Above M_c, the plots can be approximated by a straight line having the slope of 7.5, but below M_c it is very similar in shape to the log η_0 vs. log M curve of Fig.3-30. This portion also becomes a straight line having a slope of 3.0 in the iso-free-volume state.

The molecular weight dependence of the steady-state compliance J_e^0 is shown in Fig.3-32. As is evident in this figure, J_e^0 does not depend on molecular weight in the high molecular weight region, but it is approximately proportional to molecular weight in the low molecular weight region. The break point of the curve seems to be located near M_c.

The FLW theory[1,46] predicts that J_e^0 should be proportional to M as given by eq(1-46). The straight line predicted by the equation of the FLW theory is shown in Fig.3-32 by the broken line. The experimental points diverge from this line over the entire range of molecular weight covered in this study. The independence of J_e^0 from molecular weight has also been reported by several authors for narrow-distribution polystyrene[40,41,47] and poly-α-methylstyrene[48,49]. These results obtained for such non-polar polymers agree well with the Graessley theory, which is reviewed in Section 1.3[50].

Anionic Polymethyl Methacrylates

The molecular weight dependence of zero-shear viscosity for anionic

PMMA at 220°C is shown with the open circles in Fig.3-33. The dependence can be represented by a straight line having the slope of 4.4 in the higher molecular weight region. The slope of this line is not only higher than the famous value of 3.5 but also higher than the value of 4.0 for the radical PMMA obtained in previous section (Section 3.2.4).

The critical molecular weight M_c for the anionic PMMA cannot accurately be determined from Fig.3-33, but it is likely to be located between 30,000 and 40,000, which is not too different from the reliable values of 27,500 and 31,500, given by Berry and Fox[44].

In Fig.3-34 is shown the molecular weight dependence of the steady-state compliance J_e^0, calculated by eq(1-48), for the anionic PMMA, together with that for the radical PMMA evaluated from Fig.3-7 and Fig.3-8. It is clear from Fig.3-34 that J_e^0 is independent of polymerization methods and

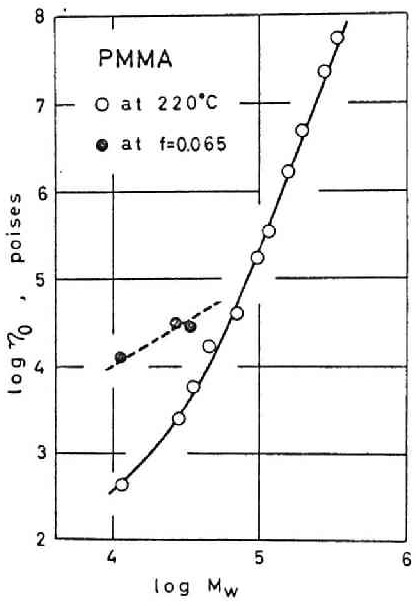

FIG.3-33. Molecular weight dependence of zero-shear viscosity η_0 for anionic PMMA at 220°C (open circles) and at f = 0.065 (closed circles).

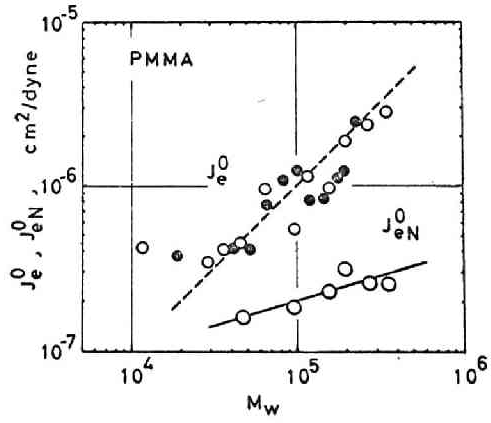

FIG.3-34. Molecular weight dependence of steady-state compliance J_e^0 and entanglement compliance J_{eN}^0 for anionic PMMA (open circles) at 220° C. Closed circles indicate the results for radical PMMA.

is roughly proportional to the molecular weight. The broken line drawn in the figure shows the prediction of the FLW theory[46] given by eq(1-64). The proportionality between the steady-state compliance and the molecular weight has also been found for polyvinyl acetate by Ninomiya et al.[51], but not for several non-polar polymers as described above. This discrepancy might be attributed to the polar groups in the polymer chain of PMMA and PVAc, though the effect of the branching in these materials should not be completely disregarded.

3.5 RHEOLOGICAL BEHAVIOR IN THE RUBBERY ZONE

Anionic Polystyrenes

The rheological behavior of polymer liquids in the rubbery zone is fundamentally affected by the entanglement couplings between the molecular chains. As pointed out in Chapter 1, almost all the theories of entanglement couplings have been based upon the treatments of Rouse and Zimm[52] for the dynamics of an isolated macromolecular chain. These theories can be classified roughly into three categories. The FLW theory[46], Marvin-Oser theory[53] and Chompff-Duiser theory[54] belong to the first category, which predict that the relaxation spectrum will have a maximum characteristic of the entanglement slipping mechanism. These theories are based on the idea that the friction factor of submolecules increases owing to the presence of entanglement couplings. The second type of theory, presented by Hayashi [55], is based on the assumption that not only the friction factor but also the elastic coefficient of submolecules (ζ_0 and κ_0, used in Section 1.3) changes due to the entanglement couplings, and it predicts a box-shaped relaxation spectrum without any maximum in the rubbery zone. The last type of theory is one presented by Graessley[50], and is based on somewhat

different model as illustrated in Fig.1-4.

The three types of theory predict distinctive behavior of various viscoelastic parameters. According to the first type, the frequency dependence curve of G" should have a maximum, and that of G' should show a very flat plateau. Furthermore, J_e^0 should be proportional to M. The Hayashi theory, on the other hand, predicts that G" will never show any maximum, and that J_e^0 will be independent of molecular weight. Although the Graessley theory, which also predicts the independence of J_e^0 on M, is built only for the entanglement relaxation spectrum, the maximum of G" and the flat plateau of G' can be easily supposed by addition of the transition spectrum, for example, the Mooney-Rouse spectrum[1,56] for transition region.

Therefore, the experimental finding that the steady-state compliance for high molecular weight polystyrenes is independent of M seems to support the Hayashi and Graessley theories. The G" curves shown in Fig.3-27, however, undoubtedly show maxima, and the G' curves shown in Fig.3-26 have very flat and long plateaus. This suggests that the narrow-distribution polystyrenes of very high molecular weights have two sets of relaxation times, which are separated from each other due to the narrow distribution of molecular weights. As the molecular weight approaches M_c, the peak associated with the entanglement slippage becomes more and more ambiguous, because of the overlapping of the two sets of relaxation times. Such features are very similar to the frequency dependence of G' and G" predicted by the Marvin-Oser theory.

In many studies hitherto published for the viscoelastic properties of various high polymers, a clear peak in the G" curves has never been observed. The reason is that the samples employed in those studies had

fairly broad distributions of molecular weights, though some of them were fractionated. The broadening of the distribution of relaxation times associated with entanglement slippage due to the broadening of molecular weight distribution will be discussed in more detail in Chapter 5.

In the conceptual scheme of entanglement coupling[1,57], the most important parameter is the average molecular weight between coupling loci, M_e, or the corresponding average chain length, $Z_e = jM_e/M_0$, where j is the number of chain atoms per monomer unit, and M_0 the molecular weight of a monomer.

As is evident in Fig.3-26, G' for high molecular weight polymers in the rubbery zone is constant, independent of frequency. The entanglement or quasi-equilibrium modulus G^0_{eN} denotes this constant value of G' and is related with the average molecular weight between the entanglement coupling loci. The value of G^0_{eN} evaluated directly from Fig.3-26 is 2.0×10^6 dynes/cm^2, and those of M_e and Z_e calculated by eq(1-51) are respectively 18,000 and 346.

When the log G' vs. log ω curve does not show a flat plateau, as in the case of broad-distribution polymers, G^0_{eN} or the entanglement compliance J^0_{eN} can be evaluated by the integration of the G" vs.lnω or J" (loss compliance) vs. ln ω curves according to the following equations[58]:

$$G^0_{eN} = \int_a^\infty H(\tau)\, d\ln\tau = \frac{2}{\pi}\int_{-\infty}^{a'} G''\, d\ln\omega \qquad (3\text{-}5)$$

$$J^0_{eN} = \int_c^b L(\tau)\, d\ln\tau = \frac{2}{\pi}\int_{b'}^{c'} J''\, d\ln\omega \qquad (3\text{-}6)$$

where $H(\tau)$ and $L(\tau)$ denote the relaxation and retardation spectra, respectively, and τ the relaxation time. The integral limits a', b' and

c' should be taken to encompass the maximum of G" or J". In Fig.3-35 are shown two examples of G" vs. log ω curves for the narrow-distribution polystyrenes, L18 and L15. The solid and broken lines show the experimental and estimated values of G". It has been confirmed that no serious error is introduced when the value of ω at which the loss tangent tan δ takes its maximum is taken as one of the integration limits or when whole curve is assumed to be symmetric.

The values of G^0_{eN} thus evaluated for several high molecular weight polymers are tabulated in Table 3-I, together with those of M_e and Z_e determined from G^0_{eN}. In this table are also listed the values caluculated from G' of the rubbery plateau in Fig.3-26. It is clear from this table that the molecular weight or chain length between entanglement couplings is almost constant independent of molecular weight, and that the result of the integration of the curves coincides very well with that obtained directly from G' of the plateau. When we assume the critical molecular weight M_c to be between 31,200 and 38,000, we obtain M_c/M_e = 1.7 to 2.1, which

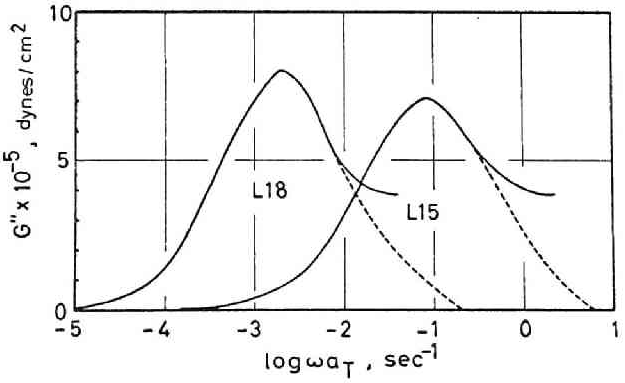

FIG.3-35. Two examples of G" vs. log ω curves for obtaining G^0_{eN} by integration.

TABLE 3-I

ENTANGLEMENT MODULUS AND ENTANGLEMENT SPACINGS OBTAINED BY INTEGRATION OF THE LOSS MODULUS

Samples	Mol. wt.	G^0_{eN}(dynes/cm^2)	M_e	Z_e
L18	581,000	2.05×10^6	17,500	337
L19	513,000	2.22×10^6	16,200	311
L22	275,000	1.80×10^6	20,100	386
L15	215,000	1.90×10^6	18,900	364
Average		1.99×10^6	18,100	347
From G' plateau		2.0×10^6	18,000	346

TABLE 3-II

ENTANGLEMENT MODULUS AND ENTANGLEMENT SPACINGS FROM THE MARVIN-OSER THEORY

Samples	Mol. wt.	G^0_{eN}(dynes/cm^2)	M_e	Z_e
L18	581,000	3.86×10^6	9,300	179
L19	513,000	4.35×10^6	8,300	159
L22	275,000	3.48×10^6	10,300	199
L15	215,000	3.48×10^6	10,300	199
Average		3.79×10^6	9,600	184

compares well with the 1.9 predicted by Bueche[59].

According to Marvin-Oser theory[53], the maximum values of G" and J" are related to G^0_{eN} and J^0_{eN} by

$$G''_{max} = 0.207\ G^0_{eN} \tag{3-7}$$

$$J''_{max} = 0.417\ J^0_{eN} \tag{3-8}$$

Therefore, from G''_{max} we can determine G^0_{eN} using eq(3-7), and hence M_e and Z_e using eq(1-51). The values thus determined for some of the narrow-distribution polystyrenes shown in Fig.2-26 are listed in Table 3-II. The values in this table differ from those in Table 3-I by a factor 1.9. Recently, it has been reported[60] that M_e calculated by the use of the Hayashi theory[55] for several polymer syatems is two or three times larger than that obtained by the Marvin-Oser theory[53].

Anionic Polymethyl Methacrylate

As seen from Fig.3-28, all of the G' curves do not show the flat rubbery plateau, and hence G^0_{eN} was determined by the integration of G" curve, using eq(3-5). In practice, the G" vs. ln ω curve was numerically integrated from ln $\omega = -\infty$ to the maximum of G" and the result was doubled, because the G" curve shows no clear peak as seen in Fig.3-29. This convenient procedure produces no serious error.

The calculated values of G^0_{eN} and J^0_{eN}, and also the value of M_e evaluated from eq(1-51) are tabulated in Table 3-III. It is clear from this table that G^0_{eN} increases gradually, while M_e decreases with decreasing molecular weight. J^0_{eN}, the reciprocal of G^0_{eN}, is logarithmically plotted against molecular weight in Fig.3-34. The plot can be approximated by a straight line having the slope of 0.3, as seen in this figure. This

TABLE 3-III

ENTANGLEMENT MODULUS AND COMPLIANCE, AND ENTANGLEMENT SPACINGS OBTAINED BY INTEGRATION OF THE LOSS MODULUS

Sample	M_w	G^0_{eN}(dynes/cm^2)	J^0_{eN}(cm^2/dyne)	M_e
MF2	342,000	3.94×10^6	2.54×10^{-7}	10,400
MF3	270,000	3.89×10^6	2.57×10^{-7}	10,500
MF5	197,000	3.12×10^6	3.20×10^{-7}	13,100
MF6	158,000	4.33×10^6	2.31×10^{-7}	9,480
MF8	96,300	5.41×10^6	1.85×10^{-7}	7,580
MF10	45,200	6.07×10^6	1.65×10^{-7}	6,760

molecular weight dependence of J^0_{eN} and M_e in the entanglement region does not agree with the generally accepted concept nor with result obtained for the anionic polystyrenes. As seen from Table 3-III, M_e ranges from 13,100 to 6,760, while M_c is estimated to be 30,000∿40,000. Therefore, the ratio M_c/M_e is as high as 2∿6, though it is about 2 for the usual non-polar polymers. The anomaly found in the molecular weight dependence of M_e and in the ratio M_c/M_e for PMMA may be attributed to the fact that the polarity affects the internal structure, which is due to the entanglement couplings between molecular chains in the polymer liquid.

3.6 EFFECT OF TEMPERATURE AND FREE VOLUME

Anionic Polystyrenes

The shift factor a_T for the polystyrene samples is plotted against temperature in Fig.3-36. The large open circles in the figure represent the

values obtained for samples having molecular weight of 28,900 (L14) and higher, the closed circles those for L12 (M = 14,800) and the small open circles for L9 (M = 8,900). It is clear from this figure that the shift factor is independent of molecular weight so far as the molecular weight exceeds a certain limiting value of about 30,000, which is close to the critical molecular weight for entanglement M_c. For the polymers of low molecular weights, the shift factor decreases with decreasing molecular weight. Log a_T for high molecular weight polystyrenes can be expressed by the following WLF-type equation:

$$\log a_T = \frac{-7.14(T - 160)}{112.1 + (T - 160)} \qquad (3\text{-}9)$$

Eq(1-81) shows that the plot of $-(T - T_r)/\log a_T$ against $(T - T_r)$ should give a straight line, and that from its slope and intercept, c_1^r, c_2^r,

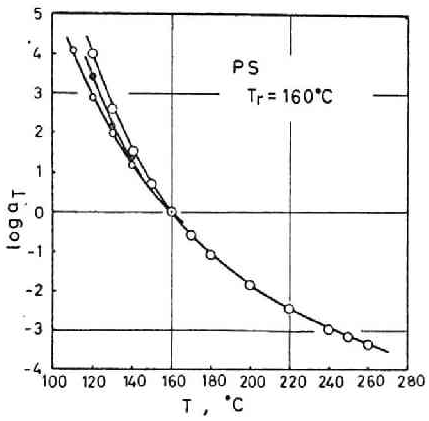

FIG.3-36. The logarithm of the shift factor a_T plotted against temperature for narrow-distribution polystyrenes. Large open circles indicate the results for $M \geq M_c$, closed circles for M=14,800 (L12), and small open circles for M=8,900 (L9).

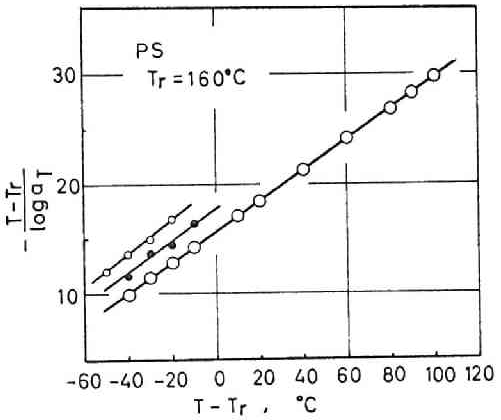

FIG.3-37. Linear plots of $-(T - T_r)/\log a_T$ vs. $T - T_r$, for narrow-distribution polystyrenes. The reference temperature is 160°C. The circles are used as in Fig.3-36.

f_r, α_f, and T_0 can be evaluated. The plot for the anionic polystyrenes is given in Fig.3-37, where the same circles as in Fig.3-36 are employed to distinguish the three types of samples. The calculated values of the free volume parameters are tabulated in Table 3-IV.

It is evident from this table that T_0 decreases with decreasing molecular weight below M_c, while α_f appears almost constant. The fractional free volume at the glass temperature, f_g, is 0.028 when we assume $T_g = 100^\circ C$. Polystyrenes having molecular weights below M_c possess excess free volume as compared with those having molecular weights above M_c at the same temperature; for example, at $160^\circ C$, $f_r = 0.0677$ for $M = 8{,}900$, while $f_r = 0.0608$ for $M \geq M_c$. This excess free volume causes the shifts of the storage modulus and loss modulus curves for low molecular weight polymers to the high frequency side in the transition zone, as seen in Figs.3-26 and 3-27.

The temperatures, T_r', at which polymers having molecular weights below M_c have the same fractional free volume as that of higher molecular weight polymers were calculated from eq(1-78) to be 155.0 and $146.8^\circ C$ for L12 and L9, respectively, instead of $160^\circ C$. Therefore, G' and G" for L12 and L9 respectively at 155.0 and $146.8^\circ C$ should correspond to those for the higher molecular weight polymers at $160^\circ C$ or in iso-free-volume state, in which $f = 0.0608$. The G' and G" curves for the seven polymers, including L12 and L9, in the iso-free-volume state are compared in Figs.3-38 and 3-39, respectively. The curves drawn with the broken lines in these figures are those for L12 and L9 at $160^\circ C$. It is evident in these figures that the curves for low molecular weight polymers corrected for the free volume unite with the others in the transition zone.

TABLE 3-IV

FREE VOLUME PARAMETERS FROM THE TEMPERATURE DEPENDENCE OF THE SHIFT FACTOR

Sample	M_w	α_f (deg^{-1})	T_0(°C)	f_{160}	f_g
	$\geq M_c$	5.42×10^{-4}	47.9	0.0608	0.0283 (T_g = 100°C)
L12	14,800	5.20×10^{-4}	38.1	0.0634	
L9	8,900	5.28×10^{-4}	31.8	0.0677	

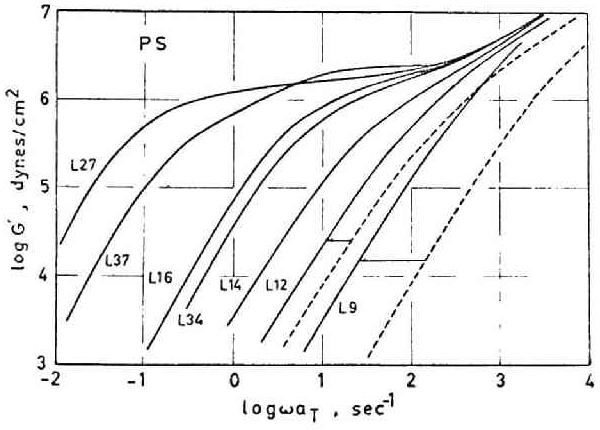

FIG.3-38. Frequency dependence of G' for narrow-distribution (anionic) polystyrenes reduced to the iso-free-volume state, f = 0.0608.

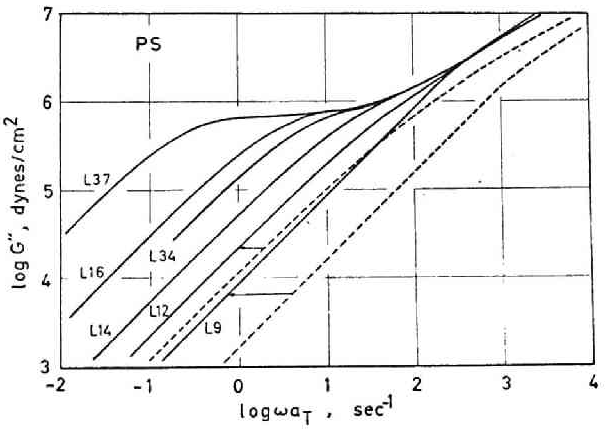

FIG.3-39. Frequency dependence of G'' for narrow-distribution (anionic) polystyrenes reduced to the iso-free- volume state, f = 0.0608.

Anionic Polymethyl Methacrylates

The shift factor a_T for the PMMA samples is plotted against temperature T in Fig.3-40. The large open circles in this figure represent the results for the samples having molecular weights of 45,200(MF10) and higher, while the other circles are those for the samples indicated. The shift factor is independent of molecular weight provided that the molecular weight exceeds a certain value. This limiting value, about 40,000, can be referred to as the critical molecular weight, M_c and will be discussed in more detail later. For the polymers of lower molecular weight, the shift factor decreases with decreasing molecular weight, as has been described above and elsewhere[45]. The WLF linear plots for the anionic PMMA are given in Fig.3-41. The free volume parameters calculated from this figure are tabulated in Table 3-V, and c_1^r and c_2^r are, respectively 6.69 and 189.8 for high molecular weight samples. When T_g is assumed to

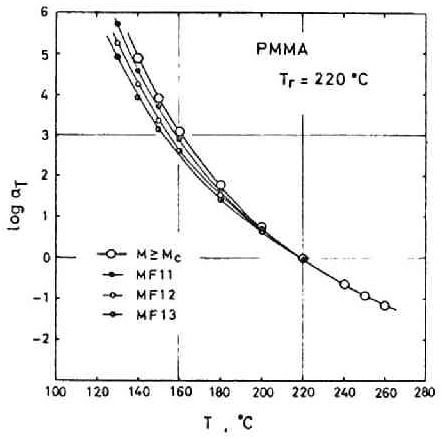

FIG.3-40. The logarithm of the shift factor a_T plotted against temperature for anionic PMMA. Large open circles represent the results for $M \geq M_c$ and the other circles for the samples indicated.

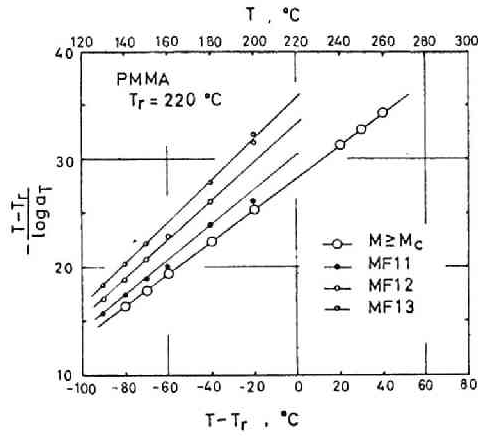

FIG.3-41. The WLF linear plots of $-(T - T_r)/\log a_T$ vs. $(T - T_r)$ for anionic PMMA. The circles are used as in Fig.3-40.

TABLE 3-V

FREE VOLUME PARAMETERS FROM THE TEMPERATURE DEPENDENCE OF THE SHIFT FACTOR OBTAINED FOR ANIONIC PMMA

Sample	M_w	$\alpha_f(deg^{-1})$	$T_0(^oC)$	f_{220}	$T_r'(^oC)$	f_g
MF2∿10	45,200	3.42×10^{-4}	30.2	0.065	220	0.026
MF11	35,100	3.96×10^{-4}	37.1	0.073	200.8	(T_g=105°C)
MF12	28,400	4.20×10^{-4}	34.4	0.078	189.1	
MF13	11,400	4.48×10^{-4}	34.4	0.083	178.9	

be 105°C for PMMA[61], c_1^g and c_2^g can be calculated to be 16.98 and 74.76, respectively.

As seen from Table 3-V, α_f increases with decreasing molecular weight below M_c, while T_0 seems to be unchanged. This is in marked contrast to the case of the anionic polystyrenes of narrow-molecular-weight distribution mentioned above , where α_f was constant and T_0 decreased. The value of f_g for the PMMA samples having molecular weights above M_c is 0.026, assuming T_g= 105°C. This value compares well with the famous value of 0.025[1].

The reference temperature in Table 3-V is the temperature at which the polymer has the fractional free volume of 0.065. The closed circles in Fig.3-33 represent the zero-shear viscosity at the temperature T_r', or the iso-free-volume state where f = 0.065. It is evident from Fig.3-33 that the molecular weight dependence of η_0 in the iso-free-volume state for lower molecular weight PMMA can be represented by a straight line. It is also found that the molecular weight at the intersection of the two straight lines drawn in this figure is around 80,000, being much higher than the

critical molecular weight M_c so far published. This is in marked contrast again to the case of the anionic polystyrenes, where M at the intersection was very close to M_c. This discrepancy is associated with the fact that the dependence of shift factor on molecular weight is very great for PMMA as shown in Fig.3-40 or 3-41. The reason why such a peculiar result is obtained for PMMA is not clear, but it appears probable that the critical molecular weight above which the free volume does not vary with molecular weight, is not always the same as M_c. The molecular weight at which the shift factor decreases may not be directly related to M_c but rather only to the chemical structure of the polymer chains, because this high value of M_c (80,000) is not believed to be true.

REFERENCES

1. J. D. Ferry,"Viscoelastic Properties of Polymers", 2nd ed., John Wiley, New York, 1970
2. M. L. Williams, R. F. Landel, and J. D. Ferry, J. Am. Chem. Soc.,77, 3701 (1955)
3. S. Onogi, T. Fujii, H. Kato, and S. Ogihara, J. Phys. Chem., 68, 1598 (1964)
4. S. Onogi, H. Kato, S. Ueki, and T. Ibaragi, J. Polym. Sci., Part C, 15, 481 (1966)
5. (a) W. P. Cox and E. H. Merz, J. Polym. Sci., 28, 619 (1958)
   (b) W. P. Cox and E. H. Merz, Official Digest, May Issue, 2 (1960)
6. T. W. DeWitt, J. Appl. Phys., 26, 889 (1955)
7. Y. H. Pao, J. Appl. Phys., 28, 591 (1957)
8. S. Onogi, I. Hamana, H. Hirai, J. Appl. Phys., 29, 1503 (1958)
9. R. L. Ballman and R. H. Simon, J. Polym. Sci., Part A, 2, 3557 (1964)

10. H. H. Zabusky and R. F. Heitmiller, SPE Trans., 4, 17 (1964)

11. R. S. Porter and J. F. Johnson, Chem Rev., 66, 1 (1966)

12. K. Ninomiya, J. D. Ferry, and Y. Oyanagi, J. Phys. Chem., 67, 2297 (1963)

13. V. C. Long, G. C. Berry, and L. M. Hobbs, Polymer, 5, 517 (1964)

14. H. P. Schreiber, Polymer, 4, 365 (1963)

15. M. Horio, T. Fujii, and S. Onogi, J. Phys. Chem. 68, 778 (1964)

16. S. Onogi, S. Ueki, and H. Kato, J. Soc. Mater. Sci., Japan, 14, 304 (1965)

17. F. Bueche, J. Appl. Phys., 30, 1114 (1959)

18. F. Bueche and S. W. Harding, J. Polym. Sci., 32, 177 (1958)

19. G. V. Vinogradov and A. Ya. Malkin, J. Polym. Sci., Part A, 2; 2357 (1964)

20. G. V. Vinogradov and A. Ya. Malkin, J. Polym. Sci., Part A2, 4, 135 (1966)

21. A. J. Charlesby, J. Polym. Sci., 17, 379 (1955)

22. W. F. Busse and R. Longworth, J. Polym. Sci., 58, 49 (1962)

23. L. D. Moore, J. Polym. Sci., 36, 155 (1959)

24. D. P. Wyman, L. H. Elyash, and W. J. Frazer, J. Polym. Sci., Part A, 3, 681 (1965)

25. G. Kraus and J. T. Gruber, J. Polym. Sci., Part A, 3, 105 (1965)

26. S. Onogi, S. Kimura, T. Kato, T. Masuda, and N. Miyanaga, J. Polym. Sci., Part C, 15, 381 (1966)

27. T. Fujimoto, H. Narukawa, and M. Nagasawa, Macromolecules, 3, 57 (1970)

28. T. Fujimoto, H. Kajiura, M. Hirose, and M. Nagasawa, Polym. J., 3, 181 (1972)

29. T. Masuda, Y. Ohta, and S. Onogi, Macromolecules, 4, 763 (1971)

30. T. Masuda, Y. Nakagawa, Y. Ohta, and S. Onogi, Polym. J., 3, 92 (1972)

31. T. Masuda, Y. Ohta, M. Minamide, and S. Onogi, J. Soc. Mater. Sci., Japan, 21, 436 (1972)

32. T. Masuda, T. Saito, Y. Ohta, and S. Onogi, J. Soc. Mater. Sci., Japan, 22, No.5, (1973) in press.

33. B. D. Coleman and W. Noll, Rev. Mod Phys., 33, 239 (1961)

34. B. D. Coleman and H. Markovitz, J. Appl. Phys., 35, 1 (1964)

35. W. Phillipoff, J. Appl. Phys., 36, 3033 (1965)

36. K. Osaki, M. Tamura, T. Kotaka, and M. Kurata, J. Phys. Chem., 69, 3642 (1965)

37. T. Kotaka and K. Osaki, J. Polym. Sci., Part C, 15, 453 (1966)

38. J. F. Rudd, J. Polym. Sci., 44, 459 (1960)

39. R. A. Stratton, J. Colloid & Interf. Sci., 22, 517 (1966)

40. G. Akovali, J. Polym. Sci., Part A2, 5, 875 (1967)

41. A. V. Tobolsky, J. J. Aklonis, and G. Akovali, J. Chem. Phys., 42, 723 (1965)

42. (a)N. J. Mills, Europ. Polym. J., 5, 675 (1969)
(b) N. J. Mills and A.Nevin, J. Polym. Sci., Part A2, 9, 267 (1971)

43. T. G. Fox, S. Gratch, and S. Loshaek, "Rheology," vol I, F.R. Eirich Ed., Academic Press, New York, 1956, Chapter 12.

44. G. C. Berry and T. G. Fox, Ad_v.Polym. Sci., 5, 261 (1968)

45. V. R. Allen and T. G. Fox, J. Chem. Phys., 41, 337 (1964)

46. J. D. Ferry, R. F. Landel, and M. L. Williams, J. Appl. Phys., 26, 359 (1955)

47. N. Nemoto, Polym. J., 1, 485 (1970)

48. T. Fujimoto, N. Ozaki, and M. Nagasawa, J. Polym. Sci., Part A2, 6, 129 (1968)

49. H. Odani, N. Nemoto, S. Kitamura, and M. Tamura, Polym. J., 1, 356 (1970)

50. W. W. Graessley, J. Chem. Phys., 54, 5143 (1971)

51. K. Ninomiya and J. D. Ferry, J. Phys. Chem., 67, 2292 (1963)

52. B. H. Zimm, "Rheology", Vol.III, F. R. Eirich, Ed., Academic Press, New York, 1960, Chapter 1.

53. (a) R. S. Marvin and H. Oser, J. Res. NBS, 66B, 171 (1962)

(b) H. Oser and R. S. Marvin, J. Res. NBS, 67B, 87 (1963)

54. (a) A. J. Chompff and J. A. Duiser, J. Chem. Phys., 45, 1505 (1966)

(b) A. J. Chompff and W. Prins, J. Chem. Phys, 48, 235 (1968)

55. S. Hayashi, J. Phys. Soc. Japan, 18,131;249 (1963)

56. M. Mooney, J.Polym. Sci., 34, 599 (1959)

57. J.D. Ferry, "Proc. 5th Intern. Congr. Rheology", S. Onogi Ed., Vol. 1, Univ. Tokyo Press, Tokyo, 1969, p.3.

58. J. F. Sanders and J. D. Ferry, Macromolecules, 2, 440 (1969)

59. F. Bueche, "Physical Properties of Polymers", Interscience, New York, 1962, p.80.

60. K. Osaki, Ph. D. Thesis, Kyoto University, 1968.

61. W. A. Lee and G. J. Knight, "Polymer Handbook", J. Brandrup and E. H. Immergut, Ed., Interscience, New York, 1966, p.III-68.

CHAPTER 4

Rheological Properties of Polymer Solutions

4.1 INTRODUCTION

In the previous chapter, the effects of temperature, molecular weight, molecular weight distribution, and branching on the rheological properties of polymer melts were surveyed on the basis of experimental results. Furthermore, the molecular weight dependence of the viscoelastic functions, some constants characteristic of the terminal and rubbery zones and free volume parameters, were discussed in detail for the well-characterized polymers. The other patameter which affects the rheological properties of polymer liquids is the concentration of the polymer in the liquid.

From a rheological view-point, the concentration of polymer solutions can be divided into various regimes depending on the intermolecular interaction between polymer molecules. Because the concentration ranges are, of course, dependent on the molecular weight of the polymer, the classification is better done with respect to $c[\eta]$ following Ferry's suggestion. [1,2] Here, c is the concentration in g/ml and $[\eta]$ is the intrinsic viscosity in ml/g. A classification might be as follows:

1. $c[\eta] < 0.5$: Very dilute polymer solutions.
   Each molecule in solution is isolated and the rheological behavior can be compared with theories based on isolated molecules.
2. $c[\eta] = 0.5 \sim 3$: Dilute polymer solutions.
   Molecules in solution interact slightly and the rheological behavior shows a significant deviation from the prediction of

theories based on isolated molecules.

3. $c[\eta] = 3 \sim 20$: Moderately concentrated polymer solutions.
   Molecules in solution interact substantially and the rheological behavior suggests the aggregation of molecules or imperfect entanglement networks.

4. $c[\eta] > 20$: Concentrated polymer solutions.
   Molecules in solution completely form a continuous network structure and the rheological behavior is dominated by the entanglement couplings.

The viscous and elastic properties of moderately concentrated polymer solutions are considerably affected not only by molecular weight and concentration but also by the solvent used. In other words, the solvent-dependent character which is important in more dilute solution is also important in this concentration range. The changes of free volume, however, have no essential effect on the viscosity of the solution. In concentrated solutions, on the other hand, the effect of free volume becomes dominant, while that of the solvent almost vanishes.

The present chapter deals with the reological properties of concentrated and moderately concentrated solutions. A superposition procedure for viscosity vs. molecular weight and viscosity vs. concentration curves is proposed and the molecular weight and concentration dependences of viscosity, as well as other rheological parameters, are discussed in relation to the solvent power. The viscoelastic properties of the concentrated polymer solutions have been measured and the concentration dependences of certain rheological parameters, such as zero-shear viscosity, steady-state compliance and entanglement compliance, are discussed. Moreover, the concentration dependence of the free-volume parameters are determined.

4.2 VISCOSITY OF MODERATELY CONCENTRATED SOLUTIONS

4.2.1 Effect of the Solvent on the Viscosity-Molecular Weight Relationship

In order to ascertain the effect of solvent on the molecular weight dependence of viscosity, log η_0 vs. log M curves for polystyrene(PS) samples (Table 2-I) in toluene were compared with those for the same samples in decalin at concentrations of 4, 6, 14, and 18%. The result is shown in Fig.4-1. In this figure, the logarithm of relative viscosity rather than viscosity itself was plotted against the logarithm of molecular weight, because the viscosity of toluene (0.466 cp at 40°C) is much lower than that of decalin (1.80 cp at 40°C). The slope of log η-log M curve is almost independent of the nature of the solvents. In the concentration range covered in this experiment, the solution in the poor solvent (decalin) shows lower relative viscosity than that in the good solvent at the same concentration. However, the concentration depencence of the viscosity is larger for solutions in the poor solvent than for those in the good solvent. Hence, as the concentration increases, the difference in viscosity of solutions in the poor and good solvents at the same concentration becomes smaller and smaller until it becomes zero at about 20%.

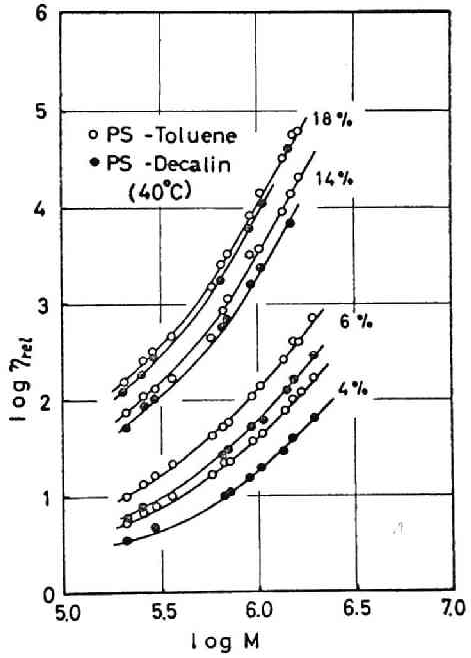

FIG.4-1. A comparison of log η_{rel} vs. log M_w curves for solutions of polystyrene in toluene with those in decalin at various concentrations at 40°C.

4.2.2 Superposition of Log η_0 versus Log M and Log η_0 versus Log c curves

Log η_0 vs. log M curves were determined for several solvent-polymer systems, such as polystyrene (PS; Table 2-I) in toluene (40°C) and decalin (40°C), and linear and branched polyvinyl acetates (PVAc; Tables 2-VII and 2-VIII, respectively) in MEK (30°C). As an example, the result for the solution of PS in toluene is shown in Fig.4-2. As seen from this figure, the approximation of each curve by straight lines is apt to depend on the range of molecular weight covered by experiment. Then the monotonical determination of M_c at the intersection of these lines is very difficult.

The solid lines in Fig.4-2 are drawn faithfully to the experimental points. When one observes these curves carefully, he will notice that the curves at different concentrations show the same slope at a given viscosity. This fact indicates that log η_0 vs. log M curves at different concentrations can be superposed by the horizontal shift along the abscissa, giving a master curve. Such a superposition was tried for the data for PS-toluene system and the result is illustrated in Fig.4-3. The reference concentration is 9.7%. As seen from this figure, the superposition is very satisfactory and gives a smooth master curve. This master curve gives the straight line having the slope of 3.4 at viscosities above 3 poises. Similarly, Figs.4-4, 4-5 and 4-6 show

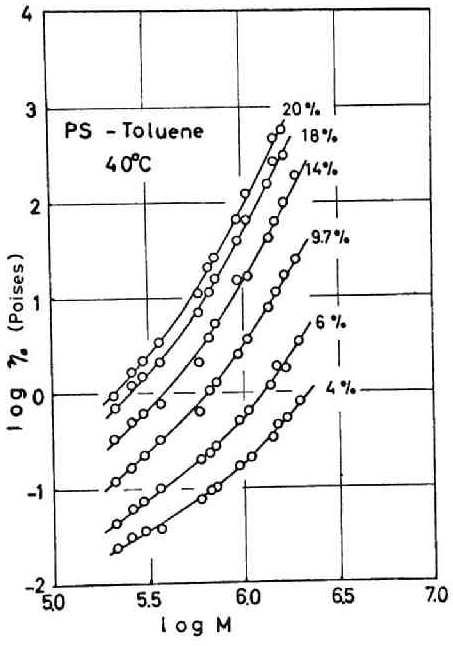

FIG.4-2. Logη_0 vs. logM curves for solution of polystyrene in toluene at various concentrations.

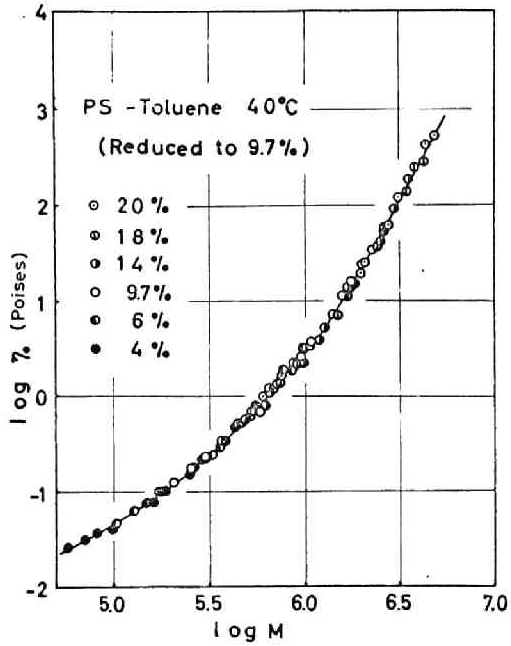

FIG.4-3. Master curve of $\log\eta_0$ vs. logM for solutions of polystyrene in toluene at 40°C. The reference concentration is 9.7%.

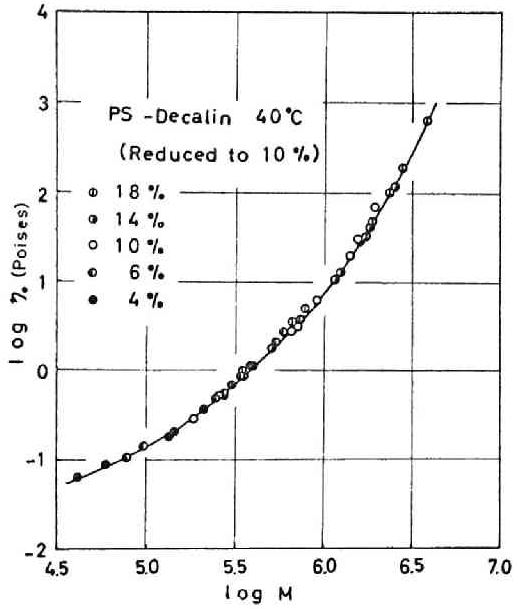

FIG.4-4. Master curve of $\log\eta_0$ vs. logM for solutions of polystyrene in decalin at 40°C. The reference concentration is 10%.

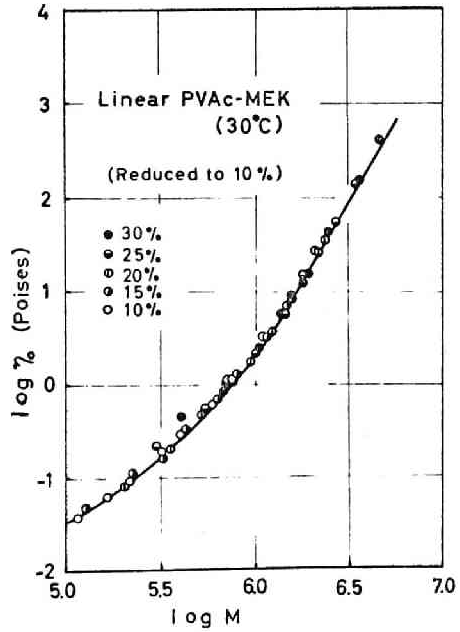

FIG.4-5. Master curve of $\log\eta_0$ vs. logM for solutions of the linear PVAc in MEK at 30°C. The reference concentration is 10%.

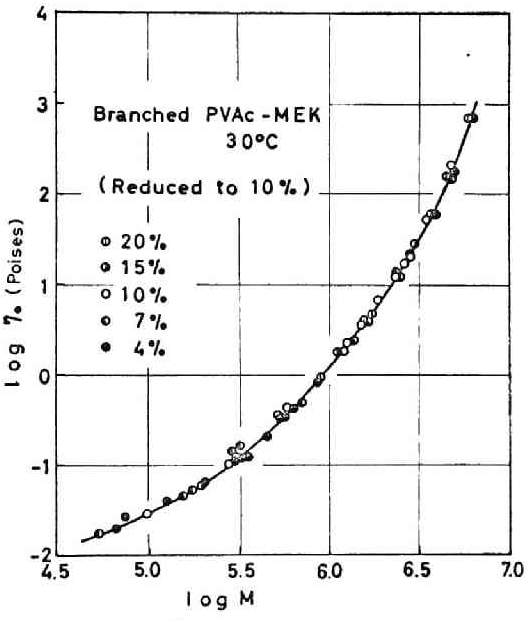

FIG.4-6. Master curve of $\log\eta_0$ vs. logM for solutions of the branched PVAc in MEK at 30°C. The reference concentration is 10%.

master curves for PS in decalin and the linear and branched PVAc in MEK, respectively. These master curves give straight portions having the slope of 3.4 at viscosities above 10 poises, above 2 poises and ranging from 7 to 100 poises, respectively.

In Fig.4-7, log η_0 versus log c curves for polystyrene in toluene (40°C) are shown. The concentration c, represents that in g/100ml, hereafter. The log η_0 vs. log c curves in this figure also show the same slope independent of the molecular weight at a given viscosity, indicating that the curves can also be superposed by the horizontal shift along the abscissa. Fig.4-8 illustrates the master curve obtained by such a superposition for PS-toluene system shown in Fig.4-7. The reference molecular weight is 925,000. As seen from the figure, the master curve gives a straight potion having the slope of 4.7 at viscosities above 3 poises. Fig. 4-9 gives the master curve obtained for PS in decalin by the superposition in reference to the molecular weight of 921,000. This curve gives a straight potion having the slope of 5.6 at viscosities above 10 poises. Figs.4-10 and 4-11 give the master curves for the solutions of the linear and branched PVAc in MEK, respectively. The reference molecular weight are respectively 756,000 and 805,000. The both curves give straight portions having the

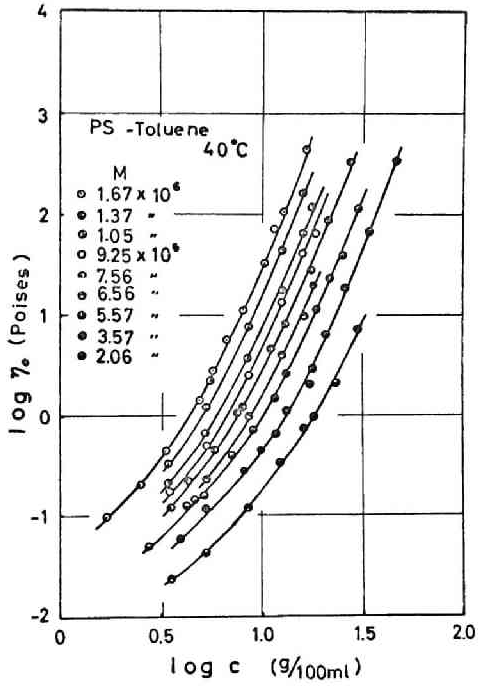

FIG.4-7. Log η_0 vs. log c curves for solutions of polystyrene having different molecular weights in toluene at 40°C.

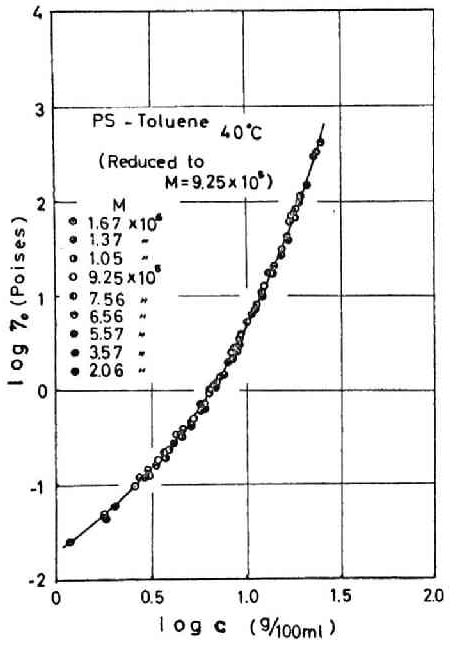

FIG.4-8. Master curve of log η_0 vs. log c for solutions of polystyrene in toluene at 40°C. The reference molecular weight is 925,000.

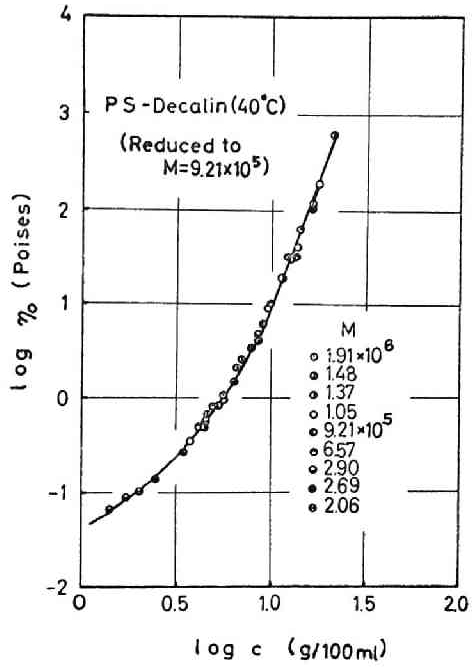

FIG.4-9. Master curve of log η_0 vs. log c for solutions of polystyrene in decalin at 40°C. The reference molecular weight is 921,000.

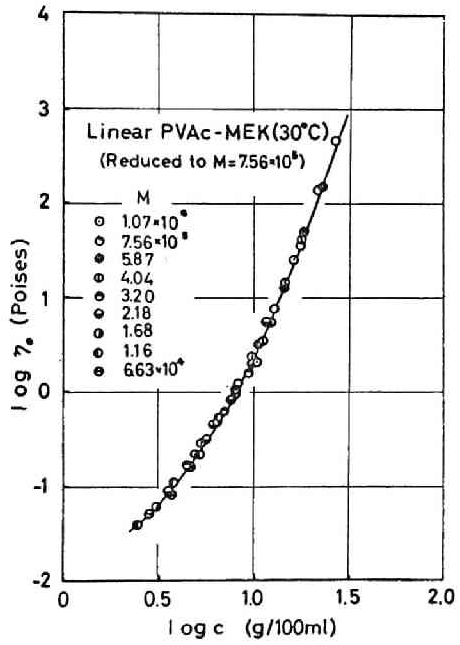

FIG.4-10. Master curve of log η_0 vs. log c for solutions of the linear PVAc in MEK at 30°C. The reference molecular weight is 756,000.

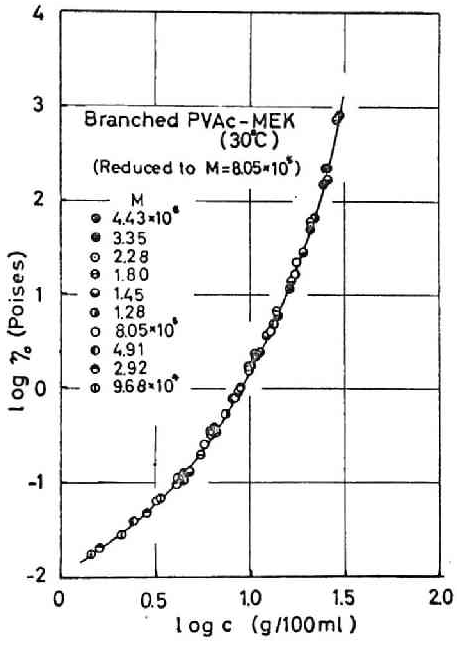

FIG.4-11. Master curve of log η_0 vs. log c for solutions of the branched PVAc in MEK at 30°C. The reference molecular weight is 805,000.

the spole of 5.4 at viscosities higher than 3 and between 7 and 100 poises respectively.

In general, the viscosity may be represented by the equation

$$\eta = K\, c^{\alpha} M^{\beta} \tag{4-1}$$

as a function of the concentration and molecular weight. In this equation K is a constant at constant viscosity and α and β are the slope of log η versus log c and logη versus log M curves, respectively. When viscosity curves can be superposed with each other as mentioned above, the following equation can be derived for a given viscosity η_c:

$$\eta_c = K\, c_0^{\alpha} M_0^{\beta} = K\, c^{\alpha} M^{\beta} \tag{4-2}$$

where the subscript 0 denotes the reference state. This equation leads to

$$\log (c/c_0) = -(\beta/\alpha) \log (M/M_0) \tag{4-3}$$

Log (M/M_0) in this equation means the shift distance by which a log η_0-log M curve at a concentration c is superposed upon the reference curve at the concentration c_0. Similarly, log (c/c_0) means the shift distance by which a log η_0-log c curve at a molecular weight M is superposed on the reference curve at M_0. Thus, these two shift factors can be determined in the superposition processes. Figs.4-12 and 4-13 show the relation between log (M/M_0) and log (c/c_0) for the systems of PVAc and PS, respectively. As seen from Fig.4-12, the relation between the two shift factors is linear in the entire range of concentration and molecular weight, and the relation obtained by the shift of log η_0-log M curves coincides completely with that obtained by the shift of log η_0-log c curves. This suggests that the superposition proposed here is quite reasonable, and that the value of β/α in eq(4-3) is always constant in entire ranges of M and c covered in this experiments. The slope of the straight line in the figure gives the

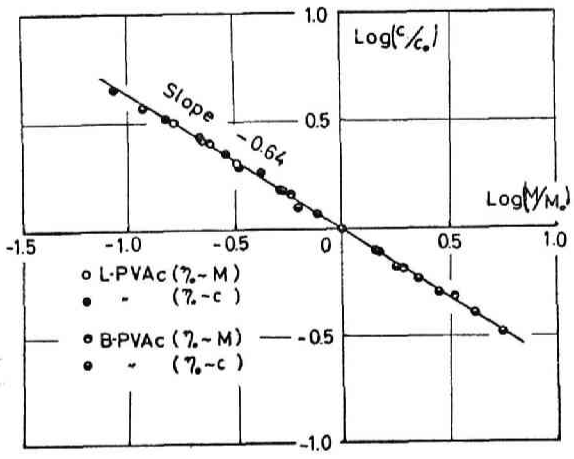

FIG.4-12. The relation between log (M/M_0) and log (c/c_0) for solutions of the linear and branched PVAc in MEK at 30°C. The slope of the line is -0.64.

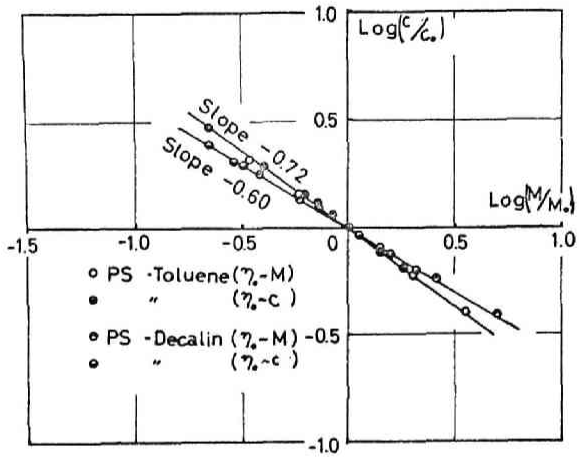

FIG.4-13. The relation between log (M/M_0) and log (c/c_0) for solutions of polystyrene in toluene and in decalin at 40°C. The slopes of the lines are -0.72 and -0.60, respectively.

value of β/α in eq(4-3) to be 0.64. The results given in Fig.4-13, on the other hand, show that $\beta/\alpha = 0.72$ for PS in toluene and $\beta/\alpha = 0.60$ for PS in decalin. In Table 4-I are summarized for the four systems the value of

TABLE 4-I

THE VALUE OF β/α AND α IN THE REGION OF $\beta = 3.4$

System	β/α	α ($\beta = 3.4$)
Linear PVAc-MEK, 30°C.	0.64	5.4 ($\eta_0 \geq 2$ poises)
Branched PVAc-MEK, 30°C.	0.64	5.4 ($100 \geq \eta_0 \geq 7$)
PS-Toluene, 40°C.	0.72	4.7 ($\eta_0 \geq 3$)
PS-Decalin, 40°C.	0.60	5.6 ($\eta_0 \geq 10$)

β/α and that of α in the viscosity range where the viscosity is proportional to $M^{3.4}$. It is clear from this table and above figures that the value of β/α is not affected by the branching but dependent upon the nature of the solvent used.

4.2.3 η_0-M-c Relations at Θ-Conditions

The results presented in the previous section, seems to suggest that the measurements in the poorer solvent give the smaller value of β/α. Furthermore, " Is the β/α value equal to 0.5 under Θ-condition?" is a new question.

Ethyl n-butyl ketone (EBK) was employed as the Θ-solvent for the linear PVAc. The viscosity of the solutions was measured at 29°C. Decalin was used again as the Θ-solvent for PS. This decalin contained cis and trans isomers in the ratio of 38.5 : 61.5, and then 15°C is considered to be very close to the Θ-temperature. The viscosity of solutions of PS was measured at 15°C.

The plots of log η versus log M and log η versus log c for the solutions of these systems also can be superposed upon the reference curves chosen arbitrarily by the horizontal shifts, giving master curves.

In Figs.4-14~4-19 are shown the master curves for the above systems. The superpositions in all systems are satisfactory. In Figs.4-20, 4-21 and 4-22, log (c/c_0) is plotted against log (M/M_0) for the same systems of the linear and branched PVAc and PS respectively. The open circles in these figures represent the data which were obtained from the shift of log η vs. log M curves and the closed circles from the shift of log η vs. log c curves. The plots in both the cases give the same straight line as in Figs. 4-20~4-22. The straight lines in the figures have the slopes of -0.55 and -0.50 for the linear and branched PVAc, and PS, respectively.

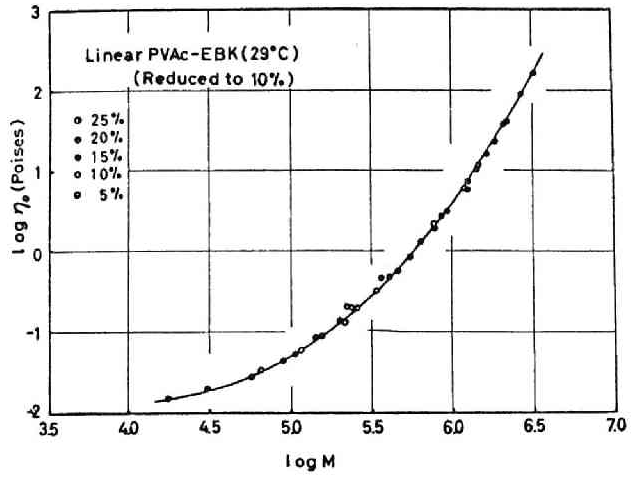

FIG.4-14. Master curve of log η_0 vs. log M for solutions of linear PVAc in EBK at 29°C. The reference concentration is 10%.

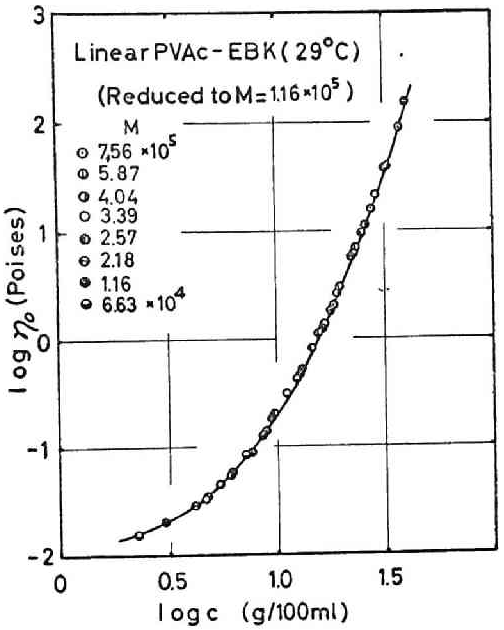

FIG.4-15. Master curve of log η_0 vs. log c for solutions of linear PVAc in EBK at 29°C. The reference molecular weight is 116,000.

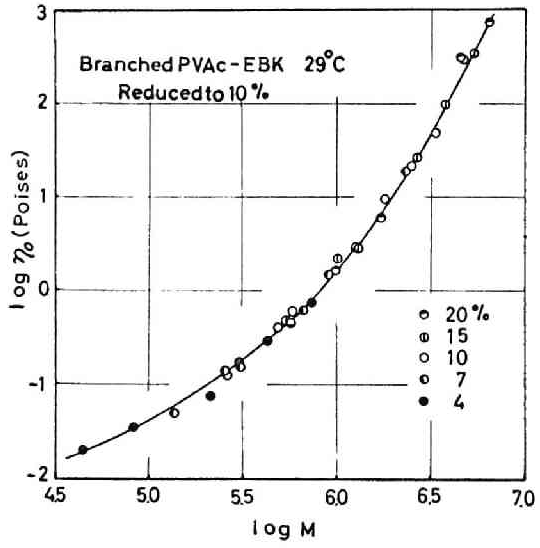

FIG.4-16. Master curve of log η_0 vs. log M for solutions of branched PVAc in EBK at 29°C. The reference concentration is 10%.

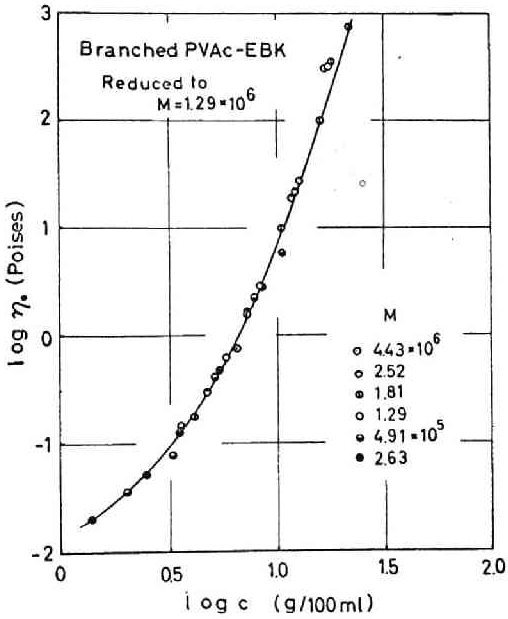

FIG.4-17. Mssster curve of log η_0 vs. log c for solutions of branched PVAc in EBK at 29°C. The reference molecular weight is 1,290,000.

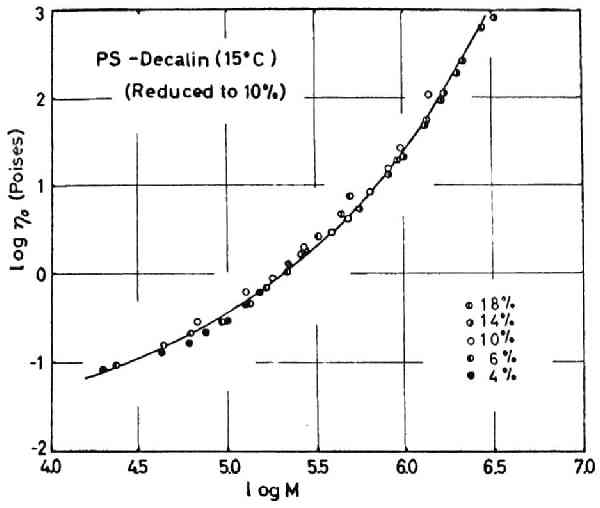

FIG.4-18. Master curve of log η_0 vs. log M for solutions of PS in decalin at 15°C. The reference concentration is 10%.

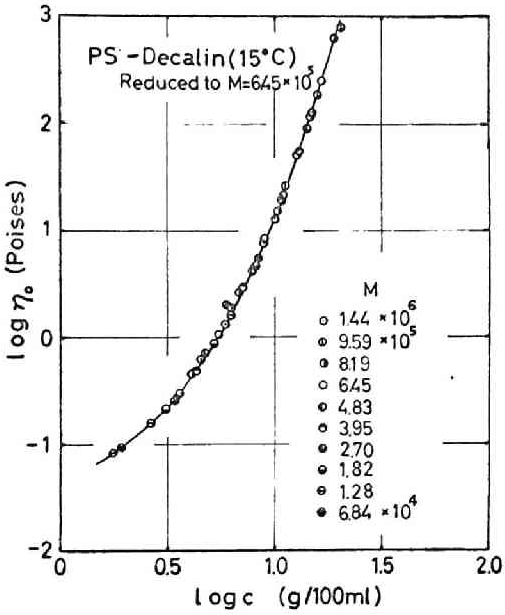

FIG.4-19. Master curve of log η_0 vs. log c for solution of PS in decalin at 15°C. The reference molecular weight is 645,000.

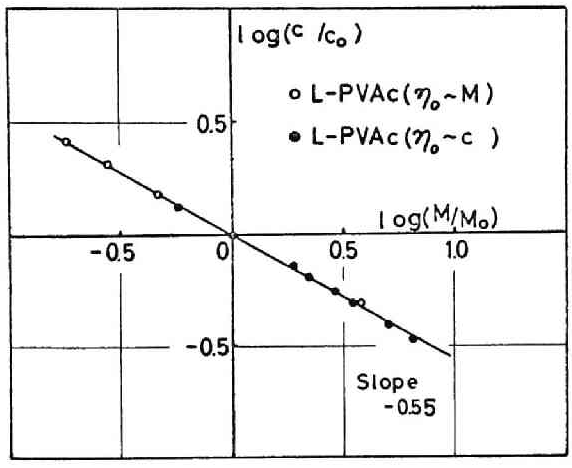

FIG.4-20. Relation between log (M/M_0) and log (c/c_0) for solutions of linear PVAc in EBK at 29°C. The slope of the line is -0.55.

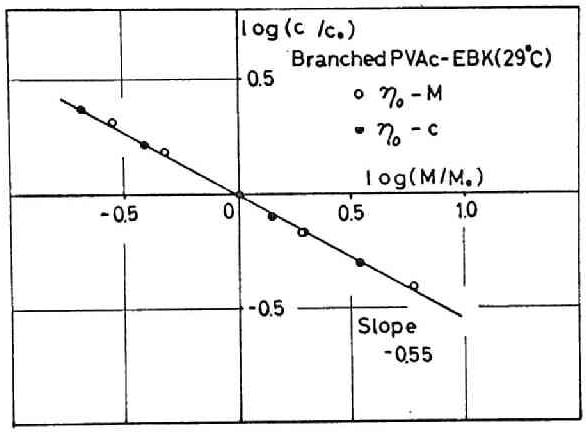

FIG.4-21. Relation between log (M/M_0) and log(c/c_0) for solutions of branched PVAc in EBK at 29°C. The slope of the line is -0.55.

These values of the slope are not always equal to 0.50, but they are much lower than those obtained for solutions in good solvents. Even 0.55 for PVAc is much closer to 0.50 than the previous value of 0.64. Ueda et al.[3] found that the θ-temperature for PVAc in EBK was 27°C., rather than 29°C.

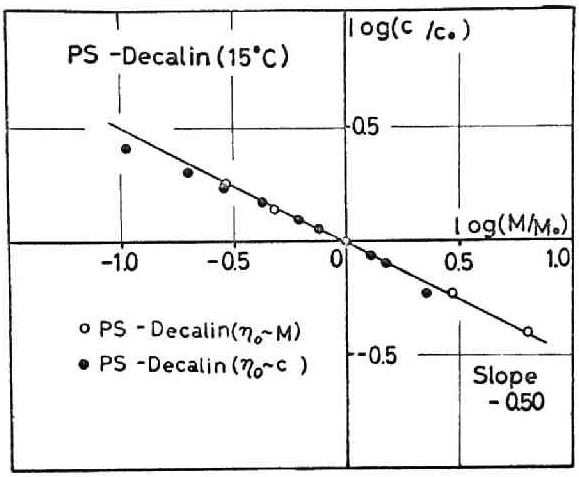

FIG.4-22. Relation between $\log(M/M_0)$ and $\log(c/c_0)$ for solutions of PS in decalin at 15°C. The slope of the line is -0.50.

4.2.4 Application of the Superposition to Other Data

The superposition principle described above was applied to some other existing viscosity data obtained for moderately concentrated polymer solutions in a wide range of molecular weight or concentration, in order to ascertain its universality.

Pezzin and Gligo[4] reported log η versus log c curves over wide range of concentration for the samples of polyvinyl chloride (PVC) having different molecular weights. The viscosity curves for the samples can be superposed well by the horizontal shift giving a smooth curve as shown in Fig.4-23. From the above-mentioned η versus concentration curves, the η versus M curves at different concentrations were redrawn, and the superposition was also applied to these curves. In Fig.4-24, the shift factor $\log(c/c_0)$ is plotted against $\log(M/M_0)$ for this system. The straight line in this figure has the slope of -0.74.

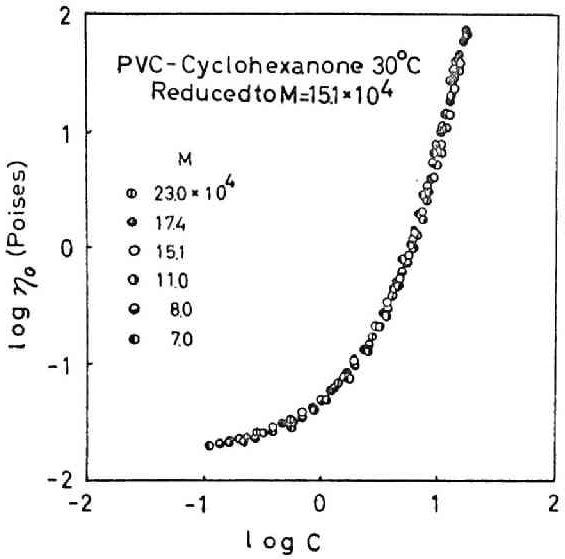

FIG.4-23. Master curve of log η_0 vs. log c for solutions of PVC in cyclohexanone at 30°C. The reference molecular weight is 151,000.

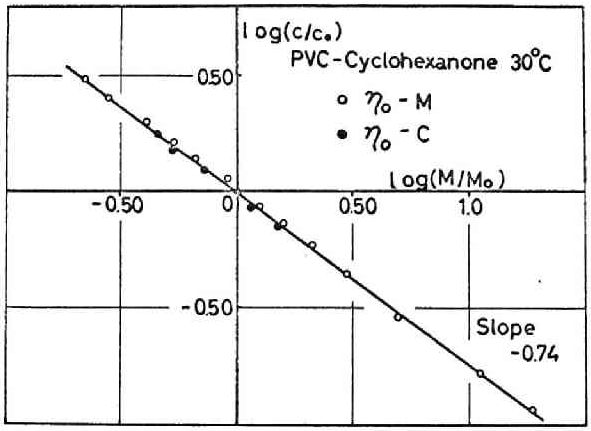

FIG.4-24. Relation between $\log(M/M_0)$ and $\log(c/c_0)$ for solutions of PVC in cyclohexanone at 30°C. The slope of the line is -0.74.

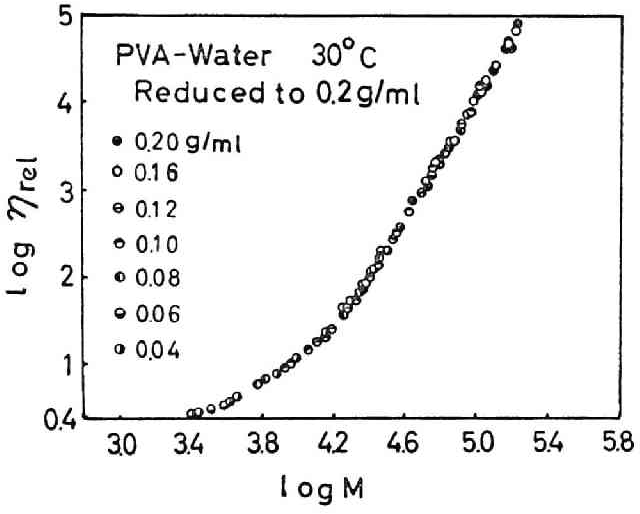

FIG.4-25. Mastercurve of log η_{rel} vs. log M for solutions of PVA in water at 30°C. The reference concentration is 0.2g/ml.

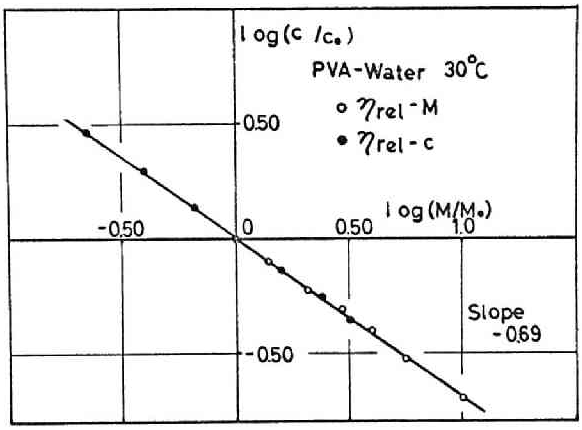

FIG.4-26. Relation between $\log(M/M_0)$ and $\log(c/c_0)$ for solutions of PVA in water at 30°C. The slope of the line is -0.69.

On the other hand, Oyanagi and Matsumoto[5] reported log η_{rel} vs. log M curves for aqueous solutions of polyvinyl alcohol (PVA) at various concentrations ranging from 0.04 to 0.20 g/ml. These curves and the redrawn log η_{rel} vs. log c curves are also superposed into smooth master curves. As an example, the master log η_{rel} vs. log M curve for this system is shown in Fig.4-25. Fig.4-26 shows a log-log plot of (c/c_0) and (M/M_0). The straight line in this figure has a slope of -0.69.

The superposition method was also applied to the data for polyisobutylene in xylene[6], for cellulose tributyrate in 1,2,3-trichloropropane [7] and for copolymer of acrylonitrile and methyl methacrylate in aqueous NaCNS[8]. These systems gave the β/α values of 0.63, 0.73 and 0.54, respectively.

4.2.5 Discussion on the Relation between Molecular Weight and Concentration

In the equivalent sphere model proposed by Onigi et al.[9], the radius of the equivalent sphere was assumed to be proportional to the square of the number of chain atoms per molecule, Z, namely, $r = k Z^{1/2}$. However, it will be more general to assume that $r = k Z^{(1/2)+\varepsilon}$, where ε is between 0 and 0.5, depending on the conbination of polymer and solvent, as well as the temperature. With this assumption, eq(4-4) can be derived in quite the same manner:

$$c Z^{(1/2)+3\varepsilon} = 300 v_0 M_0/8\pi k^3 N_0 \qquad (4\text{-}4)$$

were v_0 is the volume fraction of spheres, M_0 is the molecular weight of the monomer unit, and N_0 is Avogadro's number. When we assume that η_0 is constant at constant v_0, we get

$$c M^{(1/2)+3\varepsilon} = \text{const.} \quad (\text{at const. } v_0 \text{ or } \eta_0) \qquad (4\text{-}5)$$

The fact that the viscosity curves at different molecular weights or concentrations can be superposed well, as described above, lead to eq(4-6) for a given viscosity from eq(4-2):

$$c\,M^{\beta/\alpha} = \text{const. (at const. } \eta_0) \qquad (4\text{-}6)$$

This equation is the same as eq(4-5) when we put

$$(1/2) + 3\varepsilon = \beta/\alpha \qquad (4\text{-}7)$$

As to the relationship between molecular weight and concentration which determine the the viscosity, several investigators have given different equations of the same form as eqs(4-5) and (4-6) as follows:

Bueche[10] and Fox et al.[11]:

$$c\,M_c = \text{const.} \qquad M = M_c \qquad (4\text{-}8)$$

Bueche et al.[12]:

$$c\,M_c^{0.83} = \text{const.} \qquad M = M_c \qquad (4\text{-}9)$$

Ferry and others[2]:

$$c\,M^{0.68} = \text{const.} \qquad M > M_c \text{ or } c > c_c \qquad (4\text{-}10)$$

Onogi et al.[9] and Cornet[13]:

$$c\,M^{0.50} = \text{const.} \qquad c = c_c \qquad (4\text{-}11)$$

Here M_c and c_c denote the critical molecular weight and critical concentration. Eqs.(4-8)∿(4-11) correspond to the special case of eq(4-5) where 3ε is 0.50, 0.33, 0.18 and 0, respectively. According to experimental results described in Section 4.2.2∿4, eqs(4-5) and (4-6) hold for not only the critical points but also in wide ranges of molecular weight and concentration.

The values of β/α $(= \frac{1}{2} + 3\varepsilon)$ for the systems studied here are summarized in Table 4-II with values of a in the well-known equation, $[\eta]=KM^a$,

relating the intrinsic viscosity to the molecular weight for the same systems. The values of a were taken from the literature.[3]

TABLE 4-II

A COMPARISON OF $\beta/\alpha = (1/2) + 3\epsilon$ WITH a IN $[\eta] = KM^a$

System	Temp., °C	$\beta/\alpha = 1/2 + 3\epsilon$	α
Linear PVAc in MEK	30	0.64	0.71
Linear PVAc in EBK	29	0.55	0.50
Branched PVAc in MEK	30	0.64	
Branched PVAc in EBK	29	0.55	
PS in Toluene	40	0.72	0.72 (34°C, 45°C)
PS in Decalin (61.5% trans)	40	0.60	0.58 (73% trans)
	15	0.50	0.50
PMMA in MEK/Isopropanol (50/50 vol)	25	0.57	0.50
	35	0.55	
	45	0.56	
PMMA in Toluene	15	0.55	0.50 (10°C)
	25	0.55	0.56
	35	0.60	0.58
P(AN-MMA) in NaCNS aq.	30	0.54	
PVC in Cyclohexanone	30	0.74	0.77
PVA in Water	30	0.69	0.64

It is very interesting to note from Table 4-II that there is a good correlation between the values of a and β/α for all the systems studied. If one makes allowance for the considerable scattering of the a values obtained for a given system by different authors, this good correlation between β/α and a is rather surprising. This result indicates that chain molecules in moderately concentrated solutions maintain the same individuality as in dilute solutions.

It is necessary to touch on the limitation of the correlation between β/α and a. As will be described later in this chapter and also elsewhere[14], the α value increases more and more with increasing concentration at constant temperature, while β value probably does not exceed a constant value around 3.5. This fact clearly suggests that there may exist an upper limit of concentration above which the above correlation fails. The limit of concentration depends on the molecular weight and then can not be determined uniquely. However, it is believed that this limit of the correlation and then the superposition, should be a transition concentration from the moderately concentrated solution to the concentrated solution. The viscosity of the latter is dominated by the free volume.

Turning to lower concentrations, it seems clear that considerations that works for dilute polymer solutions cannot be applied to more concentrated solutions. Nevertheless, it is very surprising that β/α obtained from the viscosity data for such solutions is constant and seemingly equal to a obtained from those for dilute solutions. Even if we should employ the relative viscosity η_{rel} or specific viscosity η_{sp} instead of the viscosity itself, it is required that the above-mentioned superposition should be applied. Now, we will consider the Huggins type of expansion of the specific viscosity,

$$\eta_{sp} = [\eta]c\{1 + k'[\eta]c + k''[\eta]^2c^2 + \ldots \} \tag{4-12}$$

which can be rewritten as

$$\eta_{sp} = KM^ac\ [1 + K'M^ac + K''M^{2a}c^2 + \ldots\ ] \tag{4-13}$$

For very dilute solutions, this equation reduces to

$$\eta_{sp} = KM^ac \tag{4-14}$$

which is equivalent to eq(4-1) when $\alpha = 1$, $\beta = a$, and $\beta/\alpha = a$.

At higher concentrations, α in eq(4-1) should increase with increasing viscosity and reach as large a value as 5 or 6 for vinyl polymers in the entanglement region.[2,15] Therefore, β also should increase at the same rate as α does because $\beta/\alpha = a$ must be maintained. It is noteworthy that every term on the right-hand side of eq(4-13) satisfied this condition. From the log-log plots of viscosity against concentration and molecular weight, α and β were determined for the solutions of linear and branched PVAc and PS in different solvents and plotted against the viscosity in Figs.4-27, 4-28 and 4-29, respectively.

As seen from these figures, α and β increase at the same rate with increasing viscosity, giving a constant value of β/α, but the slope of the curves differs from system to system. For PS and the linear PVAc, α and β increase almost linearly first and then level off with increasing viscosity, while for the branched PVAc both α and β increase more rapidly at higher viscosities. For a particular polymer, the variation of solvent brings about a greater change in α than in β. The poorer the solvent, the steeper the curve of α. In other words, the effect of the concentration on the viscosity is more strongly dependent on the solvent power than that of the molecular weight.

As seen from the above discussions, α and β in eq(4-1) are not constants, but are functions of η_0. Nevertheless, the raio β/α remains constant. In recent years, the flow properties of polymer solutions have been investigated extensively and expressed in various manners by several authors[14~18]. It appears difficult to interrelate their expressions, but it is highly desired to consolidate divergent expressions into a simple but universal one.

FIG.4-27. Variation of α and β with log η_{rel} for linear PVAc in MEK and EBK.

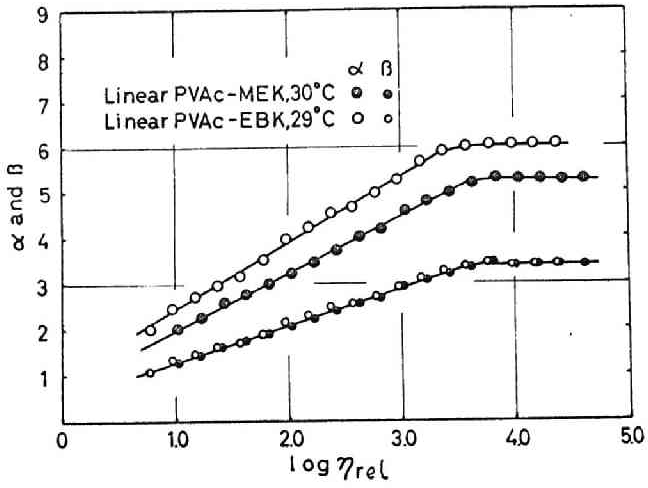

FIG.4-28. Variation of α and β with log η_{rel} for branched PVAc in MEK and EBK.

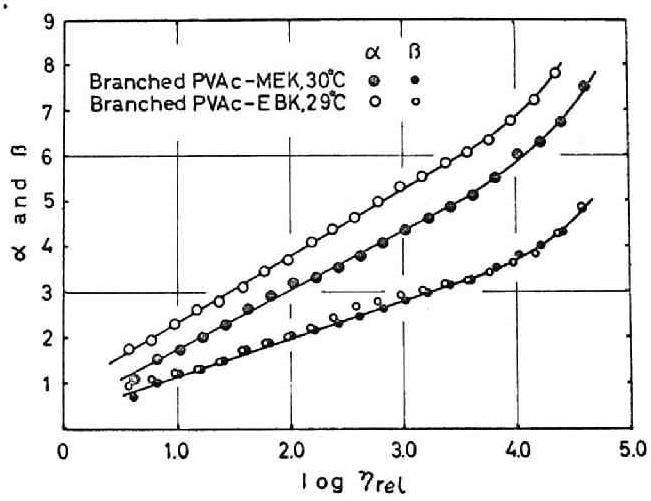

FIG.4-29. Variation of α and β with log η_{rel} for PS in toluene and decalin.

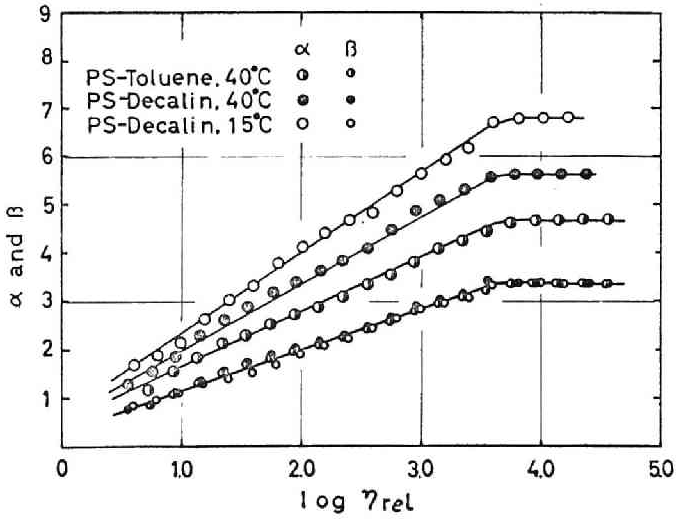

4.3 RHEOLOGICAL PROPERTIES OF MODERATELY CONCENTRATED SOLUTIONS

4.3.1 Rate of Shear Dependences of the Shear and Normal Stresses

In Figs.4-30 and 4-31, are shown the rate of shear (κ) dependences of shear stress σ_{12} and normal stress difference, $\sigma_{11} - \sigma_{22}$, for 4% solutions of anionic polystyrenes in chlorinated diphenyl (KC4; viscosity at 20°C = 6.0 poises) measured at 20°C. The molecular weights of the narrow-distribution polystyrenes used here, are tabulated in Table 2-II. The calculated values of $c[\eta]$ for these 4% solutions of L48, L44, L49 and L50 are, respectively, 4.93, 4.26, 3.64 and 2.66.

The shear stress was measured by means of the coaxial cylinder viscometer, and the normal stress difference was calculated from the extinction angle χ which was measured by flow birefringence method, as well as σ_{12} using eq(1-45). As is known in these figures, the slopes of log σ_{12} vs. log κ and log $(\sigma_{11} - \sigma_{22})$ vs. log κ curves are respectively 1.0 and 2.0 at the low rates of shear. This indicates that the η_0 and θ_0 values defined by eq(1-46) and eq(1-47) can be evaluated from these curves. Similar dependence curves for diethyl phthalate (DEP; viscosity at 20°C = 0.116 poises) solutions of anionic polystyrene (L48) at various concentrations are shown in Fig.4-32. Comparing Fig.4-30 with Fig.4-32, there is marked contrast that the log σ_{12} vs. log κ curves for different molecular weights seem to unite into a single curve at high shear region, while the similar curves for various concentrations do never. The κ value where the slope of σ_{12} and $\sigma_{11} - \sigma_{22}$ curves begin to concave downwards, that is, the onset of non-linear behavior, becomes lower with increasing molecular weight and concentration.

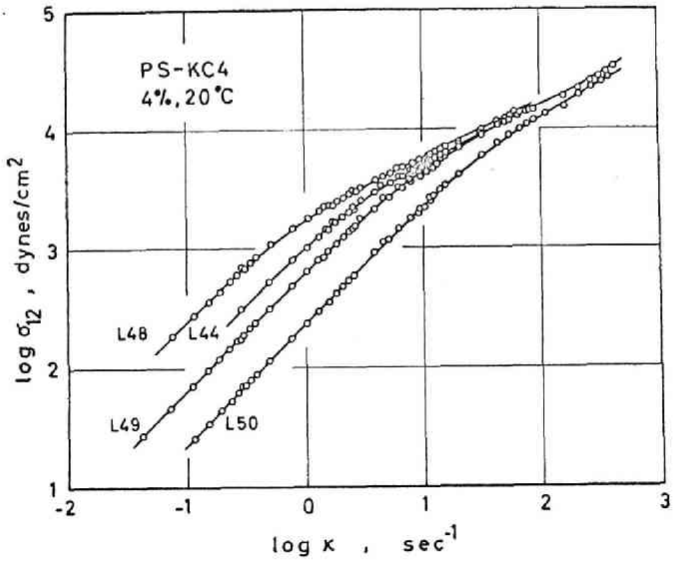

FIG.4-30. Rate of shear dependences of shear stress for 4% solutions of anionic polystyrenes having different molecular weights in chlorinated diphenyl (KC4) at 20°C.

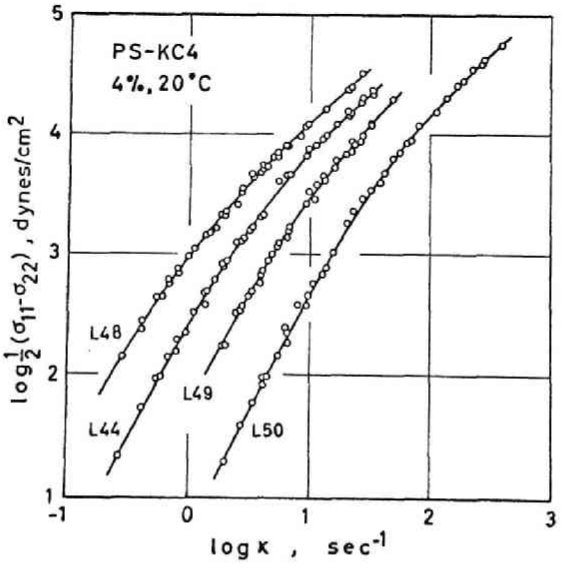

FIG.4-31. Rate of shear dependences of normal stress difference for 4% solutions of anionic polystyrenes having different molecular weights in chlorinated diphenyl (KC4) at 20°C.

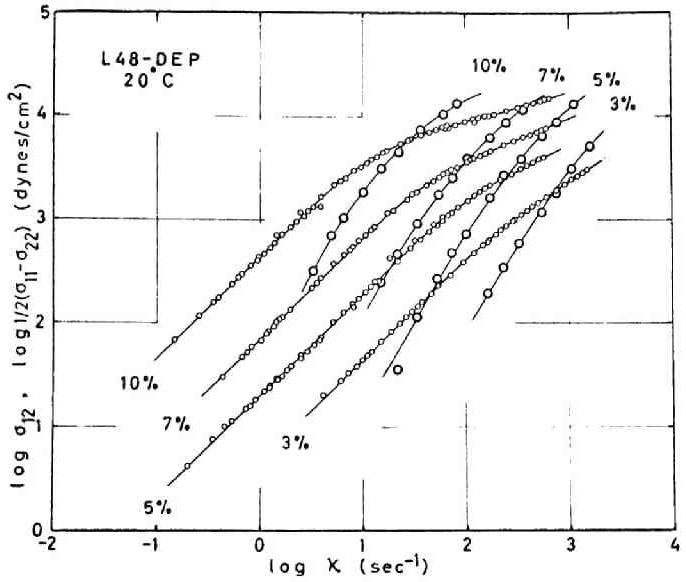

FIG.4-32. Rate of shear dependences of shear and normal stresses for anionic polystyrene (L48) solutions in diethyl phthalate (DEP) at various concentrations at 20°C.

4.3.2 Recoverable Elastic Strain

According to eqs(1-45), (1-49) and (1-50), the recoverable elastic strain s is given as cot 2χ , which can be determined by flow birefringence measurements. In Figs.4-33 and 4-34, log s thus evaluated is plotted against log σ_{12} for 3% solutions of polystyrenes of different molecular weights and for L48 solutions at various concentrations, respectively. These figures show that each log s vs. log σ_{12} curve can be approximated by a straight line having the slope of 1.0 at lower σ_{12}, but the curve deviates from the straight line with increasing σ_{12}. This means that the elastic deformation caused in polymer liquid moves from Hookian to non-Hookian with increasing the stress.[19] Furthermore, it is interesting that the all curves for 3% solutions turn downwards, but the curve for

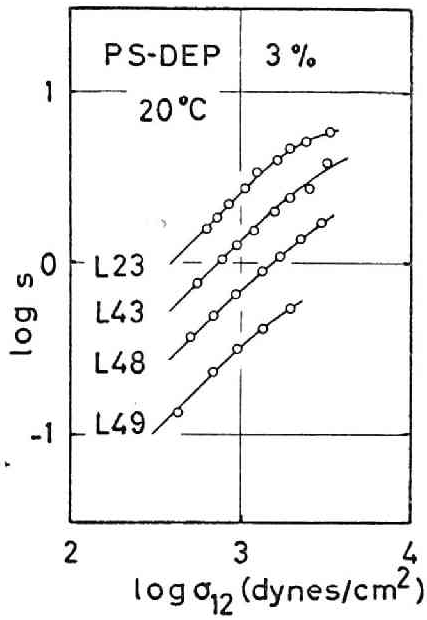

FIG.4-33. Log s plotted against $\log \sigma_{12}$ for 3% solutions of anionic polystyrenes having different molecular weights in diethyl phthalate (DEP) at 20°C.

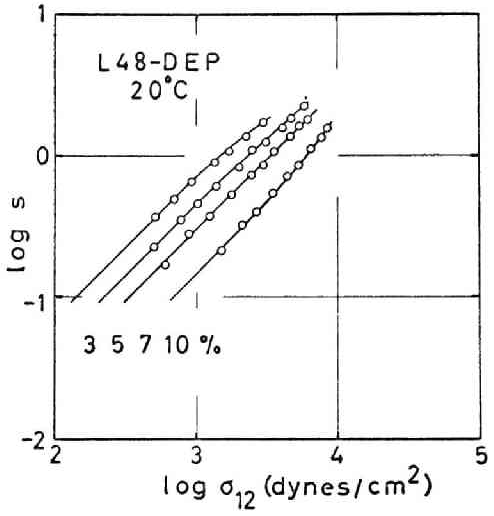

FIG.4-34. Log s plotted against $\log \sigma_{12}$ for anionic polystyrene (L48) solutions at various concentrations in diethyl phthalate (DEP) at 20°C.

10% solution upwards. On the other words, the rate-dependent compliance $J_e(\kappa)$ given by eq(1-49) decreases for 3% solution but increases for 10% solution, with increasing shear stress or rate of shear. Similar result to the latter behavior has been also found by Endo et al.[20] In Fig.4-35, the shear-stress-dependent functions, $\theta(\sigma)$,

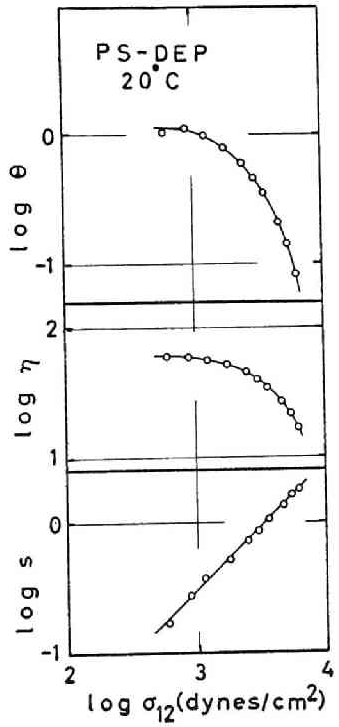

FIG.4-35. Shear stress dependences of $\theta(\sigma)$, $\eta(\sigma)$ and $s(\sigma)$ for 7% solution of anionic polystyrene (L48) in diethyl phthalate (DEP) at 20°C.

$\eta(\sigma)$ and $s(\sigma)$, are shown together for 7% solution of L48 in diethyl phthalate, for which s is proportional to σ_{12} as seen from Fig.4-34. Fig.4-35 indicates a very significant fact that the internal elastic strain for polymer liquid is still linear, even in the stress region where θ and η are bothly non-linear.

4.3.3 Zero-Shear Viscosity and Steady-State Compliance

The molecular weight dependence of zero-shear viscosity η_0 for the DEP solutions of anionic polystyrenes is given in Fig.4-36. The slopes of these curves are between 2.7 and 1.0, telling us the measurements being carried out for the moderately concentrated solutions. Further discussion on the molecular weight and concentration dependences of zero-shear viscosity will not be made here, since done extensively in Section 4.2. However, β/α value evaluated by the superposition of the curves in Fig.4-36, as well as the corresponding η_0 vs. c curves, was 0.51, suggesting that DEP is poor solvent for polystyrene.[19]

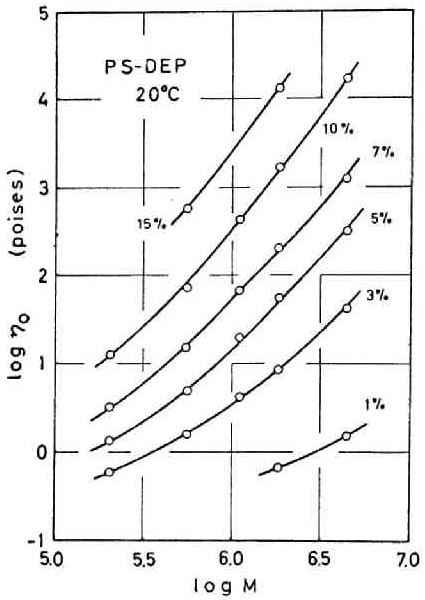

FIG.4-36. Molecular weight dependence of η_0 for the DEP solutions of anionic polystyrenes at various concentrations at 20°C.

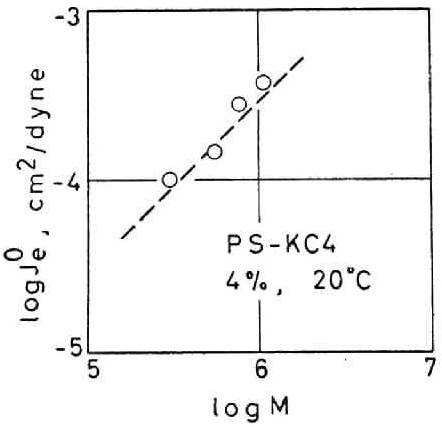

FIG.4-37. Molecular weight dependence of J_e^0 for 4% solutions of anionic polystyrenes in chlorinated diphenyl (KC4) at 20°C.

In Fig.4-37, the steady-state compliance J_e^0 calculated by eq(1-48) is plotted against molecular weight for 4% solutions of anionic polystyrenes in chlorinated diphenyl (KC4). The broken line in this figure represents the relation predicted by the Rouse theory or the FLW theory, eq(1-64). The experimental results agree with the prediction of the theories very well. The concentration dependences of steady-state compliance for polystyrene solutions are shown in Fig.4-38, where w_2 and ρ respectively denote the weight fraction of polymer in solution and the density of solution and then $w_2\rho$ is the concentration in g/ml. As seen from this figure, at lower concentrations, J_e^0 is inversely proportional to $w_2\rho$ and with increasing concentration, J_e^0 values become to decrease more rapidly. As will be shown in the next section, J_e^0 of concentrated solutions is inversely proportional to $(w_2\rho)^2$. Then the figure illustrates the transition between the two concentration ranges, clearly. More extensive investigations for the rheological properties of moderately concentrated solutions have been carried out by Osaki et al.[19,21,22]

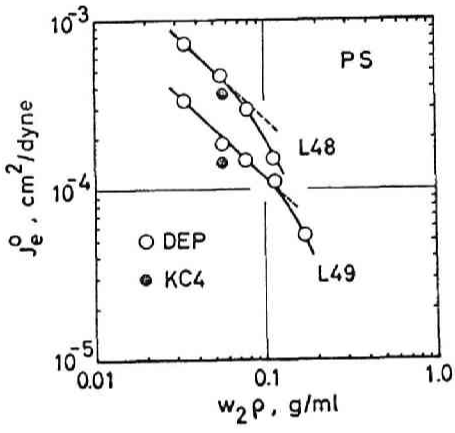

FIG.4-38. Concentration dependence of steady-state compliance for the anionic polystyrene (L48 and L49) solutions in DEP. Closed circles represent the data for solutions in KC4.

4.4 RHEOLOGICAL PROPERTIES OF CONCENTRATED SOLUTIONS

4.4.1 Effect of Temperature and the Vogel Parameters

As shown in Sections 1.3 and 1.4, almost all the rheological properties of polymer liquid depend not only on the molecular weight and concentration but also on the segmental friction factor ζ, which is strongly dependent on concentration and temperature.[2] Therefore, the concentration dependence of rheological properties of the concentrated solutions must be discussed in the iso-free-volume state.

The shift factor a_T obtained in the course of the time-temperature superposition for frequency dependence curve of viscoelastic functions, G' and G" of MC1 series and the bulk polymer 715 is plotted against temperature in Fig.4-39. The solution samples used here, can be referred to Table 2-IX. The reference temperature T_r was chosen arbitrarily for all samples. The polt of $-\log a_T/(T - T_r)$ against $(T - T_r)$ for each sample can be represented by a straight line, and hence it is clear that the temperature dependence of the shift factor shown in this figure can be expressed by the WLF type equation, eq(1-81). The reference temperature T_r and two constants c_1^r and c_2^r in this equation are tabulated in Table 4-III, as well as the Vogel parameters α_f and T_0, and T_r' caluculated from eqs(1-81) and (1-78). Here, T_r' is the temperature at which each solution has the same fractional free volume of 0.062, as that of bulk polymer 715

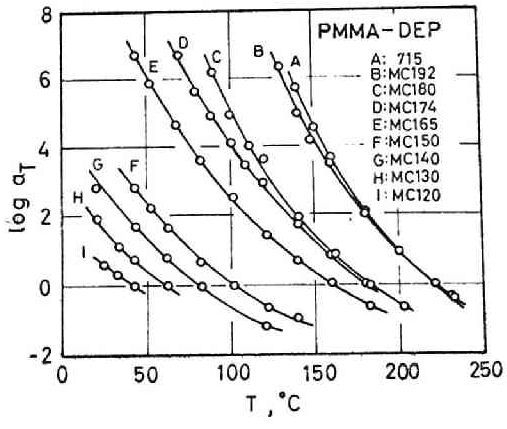

FIG.4-39. Temperature dependence of shift factor a_T for bulk PMMA (715) and its solutions(MC1 series). The last two figures in sample code represent the wt% of polymer.

TABLE 4-III

REFERENCE TEMPERATURE T_r, WLF CONSTANTS c_1^r AND c_2^r, THE VOGEL PARAMETERS α_f AND T_0, AND THE TEMPERATURE CORRESPONDING TO f = 0.062 FOR BULK PMMA (715) AND ITS SOLUTIONS (MC1 SERIES)

Sample	w_2	T_r(°C)	c_1^r	c_2^r	$\alpha_f x10^4$	T_0(°C)	T_r'(°C)
715	1.00	220	7.00	173	3.59	47.2	220
MC192	0.92	221	6.94	183	3.43	38.4	219
MC180	0.80	182	6.99	181	3.43	1.0	182
MC174	0.74	180	6.71	196	3.29	-16.0	169
MC165	0.65	160	6.50	209	3.20	-48.7	145
MC150	0.50	102	7.06	205	3.01	-103	104
MC140	0.40	82	6.99	195	3.19	-112	82.7
MC130	0.30	63	6.67	202	3.22	-139	53.5
MC120	0.20	43	6.25	205	3.39	-162	21.0

TABLE 4-IV

REFERENCE TEMPERATURE T_r, THE WLF CONSTANTS c_1^r AND c_2^r, AND THE VOGEL PARAMETERS α_f AND T_0, FOR PMMA SOLUTIONS (MC2 SERIES) AND THE SOLVENT DEP

Sample	w_2	T_r(°C)	c_1^r	c_2^r	$\alpha_f x10^4$	T_0(°C)
MC205	0.05	0	3.13	112	12.5	-112
MC202	0.02	0	2.98	111	13.1	-111
MC201	0.01	0	2.60	92.3	18.1	-92.3
DEP	0.00	0	2.42	84.1	21.4	-84.1

at 20°C. This condition is referred to as the iso-free-volume state, where each polymer in solution has the same segmental friction factor. The parameters evaluated from the temperature dependence of zero-shear viscosity are shown in Table 4-IV for MC2 series and the solvent, DEP. T_r', T_0 and α_f are plotted against the weight fraction of polymer, w_2, in Fig. 4-40. Similar results for SC2 series as well as the bulk polymer L50 and the solvent, chlorinated diphenyl KC5, are shown in Table 4-V and Fig.4-41.

There is remarkable resemblance between the results illustrated in Fig.4-40 and Fig.4-41. That is, with decreasing concentration, T_r' and T_0 decreases at higher concentrations and after passing through a minimum they increase at lower concentrations. The temperature coefficient of the fractional free volume, α_f, is almost constant at concentrations ranging from w_2=1.0 to 0.2. At lower concentrations, however, α_f increases rapidly with decreasing w_2. The critical concentration of entanglement couplings for the both system is probably located at around w_2=0.2, as will be discussed later. From the results shown in Figs.4-40 and 4-41, it concluded that α_f of polymer solutions is almost constant in the entanglement region and changes in the low concentration region where no entanglement can be formed in the solution. This constancy of α_f is also reflected on the fact that the difference between T_r' and T_0 is almost constant in entanglement region, as seen from these figures. The fractional free volume of bulk PMMA at glass temperature T_g was calculated to be 0.021, assuming T_g = 105°C. This value is close to the well-known value of 0.025 and 0.026 obtained for the anionic PMMA in the previous chapter (see Table 3-V). However, the value is rather different from the literature value of 0.013[2]. The value for bulk polystyrene is given in

Table 3-IV to be 0.028 at T_g = 100°C.

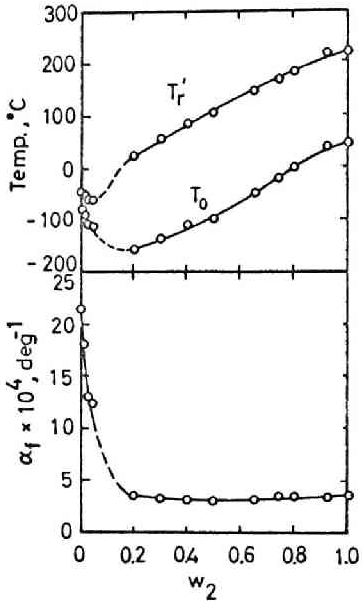

FIG.4-40. T_r', T_0 and α_f plotted against w_2 for bulk PMMA(715), its solutions(MC1 and MC2 series) and the solvent DEP.

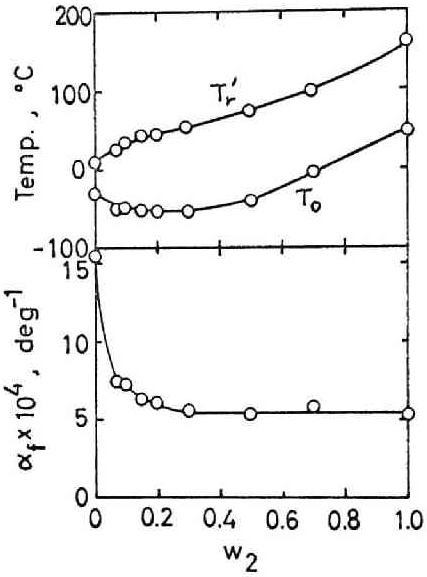

FIG.4-41. T_r', T_0 and α_f plotted against w_2 for bulk polystyrene(L50), its solutions(SC2 series) and the solvent KC5.

TABLE 4-V

REFERENCE TEMPERATURE T_r, THE WLF CONSTANTS c_1^r AND c_2^r, THE VOGEL PARAMETERS α_f AND T_0, AND T_r' AT f = 0.0608 FOR POLYSTYRENE(L50), ITS SOLUTIONS(SC2 SERIES) AND THE SOLVENT KC5.

Sample	w_2	T_r(°C)	c_1^r	c_2^r	$\alpha_f \times 10^4$	T_0(°C)	T_r'(°C)
L50	1.00	-	-	-	5.42	47.9	160.0
SC270	0.70	50	13.83	53.6	5.86	-3.6	100.0
SC250	0.50	50	9.28	88.6	5.28	-40.5	75.2
SC230	0.30	50	7.50	103.2	5.61	-53.2	55.2
SC220	0.20	50	6.84	103.4	6.14	-53.5	45.6
SC215	0.15	50	6.70	102.0	6.35	-52.0	43.8
SC210	0.10	50	6.06	99.0	7.23	-49.1	35.0
SC207	0.07	50	5.45	105.8	7.53	-55.9	24.8
KC5	0.00	50	3.52	79.6	15.5	-29.6	9.6

4.4.2 Frequency Dependence of Viscoelastic Functions

When we compare the frequency dependence curves of polymer solutions, it is important to compare them in the iso-free-volume state, where the monomeric friction factor is kept constant. In Fig.4-42 are shown the master curves of G' for the polymer 715 and its solutions at different concentrations in the iso-free-volume state. The abscissa of the figure is the reduced angular frequency ωa_T, and the reference temperatures were tabulated in Table 4-IV as T_r'. As is evident from this figure, master curves for highly concentrated solutions show the rubbery plateau and terminal zone clearly. The height of the rubbery plateau becomes lower and lower, and the terminal zone shifts to higher frequency side, as concentration decreases. The G' curves for solutions of low concentrations, such as MC130 and MC120, seem to have the rubbery plateau. This suggests that the critical concentration for entanglement couplings is probably located at about $w_2 = 0.2$. Although it is not so clear from Fig.4-42, the transition zone seems to be slightly dependent on the polymer concentration. The master curves for the loss modulus G" at f = 0.062 are shown in Fig.4-43. The frequency dependence curves of G" for samples having higher concentrations show maxima in the intermediate region between the terminal and rubbery zones. Such maxima enable us to calculate the quasi-equilibrium modulus by the integration method eq(3-5) proposed by Sanders et al.[23] The results for SC2 series are almost the same and then similar descriptions are not repeated here.

4.4.3 Rheological Behavior in the Terminal Zone

The concentration dependence of zero-shear viscosity η_0 for PMMA solutions (MC1 series) and polystyrene solutions (SC2 series) are

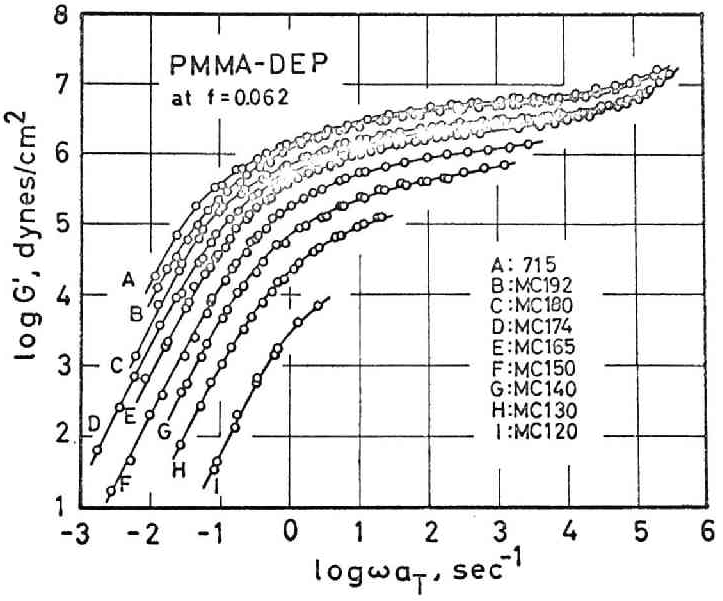

FIG.4-42. Master curves of G' for bulk PMMA(715) and its solutions (MC1 series) at f = 0.062.

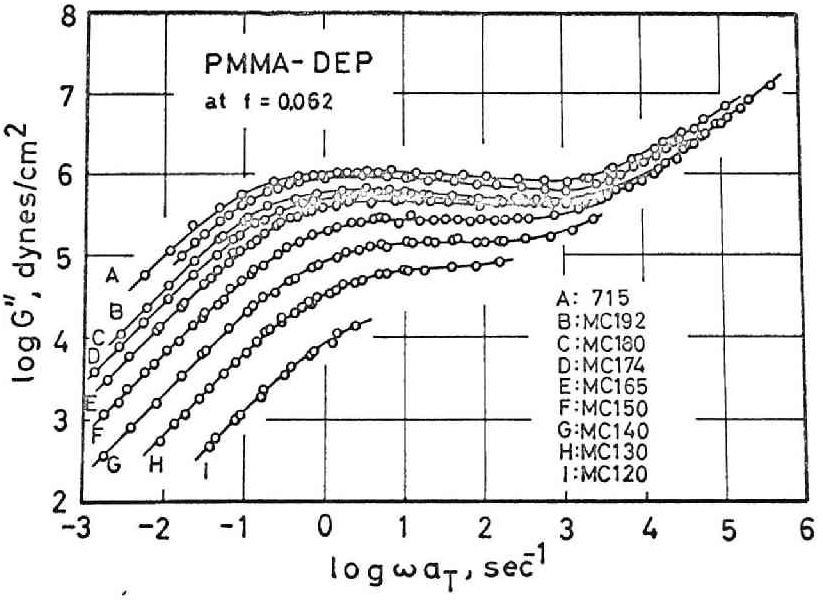

FIG.4-43. Master curves of G" for bulk PMMA(715) and its solutions (MC1 series) at f = 0.062.

respectively shown in Figs.4-44 and 4-45, where η_0 is defined by eq(1-46). In these figures, the closed and open circles represent, respectively, the zero-shear viscosities for the solutions at a constant temperature ($_T$ = 220°C for PMMA and 50°C for PS), and in the iso-free-volume state (f = 0.062 for PMMA and 0.0608 for PS). As the abscissa, in Fig.4-44, the weight fraction of polymer in solution, w_2, is employed instead of $w_{2\rho}$ or volume fraction of polymer, ϕ_2, while $w_{2\rho}$ is used in Fig.4-45. The densities of the solvent DEP and the solute polymer PMMA are respectively 1.12 and 1.17 at room temperature. The thermal expansion coefficient of these solutions can be estimated to be around 5×10^{-4} from the α_f values shown in Table 4-IV. Terefore the density of each solution at 220°C is close to unity, and w_2, $w_{2\rho}$, and ϕ_2 give almost the same value when we assume the additivity of volume in mixing. And hence the use of these different concentrations as the abscissa bears no serious difference in the concentration dependence curves of viscoelastic parameters which will be disscussed hereafter.

As shown in Fig.4-44, the concentration dependence of η_0 for PMMA at 220°C (closed circles) gives a smooth curve, and its slope varies from 4 at lower concentrations to 17 at higher concentrations; η_0 is proportional to $w_2^{4\sim17}$ at w_2=0.2~1.0. The plot of log η_0 against log w_2 in the iso-free-volume state at f = 0.062, however, can be represented by a straight line having the slope of 4.0 over the entire range of concentration; η_0 is proportional to $w_2^{4.0}$ at f = 0.062. This value of the exponent of w_2 coincides well with that of molecular weight (M) in the relation, $\eta_0 \propto M^{4.0}$, found previously in Fig.3-14. This behavior of η_0 seems to support the suggestion of Fox et al.[10] that $\eta_0$can be expressed by the power dependence of ($M\ \phi_2$): η_0 should be proportional to $(M\phi_2)^{4.0}$ in this

case. In the case of polystyrene solutions, as shown in Fig.4-45, the concentration dependence of the viscosity at 50°C (closed circles) becomes more and more remarkable with increasing the concentration; η_0 is proportional to $(w_2\rho)^{\sim 40}$ at $w_2 = 0.7$, owing to the low reference temperature. In the iso-free-volume atate, the viscosity of polystyrene solutions is proportional to $(w_2\rho)^{5\sim 6}$ as shown in Fig.4-45. This exponent seems to be too high as compared with that for molecular weight, 3.7, obtained from Fig.3-32.

In Figs.4-46 and 4-47 are shown the concentration dependences of steady-state compliance J_e^0 defined by eq(1-48), for the PMMA and polystyrene solutions, respectively. It is clear from these figures, that the dependence of J_e^0 on concentrations for the concentrated polymer solutions can be represented by a straight line having the slope of -2. Furthermore, as seen from Fig.4-47, the dependence of the steady-state compliance on concentration becomes more weak at lower concentrations. This behavior in low concentration region in this figure seems to be smoothly connected with that in higher concentration region in Fig.4-38, taking account of the difference in the molecular weights of the samples employed.

4.4.4 Rheological Behavior in the Rubbery Zone

The quasi-equilibrium modulus of the entanglement network, G_{eN}^0, denotes the height of the rubbery plateau in the frequency dependence curve of G'. The value of G_{eN}^0, as well as the entamglement compliance J_{eN}^0, can be related to the average molecular weight between entanglement coupling loci, M_e, by eq(1-51), in which $w_2\rho$, instead of ρ, must be used for the polymer solutions. The concentration dependence of J_{eN}^0 for PMMA

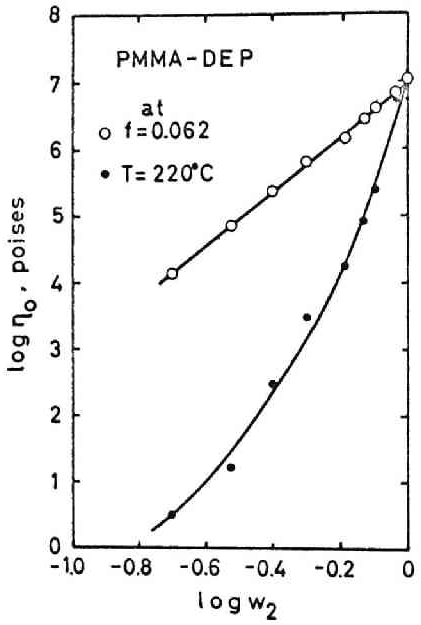

FIG.4-44. Concentration dependence of zero-shear viscosity η_0 for PMMA solutions in DEP at 220°C (closed circles) and f = 0.062 (open circles).

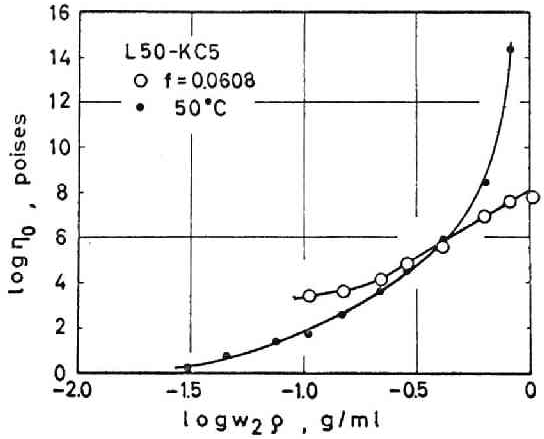

FIG.4-45. Concentration dependence of zero-shear viscosity η_0 for PS solutions in KC5 at 50°C (closed circles) and f=0.0608 (open circles).

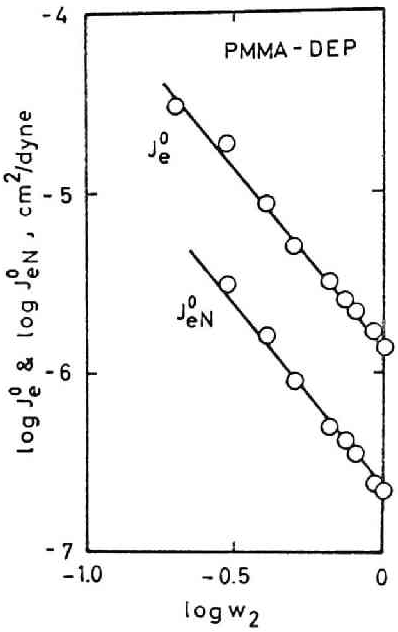

FIG.4-46. Concentration dependence of steady-state compliance J_e^0 and entanglement compliance J_{eN}^0 for PMMA solutions in DEP.

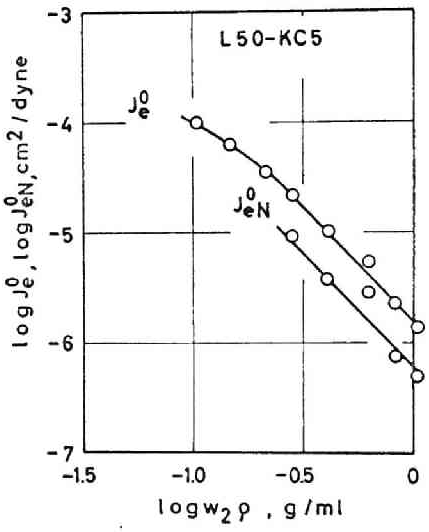

FIG.4-47. Concentration dependence of steady-state compliance J_e^0 and entanglement compliance J_{eN}^0 for PS solutions in KC5.

and polystyrene solutions are compared with those of the steady-state compliance J_e^0 in Figs.4-46 and 4-47, respectively. J_{eN}^0 is also inversely proportional to the square of the concentration. This experimental result means that the average molecular weight between entanglement coupling loci M_e is in proportion to the reciprocal of the concentration. It is very interesting that J_e^0 is 5∿6 times higher than J_{eN}^0 for the PMMA solutions, while it is 2∿3 times for polystyrene solutions. The similar result was pointed out in Section 3.5 for the bulk polymers.

REFERENCES

1. J. D. Ferry, Lecture Note for Viscoelastic Properties of Polymers, at Kyoto University, 1968.
2. J. D. Ferry, "Viscoelastic Properties of Polymers", 2nd ed., John Wiley New York, 1970.
3. M. Kurata, M. Iwama, and K. Kamada, "Polymer Handbook", J. Brandrup and E. H. Immergut, Ed., John Wiley, New York, 1966, Capter IV.
4. G. Pezzin and N. Gligo, J. Appl. Polym. Sci., 10, 1 (1966)
5. Y. Oyanagi and M. Matsumoto, J. Colloid Sci., 17, 426 (1962)
6. M. F. Johnson, W. W. Evans, I. Jordan, and J. D. Ferry, J. Colloid Sci., 7, 498 (1952)
7. R. F. Landel, J. W. Berge, and J. D. Ferry, J. Colloid Sci., 12, 400 (1957)
8. S. N. Chinai and W. C. Schneider, J. Polym. Sci., Part A, 3, 1359 (1965)
9. S. Onogi, T. Kobayashi, Y. Kojima, and Y. Taniguchi, J. Appl. Polym. Sci., 7, 847 (1963)
10. F. Bueche, "Physical Properties of Polymers", John Wiley, New York, 1961, p.378.

11. G. C. Berry and T. G. Fox, Adv. Polym. Sci., 5, 261 (1968)

12. F. Bueche, C. J. Coven, and B. J. Kinzig, J. Chem. Phys., 39, 128 (1963)

13. C. F. Cornet, Polymer, 6, 373 (1965)

14. G. C. Berry, J. Phys. Chem., 70, 1194 (1966)

15. S. Onogi, I. Hamana, and H. Hirai, J. Appl. Phys., 29, 1503 (1958)

16. L. Utracki and R. Simha, J. Polym. Sci., Part A, 1, 1089 (1963)

17. L. Utracki and R. Simha, J. Phys. Chem., 67, 1052 (1963)

18. T. G. Fox, J. Polym. Sci., Part C, 9, 35 (1965)

19. K. Osaki, Ph. D. Thesis, Kyoto University, 1968.

20. H. Endo, T. Fujimoto, and M. Nagasawa, J. Polym. Sci., Part A2, 9, 345 (1971)

21. K. Osaki, M. Kurata, and M. Tamura, Polym. J., 1, 334 (1970)

22. Y. Einaga, K. Osaki, M. Kurata, and M. Tamura, Macromolecules, 4, 87 (1971)

23. J. F. Sanders and J. D. Ferry, Macromolecules, 2, 440 (1969)

CHAPTER 5

Rheological Properties of Blends of Polymers

5.1 INTRODUCTION

Many investigations of the effect of molecular weight distribution on the rheological properties of amorphous polymers have revealed that the rheological properties in the terminal and rubbery zones are strongly affected by the molecular weight distribution.[1] In Chapter 3, the viscoelastic properties of anionic polymers having narrow distributions were reported, and it was found that the change from the rubbery to the flow region is very sharp, and that the distribution of relaxation times corresponding to entanglement slippage is very narrow.

In general, the effect of molecular weight distribution on the rheological properties of polymers can be studied either employing polymer samples having a well-defined continuous distribution of molecular weights or using binary blends composed of the same species of polymers having different molecular weights. With broad-distribution polymer, however, no concrete result can be expected, because parameters to describe the shape or breadth of the distribution can hardly be found at present. In studies with blend samples, on the other hand, some parameters such as the molecular weights of the components and the blending ratio are known. However, most studies of the rheological properties of binary blends hitherto carried out did not afford sufficient information to serve for quantitative treatment of the effect of blending or molecular weight distribution, mainly because of the considerably broad distribution of

the component polymers employed, even though some of them were fractionated. Accordingly, in order to study successfully the effect of molecular weight distribution on the viscoelastic properties of blends, the component polymers should have so narrow distribution that the effect of the distribution is within experimental errors.

In the present chapter, viscoelastic properties have been measured for blends of narrow-distribution polymers having different molecular weights, and the results have been compared with those obtained with the individual components to find a quantitative relationship between the rheological properties and the molecular weight distribution. A second aim of this study is to contribute to the development of the concept of entanglement couplings of macromolecular chains by clarifying the effect of blending of narrow-distribution polymers having different molecular weights on rheological properties in the rubbery and terminal zones.

5.2 FREQUENCY DEPENDENCES OF VISCOELASTIC FUNCTIONS

5.2.1 Effect of Molecular Weight Distribution

In Fig.5-1, master curves of storage shear modulus G' and loss modulus G" of the narrow-distribution polystyrene L15 are compared with those of the broad-distribution polystyrene PS7 (see Table 2-II). This figure reveals that the viscoelastic functions depend strongly on the molecular weight distribution, especially in the terminal and rubbery plateau zones. The log G" vs. log ω curve for a narrow-distribution polystyrene has a peak at the end of the rubbery zone, while that for the broad-distribution polymer does not. Another remarkable difference between the two polymers is that the curve for the narrow-distribution polymer shows a sharp break at the transition from the rubbery to the

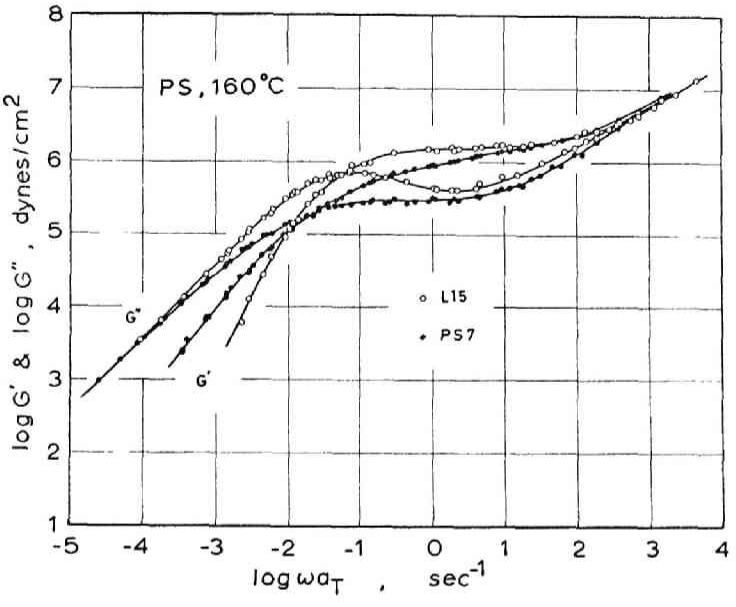

FIG.5-1. Frequency dependences of G' and G'' for the narrow-distribution polystyrene L15 and the broad-distribution PS7, reduced to 160°C.

terminal zone, in marked contrast to that for PS7. The G' curve for PS7 extends to lower frequencies owing to high molecular weight fraction included in it. All the curve unite in the transition zone, indicating that the viscoelastic properties are not affected by the molecular weight distribution at high frequencies or short time scales.

5.2.2 Viscoelastic Functions for Polymer Blends

The master curves of G' for the blends BB15 and BT1 are shown in Fig.5-2, together with those for the components, L18, L16 and L9. The G' curve for L18 has a longer and flatter plateau as compared with that of L16. The curve for L9, having a molecular weight lower than M_c, shows no plateau and diverges from the others in the transition zone owing to the excess free volume. One of the binary blends, BB15, which

contains equal amounts of L18 and L16, manifests a "two-step" plateau in the rubbery zone. The lower step on the low frequency side is clearly lower than the higher step, which is as high as the plateau of the components. The G' curve for BT1, composed of three components of equal amounts, also shows a two-step plateau; both steps are lower than those of BB15 because the contents of L18 and L16 are lower and the other component, L9, does not contribute the development of the plateau but only to the shift of the transition zone.

As seen in Fig.5-3, the master curves of G" for the blends also show two peaks, though they sometimes appear rather as shoulders, while those for each component show only one peak. The two peaks for the blends seem to correspond to those of the components. Figs.5-2 and 5-3 suggest the existence of two groups of relaxation times associated with entanglement slippage in the binary blend of narrow-distribution polymers having molecular weights higher than the critical molecular weight for entanglement couplings, M_c.

Fig.5-4 shows the frequency dependences of G' for the binary blend sample BB25 and its components. The molecular weights of the components of this blend are not very different from each other but are higher than M_c, as seen from Table 2-X, as well as Fig.2-2. Therefore, no significant change due to the blending is observed in the frequency dependences. As mentioned in Section 3.2.5, the viscoelastic functions such as dynamic viscosity $\eta' = G''/\omega$ and G' of binary blends can be superposed with respect to the blending ratio so long as the molecular weight distribution is not changed very much by the blending. The above result for BB25 is a case where the molecular weight distributions of the components overlap, and little change in viscoelastic functions is brought about by the blending.

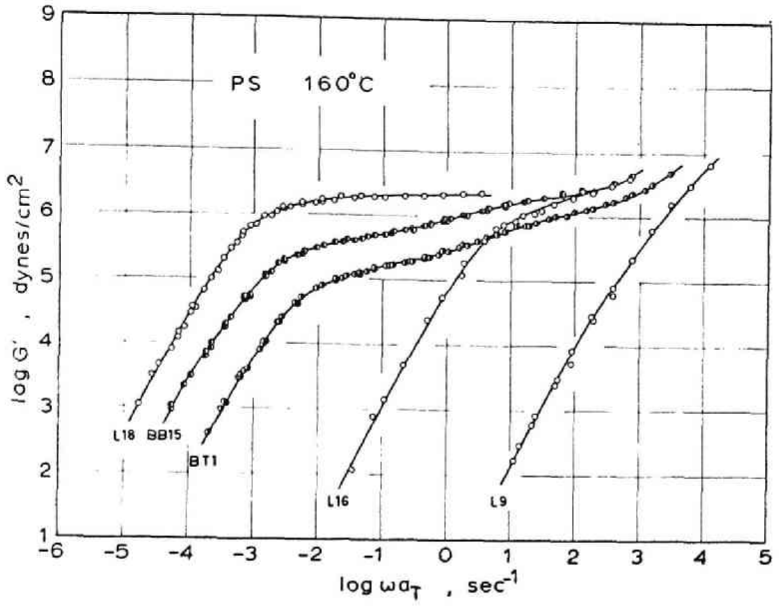

FIG.5-2. Frequency dependences of G' for BB15, BT1, and their components, reduced to 160°C.

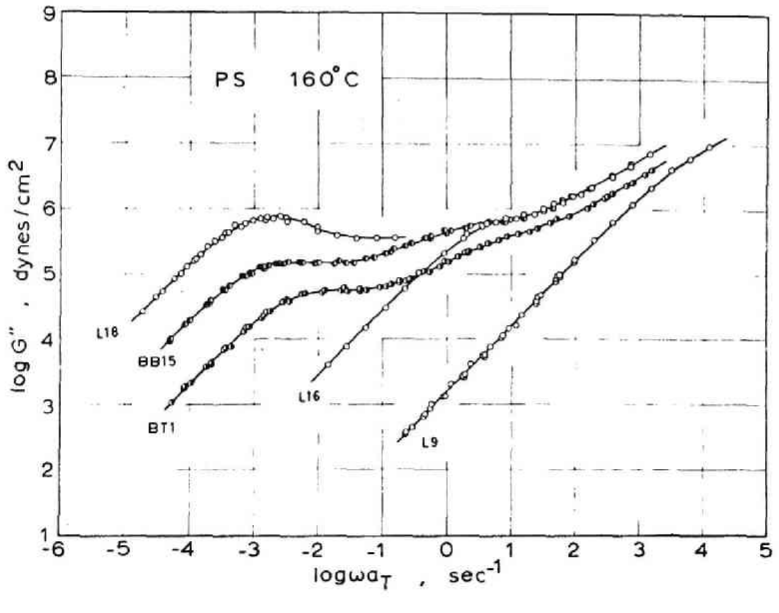

FIG.5-3. Frequency dependences of G'' for BB15, BT1, and their components, reduced to 160°C.

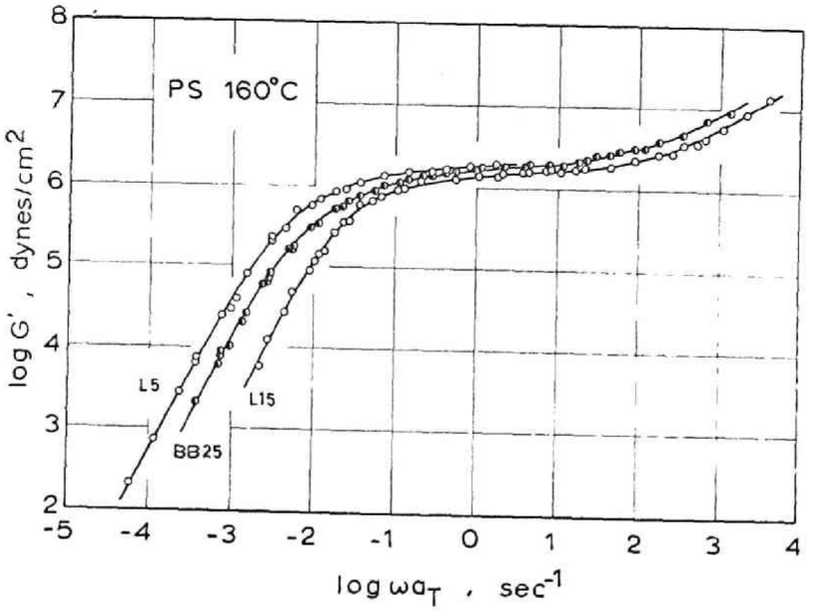

FIG.5-4. Frequency dependences of G' for BB25 and its components, reduced to 160°C.

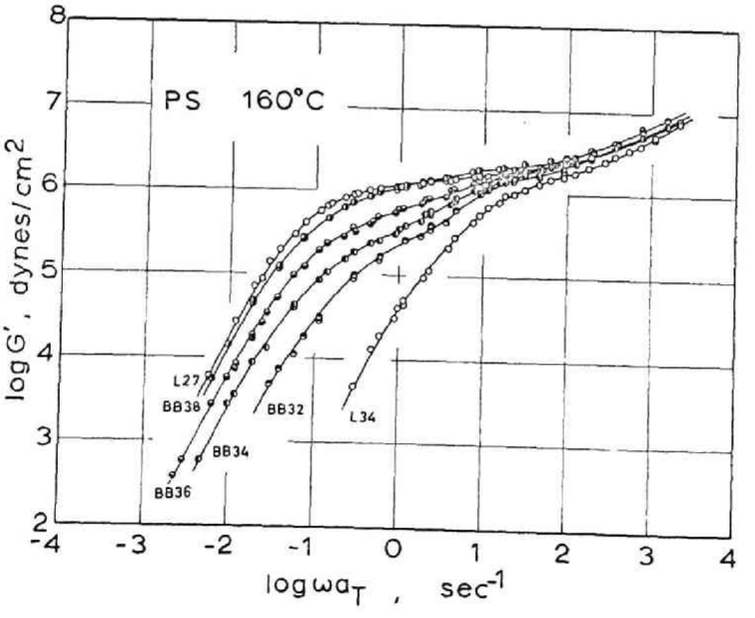

FIG.5-5. Frequency dependence of G' for the BB3 series and the components, reduced to 160°C.

In Fig.5-5 are shown similar curves for the binary blend series BB3, which include components having molecular weights above M_c and show bimodal distribution of molecular weight as seen in Fig.2-3. The behavior of these blends is intermediate between those of BB15 and BB25. Two-step plateaus are found for this series, especially for the blends, such as BB32 and BB34, containing small amounts of the high molecular weight component L27. The last figure of the sample code for binary blends used in this study represents ten times the weight fraction of the high molecular weight component.

In Figs.5-6 ∿ 5-13 are shown the frequency dependences of G' and G" for the various binary blend series, such as BB4, BB5, BB6, and BB7, as well as their components. The molecular weights and the ratios for binary blend series can be referred to Table 2-X.

For BB4 series, the molecular weight of lower molecular weight component (M_1) is higher than M_c and the ratio M_2/M_1 is fairly large (=7.10). Then the viscoelastic functions for this series clearly show the two-step plateaus. The behavior of BB5 series, for which M_1 is almost equal to M_c, seems to be in a critical condition for the two-step plateau. The curves BB6 sreies, for which M_1 is lower than M_c show such a behavior no longer, but have single plateaus likely to those of concentrated solutions as described in Section 4.4.2. G' and G" curves for the BB6 series were reduced to T'_r, the temperature at which each system has the same fractional free volume, f = 0.0608 here, because the lower molecular weight component L53 has excess free volume. For BB7 series, the M_1 is higher than M_c but M_2/M_1 is rather small (=2.18) and then the behavior resembles that of BB2 series.

In Figs.5-14 ∿ 5-17 are shown master curves of the storage shear modulus

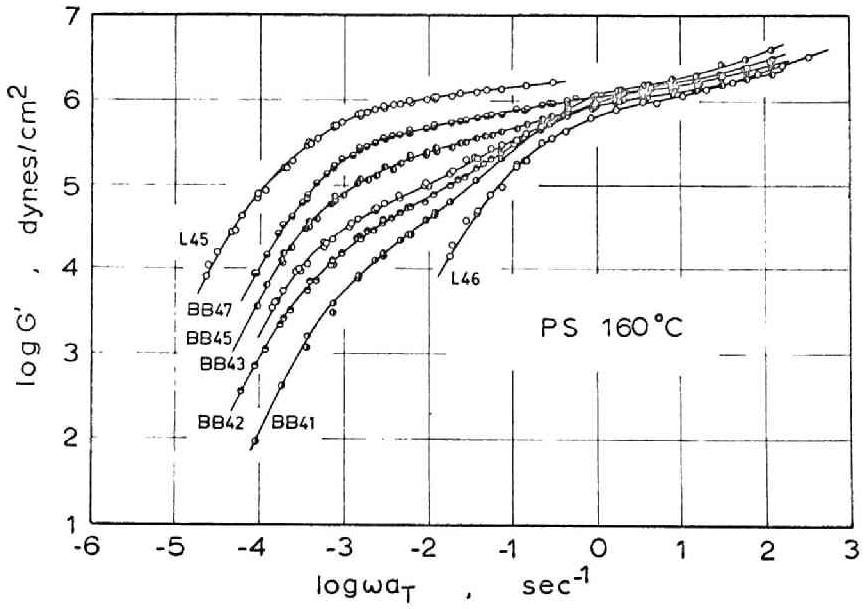

FIG.5-6. Frequency dependences of G' for the BB4 series and the components, reduced to 160°C.

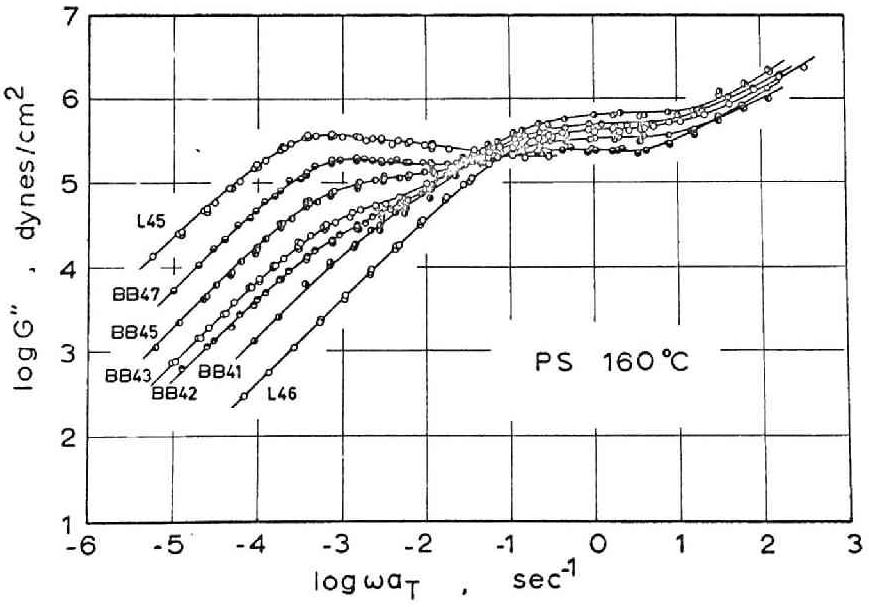

FIG.5-7. Frequency dependences of G" for the BB4 series and the components, reduced to 160°C.

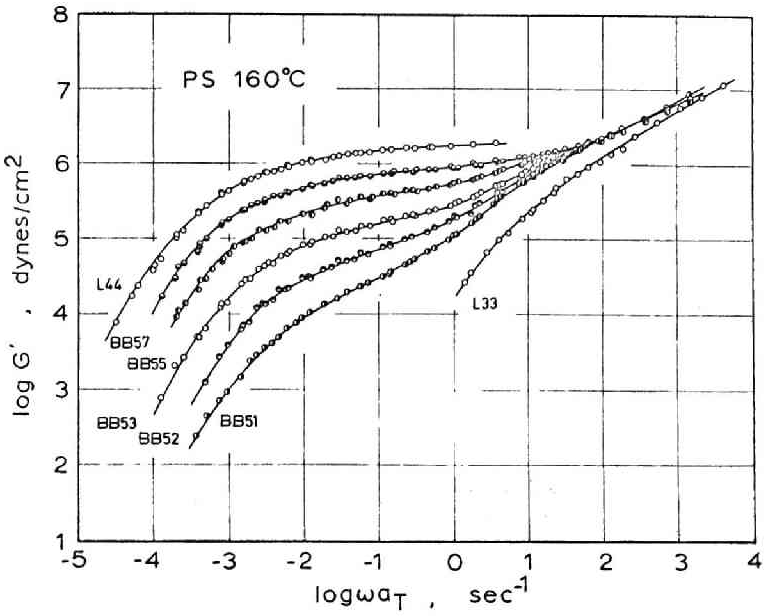

FIG.5-8. Frequency dependences of G' for the BB5 series and the components, reduced to 160°C.

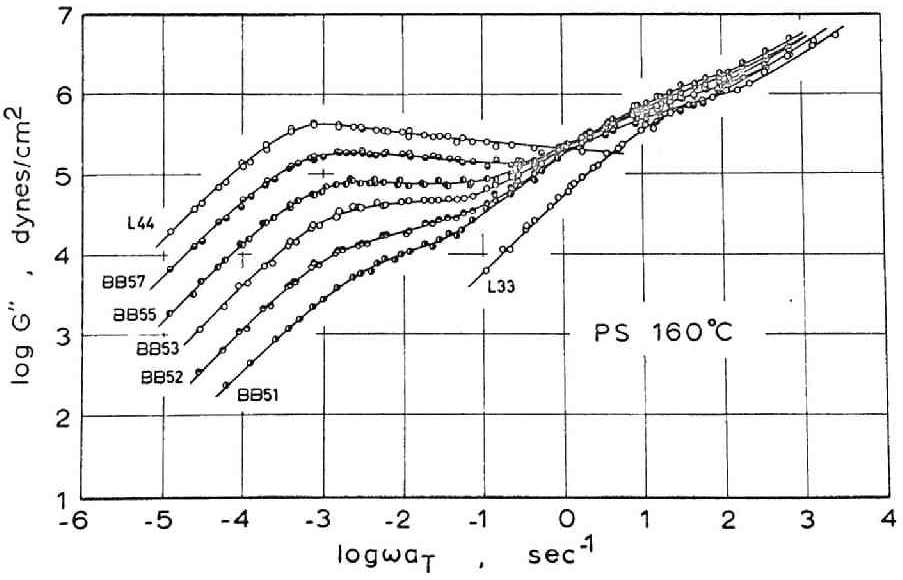

FIG.5-9. Frequency dependences of G'' for the BB5 series and the components, reduced to 160°C.

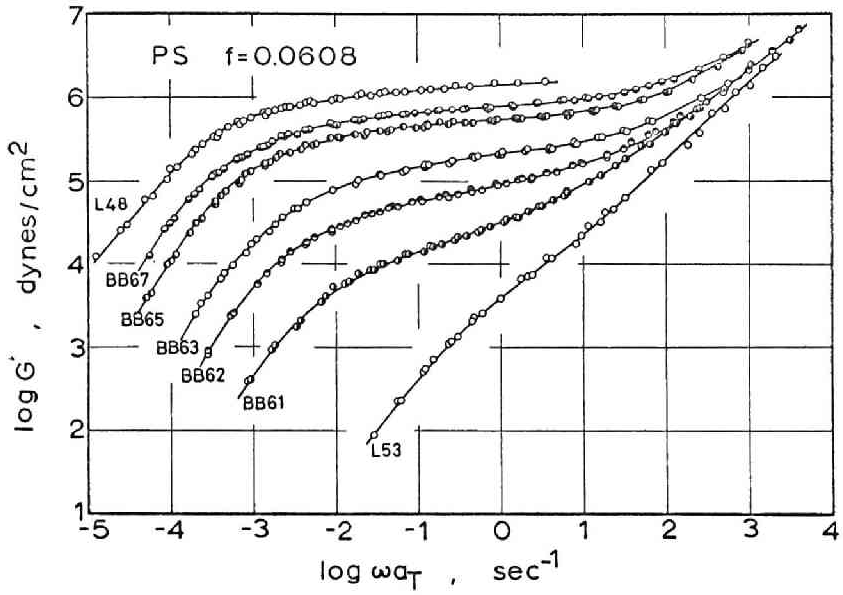

FIG.5-10. Frequency dependence of G' for the BB6 series and the components, reduced to f = 0.0608.

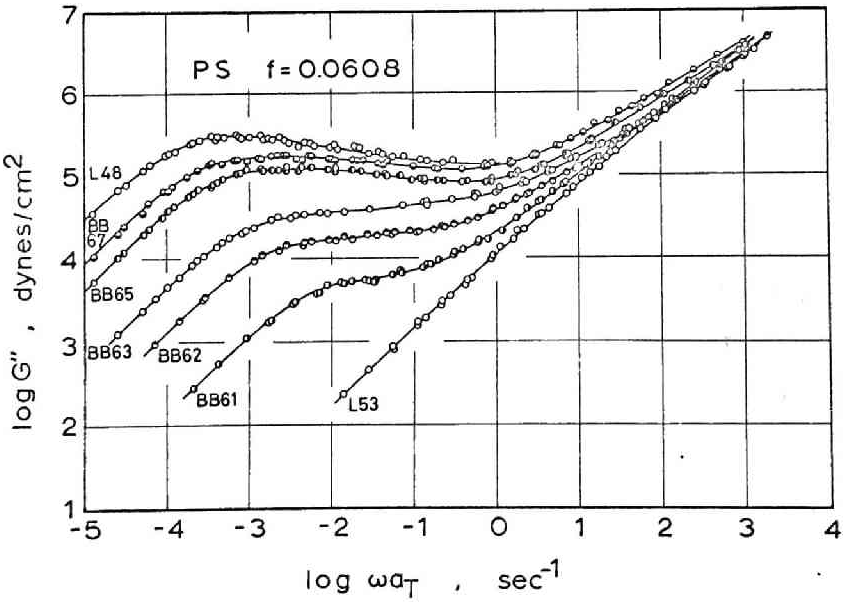

FIG.5-11. Frequency dependences of G" for the BB6 series and the components, reduced to f = 0.0608.

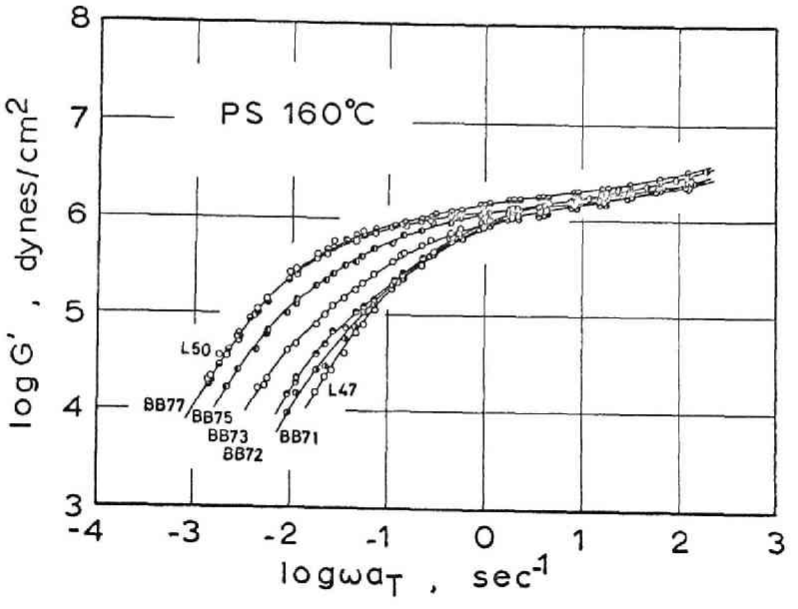

FIG.5-12. Frequency dependences of G' for the BB7 series and the components, reduced to 160°C.

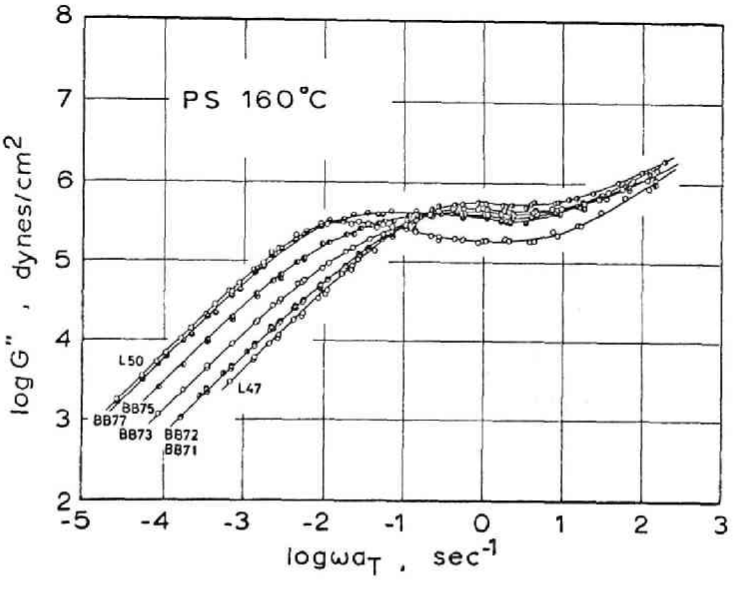

FIG.5-13. Frequency dependences of G" for the BB7 series and the components, reduced to 160°C.

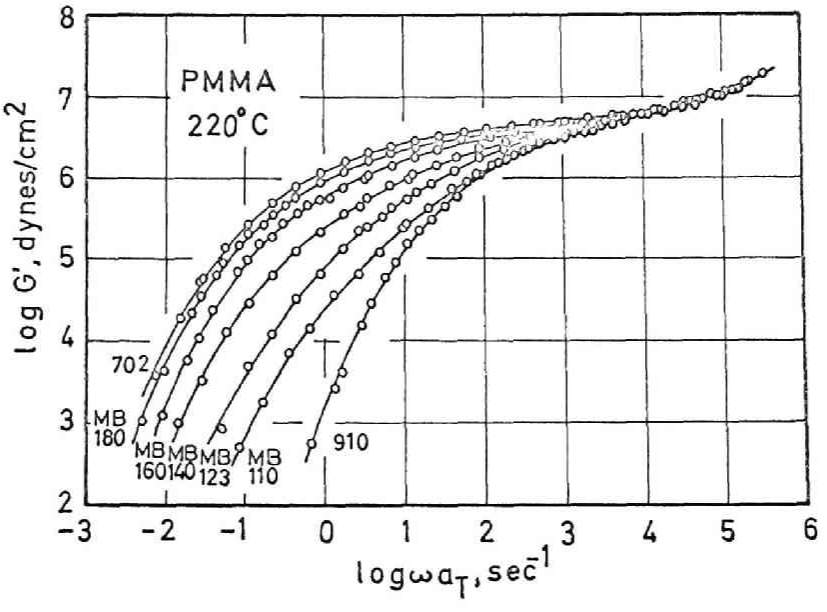

FIG.5-14. Frequency dependences of G' for the MB1 series and the components, reduced to 220°C.

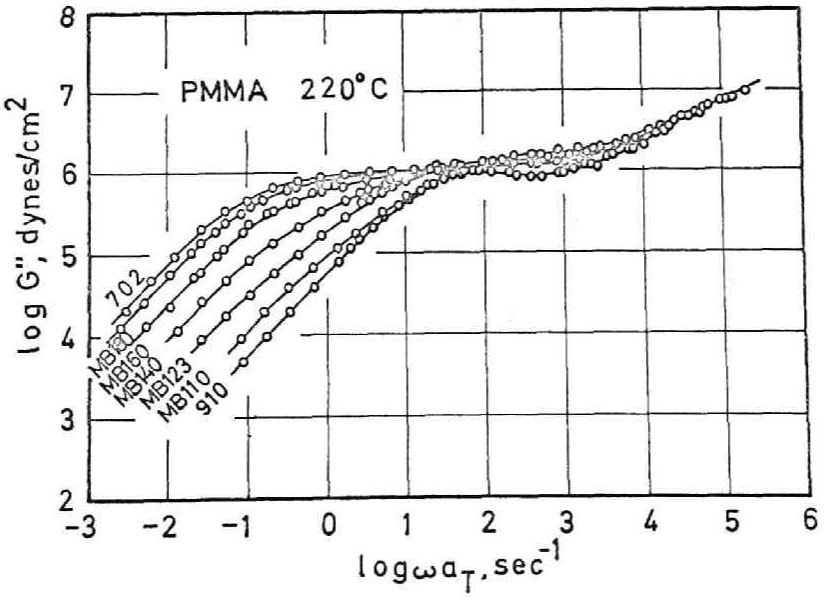

FIG.5-15. Frequency dependences of G" for the MB1 series and the components, reduced to 220°C.

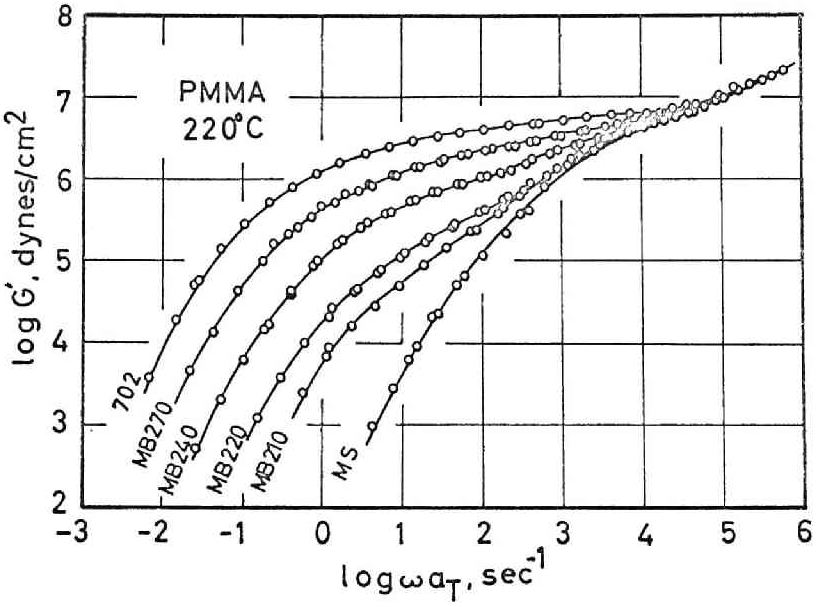

FIG.5-16. Frequency dependences of G' for the MB2 series and the components, reduced to 220°C.

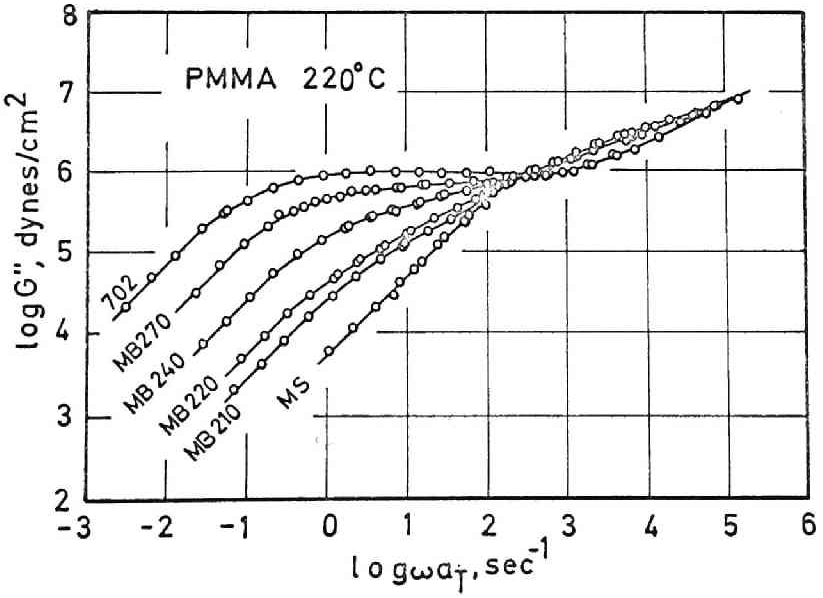

FIG.5-17. Frequency dependences of G" for the MB2 series and the components, reduced to 220°C.

G' and loss modulus G" for the MB1 and MB2 series. The G' curves in Figs. 5-14 and 5-16 as well as the G" curves in Figs.5-15 and 5-17 do not show the "two-step" plateau clearly, because the molecular weight distributions of PMMA employed in this study are not as narrow as those used in the case of the anionic polystyrenes. However, the frequency dependence curves of the viscoelastic functions, especially those for the blends containing small amounts of higher component, show the two-step behavior.

5.3 RELAXATION SPECTRUM

5.3.1 Effect of Molecular Weight Distribution

In Chapter 3, it was found for high molecular weight and narrow-distribution polystyrenes that the distribution of relaxation times characteristic of entanglement couplings appears as a peak in the G" curve and is separated from that of the glass transition. In the previous section, the frequency dependence curves of G' and G" for blends composed of two components having very different molecular weights suggested the existence of two groups of relaxation times associated with entanglement slippage. Therefore, it is very interesting to compare the relaxation spectrum of a narrow-distribution polymer with those of broad-distribution polymer or blends.

To obtain the relaxation spectrum from the dynamic viscoelasticity data, the Tschoegl equations[2] were used; they may be written as follows:

$$H(\tau) = \begin{cases} \dfrac{dG'}{d\ln\omega} + \dfrac{1}{2}\dfrac{d^2G'}{d(\ln\omega)^2}\Bigg|_{\frac{1}{\omega}=\sqrt{2}\tau} & \left(\begin{array}{l}\text{when the slope of}\\ H(\tau)\text{ is positive}\end{array}\right) \\ \dfrac{dG'}{d\ln\omega} - \dfrac{1}{2}\dfrac{d^2G'}{d(\ln\omega)^2}\Bigg|_{\frac{1}{\omega}=\tau/\sqrt{2}} & \left(\begin{array}{l}\text{when the slope of}\\ H(\tau)\text{ is negative}\end{array}\right) \end{cases} \qquad (5\text{-}1)$$

$$H(\tau) = \begin{cases} \frac{2}{\pi}\left[G'' + \frac{4}{3}\frac{dG''}{d\ln\omega} + \frac{1}{3}\frac{d^2G''}{d(\ln\omega)^2}\right]\Bigg|_{\frac{1}{\omega}=\sqrt{5}\tau} & \text{(positive)} \\ \frac{2}{\pi}\left[G'' - \frac{4}{3}\frac{dG''}{d\ln\omega} + \frac{1}{3}\frac{d^2G''}{d(\ln\omega)^2}\right]\Bigg|_{\frac{1}{\omega}=\tau/\sqrt{5}} & \text{(negative)} \end{cases} \qquad (5\text{-}2)$$

The relaxation spectrum obtained by use of these equations is very similar to that obtained by the third-order approximation method of Schwarzl and Staverman[3] or the first-order approximation method of Fujita[4]. The relaxation spectra for the narrow- and broad-distribution polystyrenes, L15 and PS7, determined from the master curve of G' using eq(5-1), are shown in Fig.5-18. These spectra agree very well with those determined from G" using eq(5-2). As seen from Fig.5-18, the spectrum for L15 has

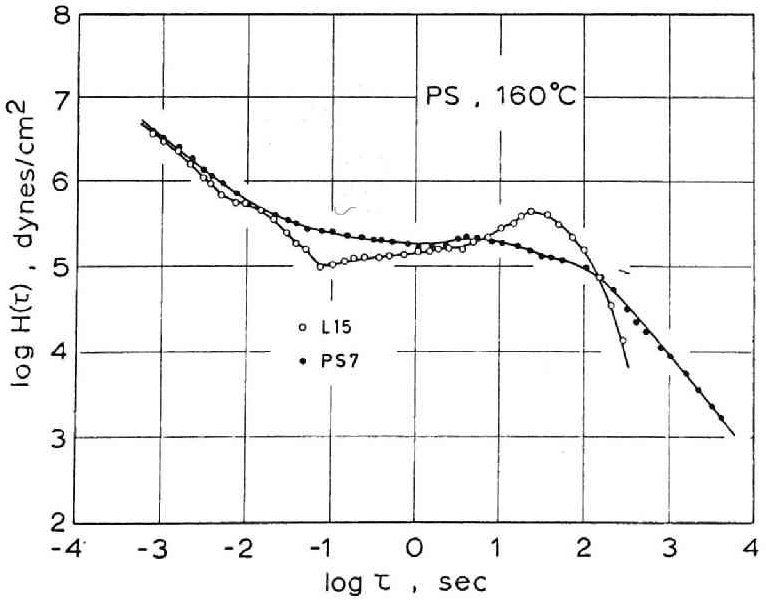

FIG.5-18. Relaxation spectra for the narrow-distribution polystyrene L15 and the broad-distribution polystyrene PS7 at 160°C.

a peak in the long time region, and then falls off rapidly with increasing relaxation time. The spectrum for PS7, on the other hand, shows no peak and extends gradually to a very long time. It can be concluded from these results that, for the narrow-distribution polystyrenes, the distribution of relaxation times associated with the entanglement couplings is not box-type as predicted by the Hayashi theory[5], but shows a peak as predicted by the other theories, such as the FLW theory[1,6] and the Chompff-Duiser theory[7], and that the broadness of the molecular weight distribution is directly reflected on the spread of the distribution of relxation times. The coincidence of the spectra for the narrow- and broad-distribution polymers in the short time region suggests that the viscoelastic properties in the transition zone are never affected by the molecular weight distribution.

5.3.2 Relaxation Spectrum for Polymer Blend

The relaxation spectra for the blrnd BB15 and its components, L18 and L16, are shown in Fig.5-19. For each component, a maximum can be observed in the relaxation spectrum. This maximum corresponds to a single plateau in the G' curve shown in Fig.5-2, and a single maximum in the G" curve in Fig.5-3. On the contrary, the spectrum for the blend BB15 has two maxima corresponding to the two-step plateau observed in the G' curve in Fig.5-2 and the G" curve in Fig.5-3. The peak on the long time side is lower than that of L18 and seems to be shifted slightly to the short time side. The other peak, on the short time side, is slightly lower and broader than that of L16 and is shifted to the long time side. Such shifts of the peak are considered to correspond to the phenomenological interaction parameters λ_1 and λ_2 in the Ninomiya theory[8] for the visco-

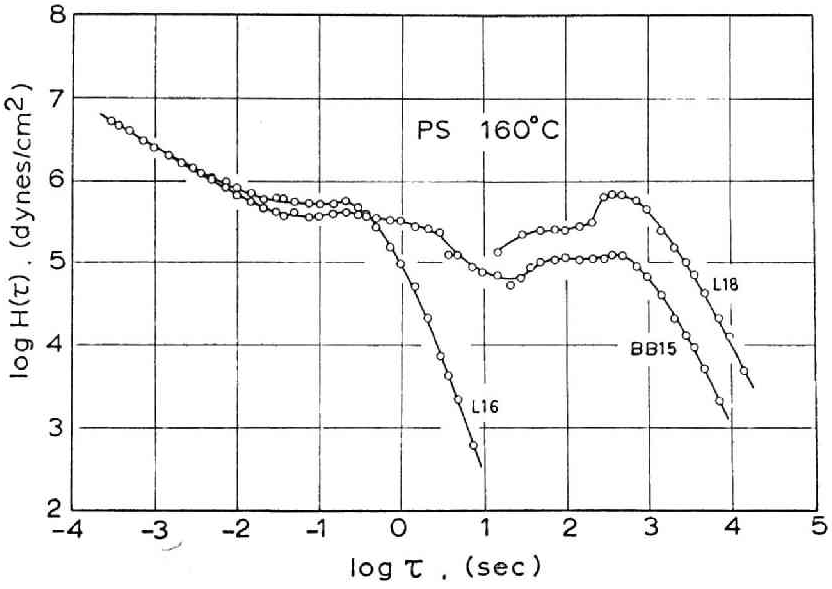

FIG.5-19. Relaxation spectra for BB5 and its component at 160°C.

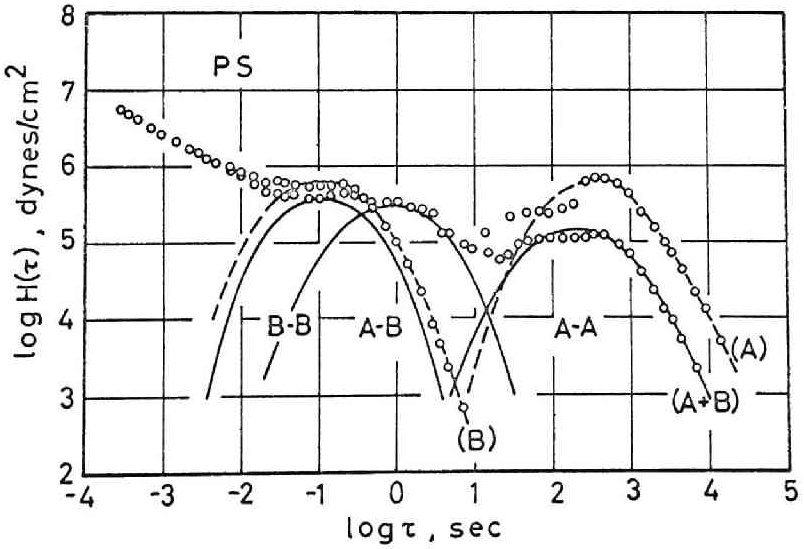

FIG.5-20. Schematic illustration of the relaxation spectra associated with the entanglement couplings for polymer blend.

elasticity of binary blends. It is also considered that a relaxation mechanism having long relaxation time (= $10^{2\sim3}$sec) is involved in the entanglement couplings between molecules of the high molecular weight component alone, while another mechanism having short relaxation times ($\sim 10^{-1}$sec) is associated with the couplings between molecules of the low molecular weight component alone. The lowering of both the peak from those of the components may be ascribed to the decrease in the content of each component.

The spread of the peak on the short time side to the long time side is probably caused by the existence of another kind of entanglement couplings between molecules of the high and low molecular weight components. This type of coupling has relaxation times longer than those of the mechanism involved in the entanglement couplings between molecules of the low molecular weight component alone. The schematic illustration of this idea is given in Fig.5-20, where A and B represent higher and lower molecular weight components respectively, and A-A, B-B and A-B denote the relaxation spectra associated with the entanglement couplings between A and A, B and B, and A and B, respectively. This fundamental concept will be applied to the establishment of the quadratic blending law, as will be described in the succeeding chapter.

5.4 RHEOLOGICAL BEHAVIOR IN THE TERMINAL ZONE

In Fig.5-21, η_0 values for the anionic polystyrenes and the blends used are plotted logarithmically against the calculated weight-average molecular weight. The open circles indicate the narrow-distribution (anionic) polystyrenes, and the closed circles the blends. The molecular weights of the blend samples were calculated by eq(2-6), since each

component has very narrow distribution of molecular weights. In the case of binary blends composed of two components having molecular weights above M_C, the weight fraction is equal to the volume fraction. As seen from Fig. 5-21, the experimental points for the blends mount fairly well on the line drawn for the narrow-distribution polymers, whose slope is 3.7 above M_C.

The molecular weight dependence of the elasticity coefficient A_G defined by eq(1-47) is shown in Fig.5-22 for the blend samples BB15, BB25 and BT1, and the BB3 series as well as for the narrow-distribution polystyrenes. The molecular weights for the blends were again calculated by eq(2-6). The slope of the solid straight line in this figure is 7.5. In marked contrast to the case of η_0, A_G values for the blends do not agree with and are clearly higher than those for the narrow-distribution polymers, excepting BB25 for which the difference from the narrow-distribution polymers

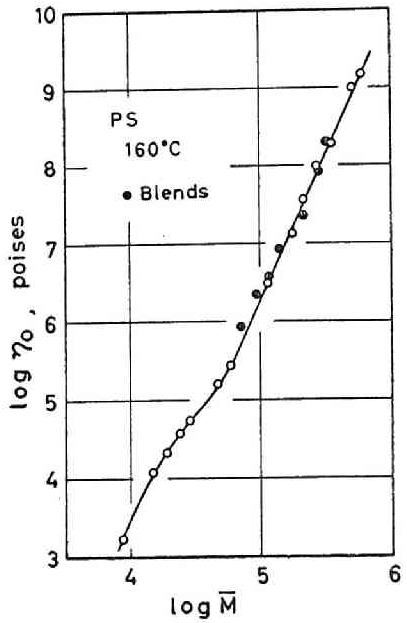

FIG.5-21. Zero-shear viscosity η_0 of the blends (closed circles) and narrow-distribution polystyrenes(open circles) plotted against $\bar{M}$, logarithmically, at 160°C.

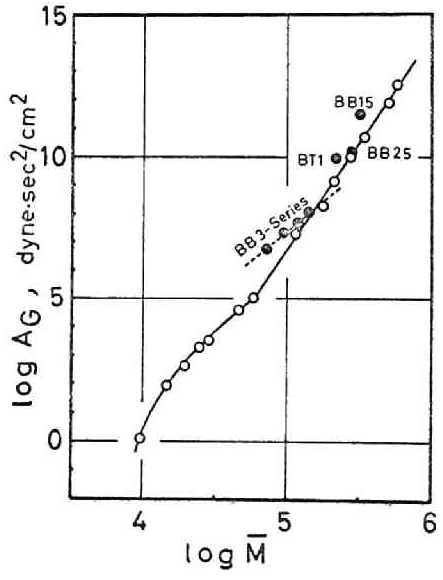

FIG.5-22. Elasticity coefficient A_G for the blends(closed circles) and narrow-distribution polystyrenes(open circles plotted against $\bar{M}$, logarithmically at 160°C.

is rather slight because the molecular weights of its components are close each other. For the BB3 series, A_G of the samples containing small amounts of the high molecular weight component deviates from the straight line for the narrow-distribution polymers, and the plot can be approximated by a straight line, shown by the broken line in Fig.5-22, having a slope of about 4.3. This result indicates that the elastic behavior of polymer liquids in the terminal zone is strongly affected by the molecular weight distribution, and that A_G will successfully be expressed not by the weight-average molecular weight but by certain higher-order moments of the molecular weight distribution.

The steady-state compliance J_e^0 of the binary blends, BB3 series, and other samples is plotted logarithmically against the weight fraction of the high molecular weight component, w_2, in Fig.5-23. In this figure, the result reported by Akovali[9] for binary blends of narrow-distribution

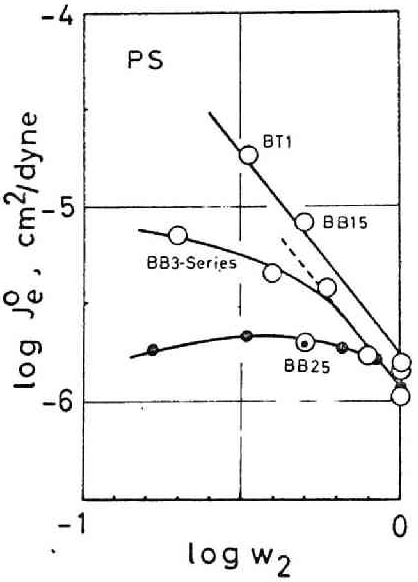

FIG.5-23. Composition dependence of steady-state compliance J_e^0 for the binary blends of anionic polystyrenes. The data indicated by the closed circles are those of Akovali[9].

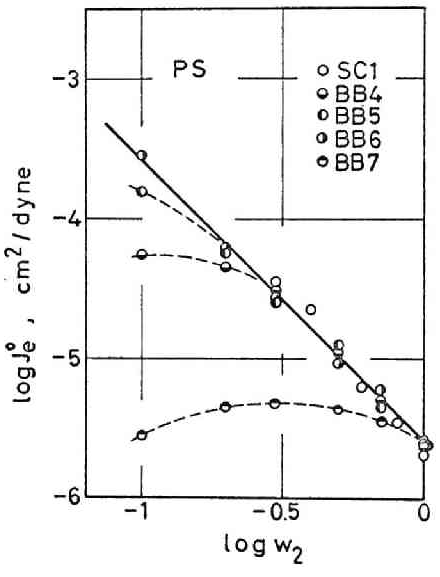

FIG.5-24. Concentration and composition dependences of steady-state compliance J_e^0 for polystyrene solutions(open circles) and binary blends of anionic polystyrenes.

polystyrene is also reproduced with the closed circles. The values of J_e^0 for binary blends are always higher than those for either component, and display a maximum at an intermediate composition. The maximum value of J_e^0 increases and the corresponding w_2 decreases as the ratio of molecular weights of the components increases. In the process of the superposition of frequency dependence curves of G' for blends with respect to the composition, the vertical shift factor c_M can be determined, as was mentioned in Section 3.2.5. This shift factor c_M represents the ratio of the steady-state compliance of the blend to that of one of the components and depends on differences in the molecular weights and distributions of the component polymers. For the blend samples of narrow-distribution polystyrenes shown in Fig.5-23, each curve can be approximated by a straight line having the slope of -2 near $w_2 = 1.0$. This does not agree with the prediction of the Ninomiya theory[8] that J_e^0 should be proportional to w_2^{-1}. The straight line extends further to the low w_2 side as the ratio of molecular weights of the components increases. It is very interesting to compare this result with that for concentrated polymer solutions, which were studied in Section 4.4.3. Such a comparison is made in Figs.5-24 and 5-25 for anionic polystyrenes and polymethyl methacrylates, respectively. The sample series used here are indicated in the figures. As seen from these figures, the dependence of J_e^0 on w_2 for the solutions can be represented by a straight line having the slope of -2, which is the asymptote of the curves for the blend samples. Therefore, it can be concluded that the low molecular weight component in a binary blend does not contribute to the steady-state compliance in the high concentration region at all, just as with solvents in polymer solutions, even when its molecular weight is higher than M_c. In other words, polymer blends and solutions should

manifest similar viscoelastic behavior at long time scales.

Here, the author feels like referring to a remarkable result obtained for the moderately concen-

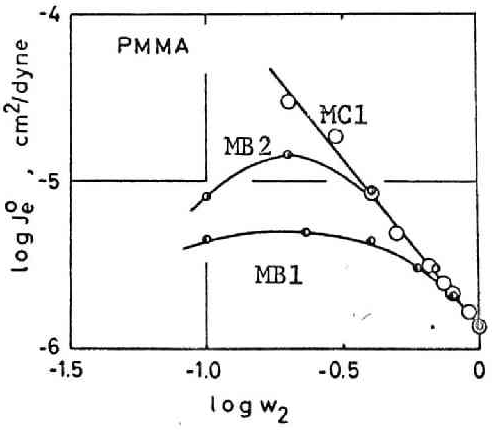

FIG.5-25. Concentration and composition dependences of steady-state compliance J_e^0 for PMMA solutions in DEP (open circles) and binary blends of PMMA (closed circles)

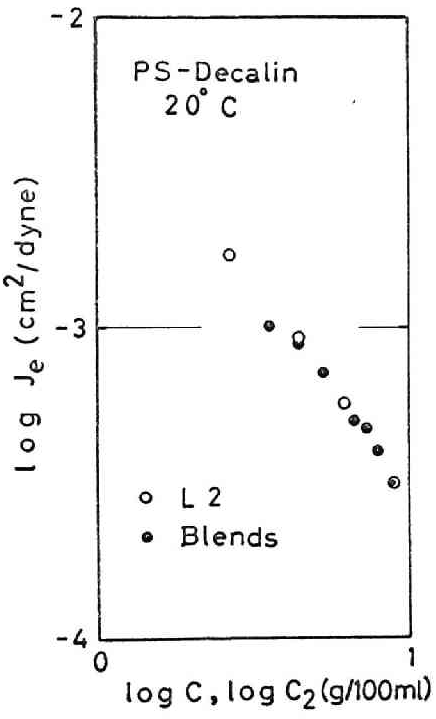

FIG.5-26. Concentration dependences of steady-state compliance J_e^0 for anionic polystyrene solutions (open circles) and 10% solution of blends of anionic polystyrenes (L2 and L5). c and c_2 denote the concentration of L2 in the solutions and the solutions of blends.

trated solutions of anionic polystyrene blends, which is shown in Fig.5-26. In this figure, the steady-state compliance J_e^0 for narrow-distribution polystyrene (L2) solution in decalin (open circles) and that for 10% solution of the blend composed of narrow-distribution polystyrenes (L2&L5) in same solvent (closed circles), are plotted against, respectively, the concentration (c) and the concentration of L2 alone in blend solution(c_2). The data represented by both circles coincide well with each other.

This result means that the steady-state compliance for solutions of polymer blends does not affected by the lower molecular weight component included in the solutions at all.

5.5 RHEOLOGICAL BEHAVIOR IN THE RUBBERY ZONE

As was seen in Fig.5-2, blends composed of narrow-distribution polystyrenes manifest the two-step plateau in the rubbery zone, and the lower step at low frequency or long time scale lowers with decreasing w_2. For the sake of quantitative considerations, the entanglement modulus G^0_{eN} and entanglement compliance J^0_{eN} of the blend samples, BB15 and BT1, and blend series, BB5 and BB6, were calculated by eq(3-5)[10]. Log J^0_{eN} for the blends BB15 and BT1 is plotted against log w_2 in Fig.5-27. For the ternary blend BT1, w_2 is regarded as 0.33. The solid line in this figure has the slope of -2, and the broken line, of -2.3, suggesting that the lower step of the two-step plateau of the G' curve in Fig.5-2 is approximately proportional to w_2^2. Similar plots for BB5 and BB6 series, as well as SC1 series (solutions) are shown in Fig.5-28. The data can be exactly represented by the solid line having the slope of -2. Comparing Figs.5-23 and 5-24 with Figs. 5-27 and 5-28, it can be said that the dependence of J^0_e and J^0_{eN} are quite similar, and J^0_e is about three times larger than J^0_{eN}.

These results appear to support the view that the lower step of the two-step rubbery plateau observed for the blends is associated with the entanglement couplings between molecules of high molecular weight component alone. Rheological studies with blends of narrow-distribution polymers seem to be very promising to clarify not only the effect of molecular weight distribution on rheological behavior but also the nature of entanglement couplings between macromolecular chains.

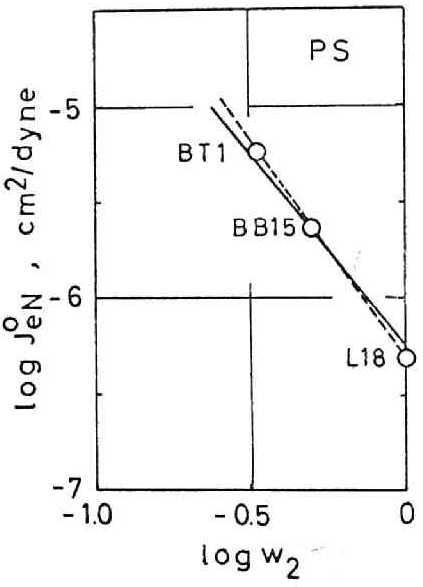

FIG.5-27. Entanglement compliance J^0_{eN} of BB15,BT1, and L18 plotted logarithmically against the weight fraction of the high molecular weight component w_2.

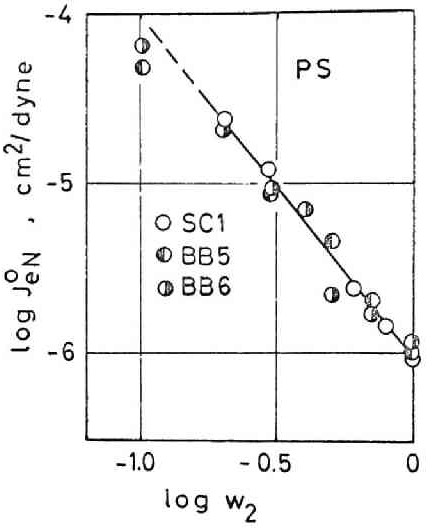

FIG.5-28. Concentration and composition dependences of entanglement compliance J^0_{eN} for SC1, BB5, and BB6 series.

5.6 FREE-VOLUME PARAMETERS

BB6 series, which contains the component L53, having lower molecular weight than M_C, shows the composition dependence of the free-volume parameters. The dependence of the Vogel parameters T_0 and α_f, the fractional free volume at 160°C, f_{160}, and the reference temperature in iso-free-volume state at f=0.0608, T'_r, on the composition for the BB6 series are shown in Fig.5-29.

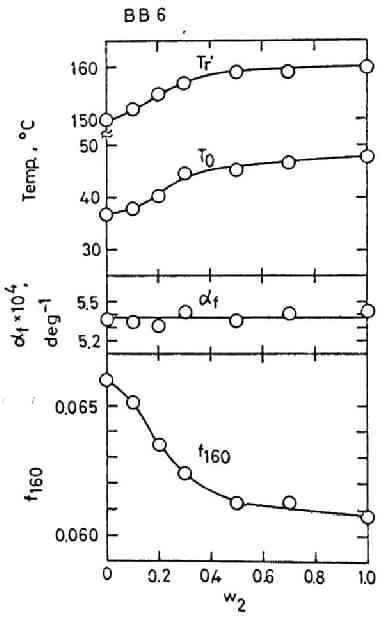

FIG.5-29. Composition dependences of the free-volume parameters, T_0, α_f, f_{160} and T'_r for BB6 series.

In this figure, α_f seems to be independent of the composition, while T_0 decreases with decreasing w_2. In Figs.5-10 and 5-11, the viscoelastic functions were reduced to T_r' in this figure. The values of T_0, α_f, and f_{160} at $w_2 = 0$ (i.e. those of L53) are quite reasonable as compared with those for narrow-distribution polystyrenes having low molecular weights given in Table 3-IV.

5.7 NON-NEWTONIAN FLOW OF POLYMER BLENDS

The rate of shear (κ) dependence of shear stress (σ_{12}) has been determined by means of the capillary rheometer described in Section 2.3.2, and using eqs(2-13), (2-14) and (2-15). The shear dependence of the viscosity is shown in the form of master curves after the time-temperature superposition. All measurements described hereafter were made at L/D ratio of 20/1, where L and D are the length and diameter of the capillary, respectively.

Fig.5-30 shows the dependence of viscosity on rate of shear for the bulk samples L56, L60 and their blend BB85. The sample codes and the components are shown in Table 2-X. The reference temperature is 240°C. The straight solid line drawn in the high shear region has the slope of -0.818, which has been predicted by Graessley[11] and supported by experimetal data[12]. The three straight lines, corresponding to the three samples, do not unite at high rates of shear; however all of the data can be converged upon a straight line when we revise the slope from -o.818 to -0.90, as shown by broken line. It is not clear which is more appropriate. The rate of shear dependent curve of viscosity for BB85 clearly shows the two-step changes, and suggests that two sets of relaxation times, corresponding to the pure components, should separately affect the viscosity- rate of shear relation.

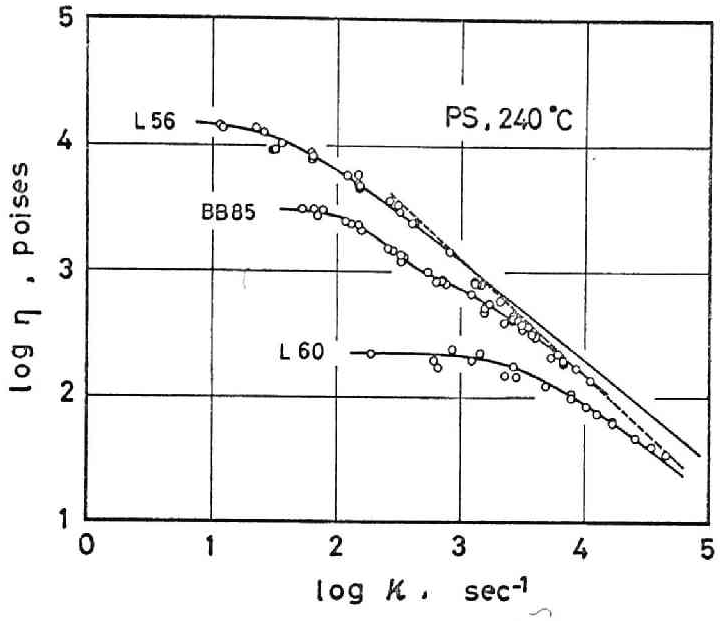

FIG.5-30. Rate of shear dependences of viscosity for the blend BB85 and its components (L56 and L60), reduced to 240°C.

In recent years, many rate-dependent relaxation spectra $H(\tau;\kappa)$ have been proposed [13~16] in connection with the constitutive equations for viscoelastic materials, as mentioned in Section 1.2. Some of the proposed relaxation spectrum have the form of

$$H(\tau;\kappa) = H(\tau)\, g(\kappa) \qquad (5\text{-}3)$$

where $H(\tau)$ and $g(\kappa)$ are the relaxation spectrum at rest (the linear relaxation spectrum) and a function of rate of shear. The presented forms of $g(\kappa)$ and the slopes of log $H(\tau;\kappa)$ at long time region at finite κ, have been reviewed by Yamamoto[17]. Recently, Shida and Shroff[18] have calculated $H(\tau;\kappa)$ as a function of τ for polyethylene using the Graessley entanglement theory, and illustrated that the slope of log $H(\tau;\kappa)$ vs. log τ at longer times is more negative than -1 and becomes steeper with increasing κ. Although the linear relaxation spectrum $H(\tau)$ of the blend samples used in this study has not been

evaluated, important idea can be gotten by the comparing the two-step changes in viscosity of the present work with the linear relaxation spectra obtained earlier for similar systems. Only theories in which the log $H(\tau;\kappa)$ vs. log τ curve has a slope more regative than -1 at long τ and finite κ can predict a two-step change of non-Newtonian viscosity.

Among the several molecular theories for the shear rate dependence of viscosity, the Graessley theory has generally been considered to be successful in representing experimental results for monodisperse systems[19]. Thus it is interesting to examine the applicability of this theory to broad-distribution and blended systems.

According to Graessley, the general equation of shear viscosity for polydisperse polymer systems is given by

$$\frac{\eta}{\eta_0} = \frac{\int_0^\infty n^2 h(\kappa,n)p(n)dn \int_0^\infty n^{7/2} g^{5/2}(\kappa,n)p(n)dn \int_0^\infty np(n)dn}{\int_0^\infty n^2 p(n)dn \int_0^\infty ng(\kappa,n)p(n)dn \int_0^\infty n^{7/2}p(n)dn} \qquad (5\text{-}4)$$

with the functions g and h and p(n). g and h are the Graessley functions and p(n) is the distribution function of the chain length n. Theoretical lines for the Schulz-Zimm distribution have been calculated for various values of the parameter Z. The ratio of M_w to M_n can be expressed in termes of Z by

$$M_w/M_n = (Z + 2)/(Z + 1) \qquad (5\text{-}5)$$

When the component polymers are monodisperse, eq(5-4) can be simplified to

$$\frac{\eta}{\eta_0} = \frac{(h_1 + p_w p_n h_2)(g_1^{5/2} + p_w p_n^{5/2} g_2^{5/2})}{(g_1 + p_w g_2)(1 + p_w p_n^{5/2})} \cdot p_1 \qquad (5\text{-}6)$$

with

$$p_n = M_2/M_1, \quad p_w = w_2/w_1 \text{ and } \quad p_1 = M_1/\bar{M} \quad , \tag{5-7}$$

and

$$h_i = \frac{2}{\pi} \left[\cot^{-1}\theta_i + \frac{\theta_i(1 - \theta_i^2)}{(1 + \theta_i^2)^2} \right] \tag{5-8}$$

$$g_i = \frac{2}{\pi} \left[\cot^{-1}\theta_i + \frac{\theta_i}{(1 + \theta_i^2)} \right] \tag{5-9}$$

$$\theta_i = F(\kappa)\left(\frac{M_i}{\bar{M}} \right)^2 h_i \tag{5-10}$$

$$F(\kappa) = \left(\frac{\kappa\tau_0}{2} \right)\left(\frac{\eta}{\eta_0} \right) \frac{1}{\bar{h}} \tag{5-11}$$

$$\bar{h} = (h_1 + p_n p_w h_2) p_1 w_1 \tag{5-12}$$

where M_1, M_2 and $\bar{M}$ are the weight-average molecular weights of the lower and higher molecular weight components and of the blend, respectively. The functions g, h and θ are certain functions defined by Graessley[11]. The procedure for calculating the theoretical line is somewhat complicated and is described by Graessley and Segal[19].

The reduced viscosity η/η_0 vs. reduced shear rate curves for the blend of bulk polymers BB85 and the components are shown in Fig.5-31. The curve fitting has been carried out such that the experimental data best fall on the theoretical curve at the low and high shear rate ends. The procedure used should be emphasized here; it is based on the fact that the shear rate dependent curves of viscosity unite into a straight line in the

high rate of shear region (power law region), regardless of the molecular weight distribution. As seen from Fig.5-31, the agreement of the theory with the experiment is very good for the narrow-distribution polystyrenes. However, the experimental data for the blend samples show higher values than the theory. Furthermore, the theory predicts a broader change of viscosity at intermediate rates of shear, as compared with the experimental curve, the latter clearly showing the two-step change of viscosity. This fact suggests that the theory probably does not account for the shift of the relaxation times by blending (λ_{ii}), as discussed in the succeeding chapter.

The characteristic relaxation time τ_0, given in eq(5-8), can be obtained by shifting the experimental curve so as to superpose on the theoretical line at lower and higher rates of shear. Values of τ_R/τ_0 are plotted against cM_w in Fig.5-32, where τ_R is the Rouse longest relaxation time and c is the concentr

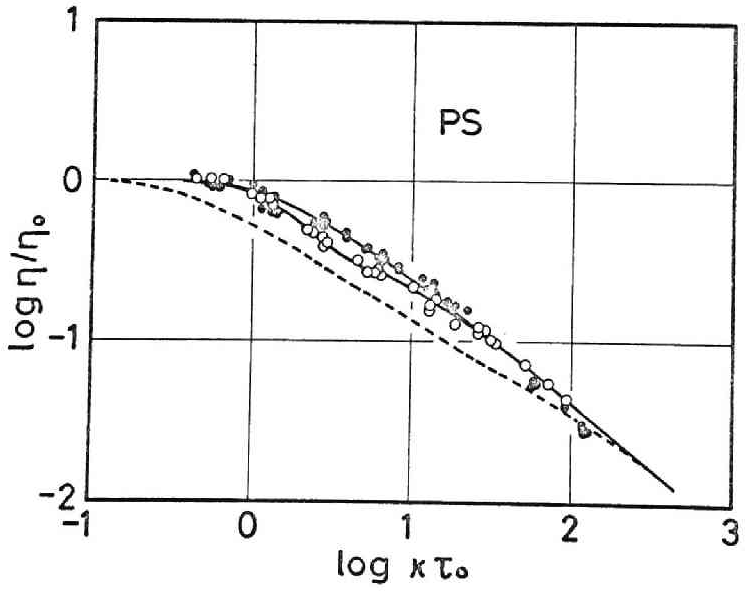

FIG.5-31. Reduced viscosity vs. reduced rate-of-shear curves for the blend BB85 (open circles) and the components, L56 and L60,(closed circles). The uppermost solid and broken lines are the prediction of the Graessley theory[11] for the monodisperse systems and the blend, respectively.

tion, measured in g/ml. In this figure, PSB and PS25 denote the broad-distribution polystyrene and the 50% solution in KC5, LC15 and LC25 the 50% solutions of narrow-distribution polystyrenes, and SB15 the 50% solution of blend of narrow-distribution polystyrenes, respectively. The solid line drawn in this figure is the empirical one obtained by Graëssley and Segal[19]. The data are somewhat scattered around the straight line, but seems to be roughly represented by the empirical line. Graessley and Segal[19] reported an extremely high value of τ_R/τ_0 for blend sample, although not so high in this figure. This discrepancy may have been caused by the difference in curve fitting, since they fitted only at lower rates of shear.

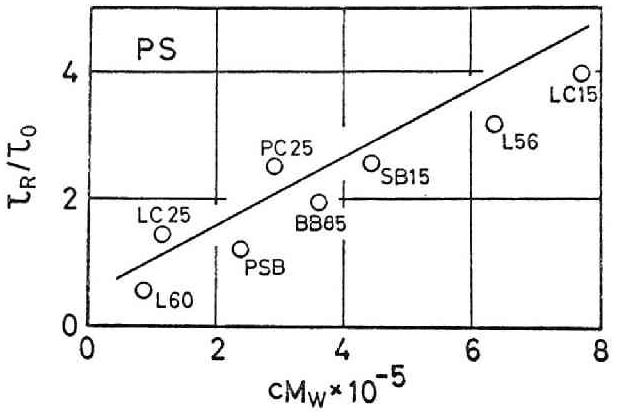

FIG.5-32. The ratios of the Rouse relaxation time τ_R to the characteristic relaxation time τ_0 plotted against the products of concentration and molecular weight.

REFERENCES

1. J. D. Ferry, "Viscoelastic Properties of Polymers", 2nd ed., John Wiley, New York, 1970, Chapter 13.
2. N. W. Tschoegl, Rheologica Acta, 10, 582 (1971)
3. F. Schwarzl and A. J. Staverman, Appl. Sci. Res., A4, 127 (1953)
4. H. Fujita, J. Appl. Phys., 29, 943 (1958)
5. S. Hayashi, J. Phys. Soc. Japan, 18, 131;249 (1963)

6. J. D. Ferry, R. F. Landel, and M. L. Williams, J. Appl. Phys.,26, 359 (1955)

7. (a) A. J. Chompff and J. A. Duiser, J. Chem. Phys., 45, 1505 (1966)
   (b) A. J. Chompff and W. Prins, J. Chem. Phys., 48, 235 (1968)

8. (a) K. Ninomiya, J. Colloid Sci., 14, 49 (1959)
   (b) K. Ninomiya and J. D. Ferry, J. Colloid Sci., 18, 421 (1963)

9. G. Akovali, J. Polym. Sci., Part A2, 5, 875 (1967)

10. J. F. Sanders and J. D. Ferry, Macromolecues, 2, 440 (1969)

11. W. W. Graessley, J. Chem. Phys., 43, 2696 (1965); 47, 1942 (1967)

12. R. A. Stratton, J. Colloid & Interf. Sci., 22, 517 (1966)

13. T. W. Spriggs and R. B. Bird, Ind. Eng. Chem., Fund., 4, 182 (1964)

14. (a) D. C. Bogue and J. L. White, "Engineering Analysis of Non-Newtonian Fluids", Agardograph Series of NASA, 1970.
   (b) I-J. Chen and D. C. Bogue, Trans. Soc. Rheology, 16, 59 (1972)

15. T. Tanaka, M. Yamamoto, and Y. Takano, J. Macromol. Sci., B4, 931 (1970)

16. M. Yamamoto, Trans. Soc. Rheology, 15, 331 (1971)

17. M. Yamamoto, Trans. Soc. Rheology, 15, 783 (1971)

18. (a) M. Shida and R. M. Shroff, Trans. Soc. Rheology, 14, 605 (1970)
   (b) R. M. Shroff and M. Shida, J. Macromol. Sci., B6, 277 (1972)

19. W. W. Graessley and L. Segal, AIChE J., 16, 261 (1970)

CHAPTER 6

Blending Laws for Polymers

6.1 INTRODUCTION

The well-known Ninomiya blending law[1~3] for binary blends of polymers was proposed more than ten years ago, and has been widely utilized[4] because of its simplicity. It has been made clear, however, that the blending law cannot be applied to the rheological properties of blends of narrow-distribution polymers. The results described in Chapters 4 and 5, as well as the other data[5~7] show definitely that the steady-state compliance J_e^0, and the quasi-equilibrium compliance J_{eN}^0 are both inversely proportional to w_2^2 or c^2, where w_2 and c are the weight fraction of the higher molecular weight component in the binary blend, and the concentration of polymer in solution, respectively. These facts do not agree with the prediction of the Ninomiya theory.

The present author and others (Bogue-Masuda-Einaga-Onogi ; BMEO[8]) proposed a quadratic blending law for the entanglement region, and obtained an expression of the steady-state compliance in terms of w_2. This theory is based on the experimental results for the narrow-distribution polymers and their blends described throughout the preceding chapter and especially on the concept mentioned in Section 5.3.2, that the three sets of relaxation times may exist in polymer blend corresponding to the three types of the entanglement couplings.

More recently Graessley[9] presented a theory involving the mean relaxa----

tion time $\langle\tau\rangle_{ij}$ of the entanglement between component molecules i and j in the blend, and formalized relations for the zero-shear viscosity and the steady-state compliance, using a blending law similar to that of BMEO. Prest[10] also presented a blending law, which might be called the modified Ninomiya blending law, taking account of the quadratic blending rule.

In the present chapter, the current blending theories are reviewed and the differences between them are made clear. Moreover, the tests of these blending theories, especially the quadratic blending laws (BMEO and Graessley) are made by use of the experimental data obtained for the binary blends of narrow-distribution polystyrenes in the preceding chapter. Finally some suggestions toward improving the present theories are presented.

6.2 A REVIEW ON THE BLENDING THEORIES

6.2.1 The Ninomiya Theory

The Ninomiya blending law can be given as[1~3]

$$H_b(\tau) = v_1 H_1(\tau/\lambda_{11}) + v_2 H_2(\tau/\lambda_{22}) \qquad (6\text{-}1)$$

where $H_b(\tau)$ and $H_i(\tau)$ are the relaxation spectra of blend and the components before mixing, and v_i and λ_{ii} denote the volume fraction and the uniform shift of relaxation times caused by mixing, respectively. To indicate the lower and higher molecular weight components, and the blend, the subscripts 1, 2 and b are used, respectively, hereafter. It is significant in this blending law that the relaxation spectrum of the blend can be obtained only by shifting the components by the amounts of $\log v_i$ and $\log \lambda_{ii}$ along the $\log H$ and $\log \tau$ axes. λ_{ii} is defined by

$$\lambda_{ii} = \frac{\tau_{mb}}{\tau_{mi}} = \frac{\tau_{pb}}{\tau_{pi}} \qquad (6\text{-}2)$$

This quantity is a function of some-average molecular weights of the blend and component polymers[1~3], where τ_m and τ_p are the maximum and the p-th (from τ_m) relaxation times.

6.2.2 The BMEO Theory

The total relaxation spectrum for blend $H_b(\tau)$ can be divided into two parts:

$$H_b(\tau) = H_b^T(\tau) + H_b^E(\tau) \qquad (6\text{-}3)$$

$H_b^T(\tau)$ is the relaxation spectrum characteristic of the glass transition region and $H_b^E(\tau)$ is that of the terminal or flow region associated with the entanglement slippage. This type of separation was already suggested in Sections 3.3 and 5.3.1. Moreover, $H_b^E(\tau)$ is expressed as follows:

$$H_b^E(\tau) = W_1^2 H_1(\tau/\lambda_{11}) + 2W_1W_2H_{12}(\tau/\lambda_{12}) + W_2^2 H_2(\tau/\lambda_{22}) \qquad (6\text{-}4)$$

where w_i and $H_i(\tau)$ respectively denote the weight fraction and the relaxation spectrum of the components in the pure state. $H_{12}(\tau/\lambda_{12})$ is a cross-relaxation spectrum which appears by mixing. Eq(6-4) suggests that the relaxation spectrum of the blend can be obtained simply by shifting the spectra of the component polymers. λ_{ii} has a similar meaning to λ_{ii} in eq(6-2), namely,

$$\lambda_{ii} = \frac{\langle\tau\rangle_{ii}}{\langle\tau\rangle_{i}} = \frac{\tau_{mii}}{\tau_{mi}} \qquad (6\text{-}5)$$

$\langle\tau\rangle$ and τ_m are, respectively, a mean and the maximum relaxation times. It should be noted that the double subscript (ii and ij) and the single(i) are used for the blended and pure states. λ_{12} is defined as the ratio of mean relaxation time for the entanglement between the high and low molecular weight components to an imaginary relaxation time $\langle\tau\rangle^*_{12}$:

$$\lambda_{12} = \frac{\langle\tau\rangle_{12}}{\langle\tau\rangle^*_{12}} \qquad (6\text{-}6)$$

BMEO theory is based on the following equations:

$$\frac{\langle\tau\rangle_{i}}{\tau_C} = \frac{M_i^{3.5}}{M_C^{3.5}} \qquad (6\text{-}7)$$

and

$$\frac{\langle\tau\rangle_{ij}}{\tau_C} = \frac{M_i M_j M_w^{1.5}}{M_C^{3.5}} \qquad (6\text{-}8)$$

where M_C is the critical molecular weight for entanglement and τ_C is the relaxation time at $M_i = M_C$. Eq(6-7) has been supported by some experiments, but eq(6-8) was purely assumed. Assuming $\langle\tau\rangle^*_{12} \propto (\sqrt{M_1 M_2})^{3.5}$, the relations

$$\lambda_{ii} = \left(\frac{M_w}{M_i}\right)^{1.5} \qquad (6\text{-}9)$$

and

$$\lambda_{12} = \left(\frac{M_w}{\sqrt{M_1 M_2}} \right)^{1.5} \qquad (6\text{-}10)$$

are obtained from eqs(6-7) and (6-8).

The expressions for the zero-shear viscosity η_{0b} and the steady-state compliance J^0_{eb} were derived by use of some approximations. In the case of " single regime dominating ", η_{0b} and J^0_{eb} are given by

$$\eta_{0b}/\eta_{01} = \left(M_w/M_1 \right)^{3.5} \qquad (6\text{-}11)$$

and

$$\frac{J^0_{eb}}{J^0_{el}} = \frac{(W_1 M_1^2 + W_2 M_2^2)^2}{(W_1 M_1 + W_2 M_2)^4} = \left(\frac{M_Z}{M_W} \right)^2 \qquad (6\text{-}12)$$

based on the component 1, and M_Z is the Z-average molecular weight.

6.2.3 The Graessley Theory

In the Graessley theory, the entanglement relaxation spectrum of the blend is given by the following equation, which is quite similar to that of BMEO:

$$H_b^E(\tau) = W_1^2 H_1(\tau) + W_1 W_2 \{H_{12}(\tau) + H_{21}(\tau)\} + W_2^2 H_2(\tau) \qquad (6\text{-}13)$$

However, $H_{12}(\tau)$ was distinguished from $H_{21}(\tau)$, this term being based on the molecular theory[11] proposed which considered the pairwise interaction between the central and passing macromolecular chains. Accordingly, $H_{12}(\tau)$ and $H_{21}(\tau)$

depend on the molecular model, but the connected spectrum $\{H_{12}(\tau)+ H_{21}(\tau)\}$ has the same physical meaning as $2H_{12}(\tau)$ in BMEO theory. It must be emphasized that $\lambda_{ii} = 1$ here and this is a weak point of this blend theory as discussed later.

The final results for η_{0b} and J^0_{eb} are

$$\eta_{0b} = (\nu_1 E_1 + \nu_2 E_2)kT[W_1^2 <\tau>_{11} + W_1 W_2 (<\tau>_{12} + <\tau>_{21}) + W_2^2 <\tau>_{22}] \qquad (6\text{-}14)$$

and

$$J^0_{eb} = \frac{1}{(\nu_1 E_1 + \nu_2 E_2)kT} \cdot \frac{W_1^2 <\tau^2>_{11} + W_1 W_2 (<\tau^2>_{12} + <\tau^2>_{21}) + W_2^2 <\tau^2>_{22}}{[W_1^2 <\tau>_{11} + W_1 W_2 (<\tau>_{12} + <\tau>_{21}) + W_2^2 <\tau>_{22}]^2} \qquad (6\text{-}15)$$

with the number of i-th component molecules /cc being ν_i; and the entanglement density of i-th component being $E_i = M_i/M_e$. M_e is the average molecular weight between the entanglement points. $<\tau>_{ij}$ is the relaxation time of the entanglement between the central (i) and passing (j) chains. Eqs(6-14) and (6-15) are also expressed in the similar form to eqs(6-11) and (6-12):

$$\frac{\eta_{0b}}{\eta_{0l}} = W_1^2 + d_1 W_1 W_2 + R W_2^2 \qquad (6\text{-}16)$$

$$\frac{J^0_{eb}}{J^0_{el}} = \frac{W_1^2 + d_2 W_1 W_2 + R^2 W_2^2}{(W_1^2 + d_1 W_1 W_2 + R W_2^2)^2} \qquad (6\text{-}17)$$

with

$$\lambda_{ii} = \frac{<\tau>_{ii}}{<\tau>_i} = 1 \qquad (6\text{-}18)$$

$$d_1 = \frac{\langle\tau\rangle_{12} + \langle\tau\rangle_{21}}{\langle\tau\rangle_1} \tag{6-19}$$

$$d_2 = \frac{\langle\tau^2\rangle_{12} + \langle\tau^2\rangle_{21}}{\langle\tau^2\rangle_1} \tag{6-20}$$

and

$$R = \frac{\langle\tau\rangle_{22}}{\langle\tau\rangle_1} = \left(\frac{E_2}{E_1}\right)^{3.5} = \left(\frac{M_2}{M_1}\right)^{3.5} \tag{6-21}$$

The numerical values for d_1 and d_2 have been tabulated in the paper, and $d_1 \propto (M_2/M_1)$ and $d_2 \propto (M_2/M_1)^2$ in the ranges of $2 \leqq M_2/M_1 \leqq 10$.

6.2.4 The Prest Theory

Prest's idea is that the relaxation spectrum for the blend can be obtained by shifting the spectra of the components along the ordinate (log H) and abscissa (log τ). This concept seems to be similar to that of the Ninomiya blending law. However, the weighting factors are some functions of the composition instead of the volume fractions. The expression is

$$H_b(\tau) = v_{11}^* H_1(\tau/\lambda_{11}^*) + v_{22}^* H_2(\tau/\lambda_{22}^*) \tag{6-22}$$

Accordingly, the sum of v_{11}^* and v_{22}^* is not equal to unity; but if the transition region response is to be independent of molecular weight distribution, one must have

$$v_{11}^*(\lambda_{11}^*)^{1/2} + v_{22}^*(\lambda_{22}^*)^{1/2} = 1 \tag{6-23}$$

The correspondence to the quadratic blending law (BMEO) is given by

$$v_{22}^{*} \frac{H_2(\tau/\lambda_{22}^{*})}{H_2(\tau/\lambda_{22})} = W_2^2 + 2W_1W_2 \frac{H_{12}(\tau/\lambda_{12})}{H_2(\tau/\lambda_{22})} \qquad (6\text{-}24)$$

or

$$v_{11}^{*} \frac{H_1(\tau/\lambda_{11}^{*})}{H_1(\tau/\lambda_{11})} = W_1^2 + 2W_1W_2 \frac{H_{12}(\tau/\lambda_{12})}{H_1(\tau/\lambda_{11})} \qquad (6\text{-}25)$$

Assuming a box-shaped relaxation spectra, the parameters v_{11}^{*}, v_{22}^{*}, λ_{11}^{*} and λ_{22}^{*} were estimated as function of the composition and molecular weight by comparison with the experimental data. However, the concept that $H_{12}(\tau/\lambda_{12})/H_2(\tau/\lambda_{22})$ = const and $\lambda_{12} = \lambda_{22}$, cannot be supported theoretically from a molecular point of view. In other words, the relaxation time $\langle\tau\rangle_{22}$ should be different from $\langle\tau\rangle_{12}$ or $\langle\tau\rangle_{21}$. The relaxation spectrum of the blend obtained in the ranges of $M_2/M_1 \leqq 4$ and $w_2 \leqq 0.4$, as presented by Prest apparently seems to be make up only by those of the components.

6.3 EXPERIMENTAL TESTS OF THE QUADRATIC BLENDING LAWS

In this section, experimental tests of the two quadratic blending laws, the BMEO and Graessley theories, are presented. The experimental data employed here are those which have been obtained for narrow-distribution polystyrenes and described in the preceding chapter. The molecular weights M_1 and M_2, and the ratios for the blending series are tabulated in Table 2-X. The SC2 series is the solution of polystyrene in chlorinated diphenyl as shown in Table 2-IX.

Integration of the relaxation spectrum eq(6-4) gives the storage and loss moduli for blend, $G_b'(\omega)$ and $G_b''(\omega)$, as follows:

$$G_b'(\omega) = W_1^2 G_1'(\omega\lambda_{11}) + 2W_1W_2 G_{12}'(\omega\lambda_{12}) + W_2^2 G_2'(\omega\lambda_{22}) \tag{6-26}$$

$$G_b''(\omega) = W_1^2 G_1''(\omega\lambda_{11}) + 2W_1W_2 G_{12}''(\omega\lambda_{12}) + W_2^2 G_2''(\omega\lambda_{22}) \tag{6-27}$$

When the 2-2 interaction dominates, (for example the concentrated solution is most typical), eqs(6-4), (6-26) and (6-27) can be rewritten as

$$H_b^E(\tau) = W_2^2 H_2^E(\tau/\lambda_{22}) \tag{6-28}$$

$$G_b'(\omega) = W_2^2 G_2'(\omega\lambda_{22}) \tag{6-29}$$

$$G_b''(\omega) = W_2^2 G_2''(\omega\lambda_{22}) \tag{6-30}$$

From these equations, η_{0b}, J_{eb}^0 and λ_{22} are expressed as

$$\eta_{0b} = \int_0^\infty H_b^E(\tau)d\tau = W_2^2\lambda_{22}\eta_{02} \tag{6-31}$$

$$J_{eb}^0 = \frac{\int_0^\infty \tau H_b^E(\tau)d\tau}{[\int_0^\infty H_b^E(\tau)d\tau]^2} = \frac{1}{W_2^2} \cdot J_{e2}^0 \tag{6-32}$$

and

$$\lambda_{22} = \frac{J_{eb}^0 \cdot \eta_{0b}}{J_{e2}^0 \cdot \eta_{02}} \tag{6-33}$$

The values of λ_{22} can be estimated from the G' and G'' for the pure components

and the blend, using the eqs(6-29) and (6-30).

In Figs.6-1 and 6-2, the values of λ_{22} obtained in the composition range in which J^0_{eb} is proportional to W_2^{-2} are plotted against $J^0_{eb}\,\eta_{0b}/J^0_{e2}\eta_{02}$. The symbols correspond to the blend series and the solutions as indicated in the figures. Although λ_{11} and λ_{12} can be estimated, in principle, as Ninomiya did, the separation was impossible because of the closeness of the G'_1 (or G''_1) and G'_{12} (or G''_{12}) functions. The difficulty is also related to the fact that d_1 and R in the Graessley theory are respectively proportional to (M_2/M_1) and $(M_2/M_1)^{3.5}$ as mentioned in the previous section.

In Fig.6- 3, the λ_{22} experimentally evaluated are plotted against (M_W/M_2) to confirm the assumption of eq(6-9). The dotted line represents eq(6-9) and the BMEO assumption seems to be adequate. Accordingly, it may be necessary that the Graessley relations eqs(6-16)and(6-17) should be rewritten under the condition $\lambda_{ii} \neq 1$ into

$$\frac{\eta_{0b}}{\eta_{01}} = W_1^2 \frac{\langle\tau\rangle_{11}}{\langle\tau\rangle_1} + W_1W_2 \frac{\langle\tau\rangle_{12}+\langle\tau\rangle_{21}}{\langle\tau\rangle_1} + W_2^2 \frac{\langle\tau\rangle_{22}}{\langle\tau\rangle_1} \tag{6-34}$$

$$\frac{J^0_{eb}}{J^0_{e1}} = \frac{W_1^2 \frac{\langle\tau^2\rangle_{11}}{\langle\tau^2\rangle_1} + W_1W_2 \frac{\langle\tau^2\rangle_{12}+\langle\tau^2\rangle_{21}}{\langle\tau^2\rangle_1} + W_2^2 \frac{\langle\tau^2\rangle_{22}}{\langle\tau^2\rangle_1}}{\left[W_1^2 \frac{\langle\tau\rangle_{11}}{\langle\tau\rangle_1} + W_1W_2 \frac{\langle\tau\rangle_{12}+\langle\tau\rangle_{21}}{\langle\tau\rangle_1} + W_2^2 \frac{\langle\tau\rangle_{22}}{\langle\tau\rangle_1}\right]^2} \tag{6-35}$$

These equations are the general formulations for η_{0b} and J^0_{eb}. For example, using the BMEO assumption [eqs(6-7) and (6-8)] and also $\langle\tau^2\rangle_{ij}=\langle\tau\rangle^2_{ij}$, eqs (6-11) and (6-12) can be obtained. These were deduced by a purely phenomenological treatment by BMEO.

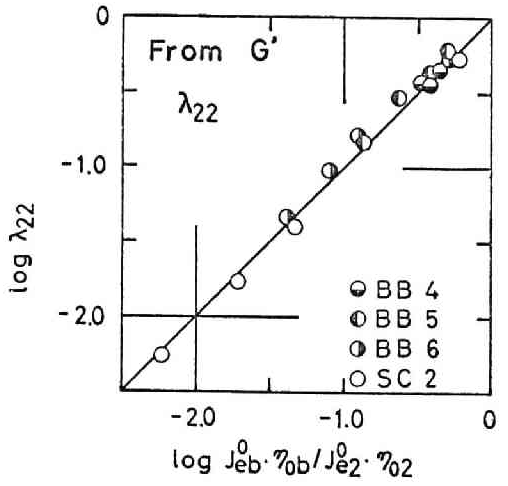

FIG.6-1. Log λ_{22} obtained from the frequency dependence curve of G', plotted against $\log(J^0_{eb}\eta_{0b}/J^0_{e2}\eta_{02})$.

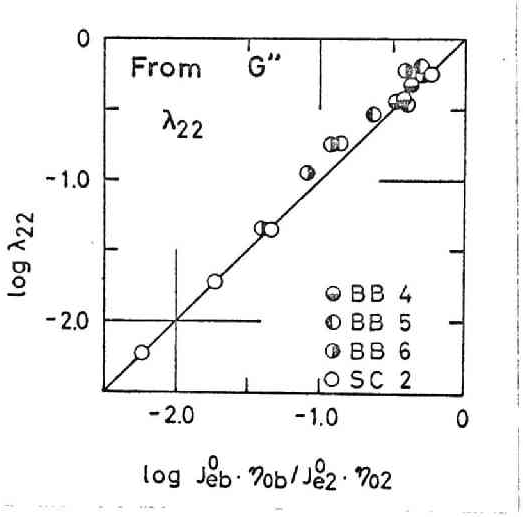

FIG.6-2. Log λ_{22} obtained from the frequency dependence curve of G", plotted against $\log(J^0_{eb}\eta_{0b}/J^0_{e2}\eta_{02})$.

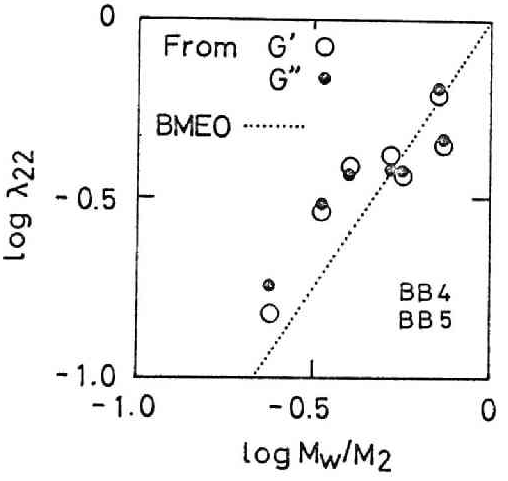

FIG.6-3. Log λ_{22} plotted against log (M_w/M_2) to confirm the eq(6-9).

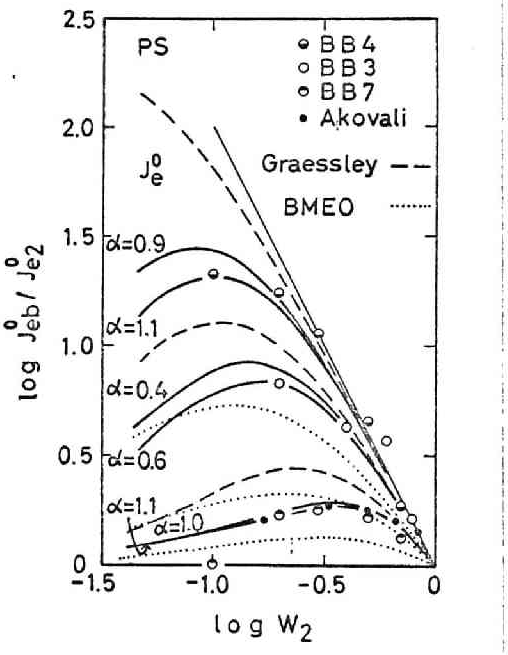

FIG.6-4. Comparison of the BMEO(dotted line), Graessley(broken line) and modified Graessley(solid line) theories with the experimental data for composition dependence of J^0_{eb}/J^0_{e2}.

Fig. 6-4 shows the comparison of the BMEO and Graessley theories with the experimental data for the composition dependence of J^0_{eb}/J^0_{e2}, as well as data of Akovali[12]. The uppermost solid straight line indicates the relation for 2-2 interaction dominating [eq(6-32)] and the other solid lines will be discussed later. As seen from this figure, the BMEO theory (dotted line) predicts too low and the Graessley theory (broken line) too high values of J^0_{eb}. It is probable that the discrepancy for BMEO theory can be attributed to the expression of the relaxation times for 1-1 and 1-2 interactions i.e. λ_{11} and λ_{12}, since the assumption for λ_{22} is acceptable as seen from Fig.6-3. On the other hand, the Graessley theory seems to have a weak point in the overestimation of the relaxation time for the 2-2 interaction in blend. This is caused by the idea that the effective frictional coefficient ζ_{22} for 2-2 interaction depends only on the length of the central and passing chains in both pure component and blend. Therefore, it is suggested that the frictional coefficient obtained for mono-disperse systems cannot be applied to the binary blend as it is.

When $\langle\tau\rangle_{22}$ and λ_{22} are written as follows using a parameter α:

$$\langle\tau\rangle_{22} = M_2^{3.5-\alpha} M_W^{\alpha} \tag{6-36}$$

$$\lambda_{22} = \frac{\langle\tau\rangle_{22}}{\langle\tau\rangle_2} = \left(\frac{M_W}{M_2}\right)^{\alpha} \tag{6-37}$$

the eqs(6-16) and (6-17) can be modified into

$$\frac{\eta_{0b}}{\eta_{01}} = W_1^2 + d_1 W_1 W_2 + R' W_2^2 \tag{6-38}$$

$$\frac{J^0_{eb}}{J^0_{el}} = \frac{W_1^2 + d_2 W_1 W_2 + R'^2 W_2^2}{(W_1^2 + d_1 W_1 W_2 + R' W_2^2)^2} \qquad (6\text{-}39)$$

Here, $\alpha=0$ and $\alpha = 1.5$ respectively correspond to the Graessley and BMEO theories, and R' is smaller than R:

$$R' = \frac{\langle\tau\rangle_{22}}{\langle\tau\rangle_1} = \left(\frac{M_2}{M_1}\right)^{3.5-\alpha} \cdot \left(\frac{M_W}{M_1}\right)^{\alpha} \leq R \qquad (6\text{-}40)$$

Values of α to represent the experimental data were evaluated by curve fitting as shown in Fig.6-4. The values for the blend series are located at about $\alpha = 1.0$, except for BB3 ($\alpha = 0.5$). This shows that the molecular weight dependence of λ_{22} should be intermediate between $\alpha = 0$ and $\alpha = 1.5$. The zero-shear viscosity of those blend series was calculated from eq(6-38), and is shown in Fig.6-5. The molecular weight dependence of η_{0b} (calculated from the α values) agrees well with the relation $\eta_{0b} \propto M_W^{3.5}$, while the Graessley theory does not.

Besides the treatments discussed above, Mills et al.[13] have been proposed the following empirical equation for J^0_{eb}:

$$\frac{J^0_{eb}}{J^0_{e2}} = \left(\frac{M_Z}{M_W}\right)^{3.7} \qquad (6\text{-}41)$$

In Fig.6-6 the recent experimental results for the blends of narrow-distribution polystyrenes are gathered to confirm the eq(6-41). The solid and dotted lines indicate the Mills equation and the BMEO prediction.

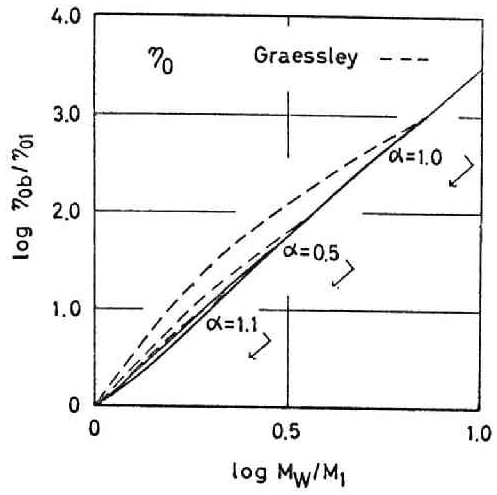

FIG.6-5. Molecular weight dependence of η_{0b} calculated from eq(6-38) at various α (solid line) and from the Graessley theory.

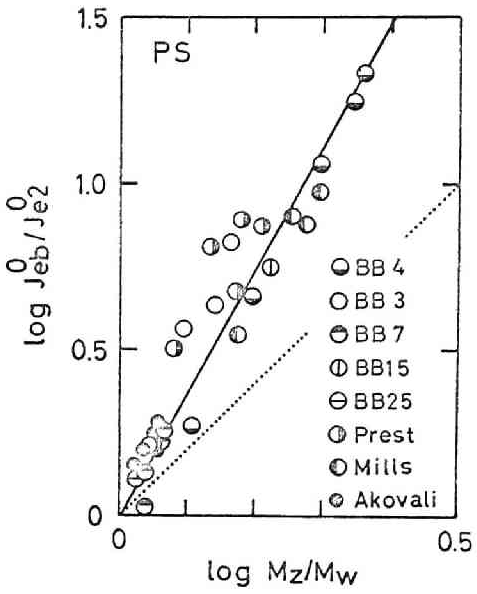

FIG.6-6. Log (J^0_{eb}/J^0_{e2}) experimentally obtained, plotted against log (M_Z/M_w) to test the Mills (solid line) and BMEO (dotted line) equations.

Although the two series of blends (Prest and BB3) show somewhat higher values, the agreement of all the data with the Mills relation is very good. Using this experimental fact and the relation obtained in Section 5.4, $\eta_{0b}/\eta_{02} = (M_W/M_2)^{3.7}$, λ_{22} given by eq(6-33) should be expressed by

$$\lambda_{22} = \frac{J^0_{eb} \cdot \eta_{0b}}{J^0_{e2} \cdot \eta_{02}} = \left(\frac{M_Z}{M_2} \right)^{3.7} \qquad (6\text{-}42)$$

To decide which expression for λ_{22} is more adequate [eq(6-37) or eq(6-42)], further investigations are required.

REFERENCES

1. J. D. Ferry, "Viscoelastic Properties of Polymers", 2nd ed., John Wiley, New York, 1970.
2. K. Ninomiya, J. Colloid Sci., 14, 49 (1959); 17, 759 (1962)
3. K. Ninomiya and J. D. Ferry, J. Colloid Sci., 18, 421 (1963)
4. K. Ninomiya and J. D. Ferry, J. Phys. Chem., 67, 2297 (1963)
5. W. W. Graessley and L. Segal, Macromolecules, 2, 49 (1969)
6. Y. Einaga, K. Osaki, M. Kurata, and M. Tamura, Macromolecules, 4, 87 (1971)
7. K. Osaki and Y. Einaga, "Progress in Polymer Science, Japan", Vol. I, M. Imoto and S. Onogi, Ed., Kodansha, Tokyo, 1971.
8. D. C. Bogue, T. Masuda, Y. Einaga, and S. Onogi, Polym. J., 563 (1970)
9. W. W. Graessley, J. Chem. Phys., 54, 5143 (1971)
10. W. M. Prest, Jr., Polym. J. 4, 163 (1973)
11. W. W. Graessley, J. Chem. Phys., 43, 2696 (1965); 47, 1942 (1967)
12. G. Akovali, J. Polym. Sci., Part A2, 5, 875 (1967)
13. (a) N. J. Mills, Europ. Polym. J., 5, 675 (1969)
    (b) N. J. Mills and A. Nevin, J. Polym. Sci., Part A2, 9, 267 (1971)

Publications

[A] PAPERS, ON WHICH THE PRESENT THESIS IS BASED

1. Effect of Molecular Weight and Concentration on Flow Properties of Concentrated Polymer Solutions.
   J. Polym. Sci., Part C, 15, 381 (1966)

2. Relationship between Molecular Weight and Concentration Determining the Viscosity of Concentrated Polymer Solutions (in Japanese).
   Nippon Kagaku Zasshi, 88, 231 (1967)

3. Dependence of viscosity of Concentrated Polymer Solutions upon Molecular Weight and Concentration.
   J. Polym. Sci., Part A2, 5, 899 (1967)

4. Rheological Properties of Polymethyl Methacrylate and Polyvinyl Acetate in the Molten State.
   Kolloid-Z & Z. Polym., 222, 110 (1968)

5. Molecular Structure and Melt Rheology (in Japanese).
   Kobunshi, 17, 640 (1968)

6. Rheological Properties of Anionic Polystyrenes I. Dynamic Viscoelasticity of Narrow-Distribution Polystyrenes.
   Macromolecules, 3, 109 (1970)

7. Rheological Properties of Anionic Polystyrenes II. Dynamic Viscoelasticity of Blends of Narrow-Distribution Polystyrenes.
   Macromolecules, 3, 116 (1970)

8. Viscoelastic Properties of Poly(methyl Methacrylate)s Prepared by Anionic Polymerization.
   Polym. J., 1, 418 (1970)

9. Viscoelastic Properties of Blends of Poly(methyl Methacrylate)s.
   Polym. J., 1, 542 (1970)

10. A Constitutive Model for Molecular Weight and Concentration Effects in Polymer Blends.
Polym. J., 1, 563 (1970)

11. Molecular Weight Distribution and Mechanical Properties of Linear Polymers (in Japanese).
Kogyo Kagaku Zasshi, 73, 1255 (1970)

12. Viscoelasticity of Narrow- and Broad-Distribution and Star-Shaped Polystyrenes (in Japanese).
Nippon Kagaku Sen-i Kenkyusho Koen shu, 28, 27 (1971)

13. Viscoelastic Properties of Concentrated Solutions of Poly(methyl Methacrylate) in Diethyl Phthalate.
Polym. J., 3, 315 (1972)

14. Rheological Properties of Anionic Polystyrenes IV. Non-Newtonian Flow of Monodisperse Polystyrenes and Their Blends.
J. Appl. Polym. Sci., Part C, to be published.

15. Steady-State Compliance of Polymer Blends.
J. Appl. Polym. Sci., Part C, to be published.

[B] OTHERS

16. Flow Properties of Some Suspensions (in Japanese).
Nippon Kagaku Zasshi, 88, 854 (1967)

17. Viscoelastic Properties of High Polymer - Particle Systems (in Japanese).
Nippon Kagaku Zasshi, 89, 464 (1968)

18. Rheology of Polymer - Particle Systems (in Japanese).
Nippon Kagaku Sen-i Kenkyusho Koen Shu, 25, 15 (1968)

19. Rheological Properties of Disperse Systems of Butyl Rubber Solutions and Carbon Black (in Japanese).
Nippon Kagaku Zasshi, 90, 360 (1969)

20. Non-Linear Viscoelasticity of Disperse Systems (in Japanese).
Zairyo, 19, 341 (1970)

21. Non-Linear Behavior of Viscoelastic Materials I. Disperse Systems of Polystyrene Solution and Carbon Black.
Trans. Soc. Rheology, 14, 275 (1970)

22. A Modified Casson Equation for Dispersions.
Trans. Soc. Rheology, 14, 617 (1970)

23. Rheological Properties of Anionic Polystyrenes III. Characterization and Rheological Properties of Four-Branch Star Polystyrenes.
Macromolecules, 4, 763 (1971)

24. Viscoelastic Properties of Concentrated Solutions of Randomly Branched Polystyrenes.
Polym. J., 3, 92 (1972)

25. Viscoelastic Properties of Concentrated Solutions of Star-Shaped Polystyrenes (in Japanese).
Zairyo, 21, 436 (1972)

26. Viscoelastic Properties of Star-Shaped Polystyrenes Having Six Branches and Their Concentrated Solutions (in Japanese).
Zairyo, 22, (1973).